WMRC Reports
Waste Management and Research Center

Stabilization of Arsenic Wastes

Max Taylor,
Robert Fuessle
Bradley University

RR-E73
January 1994
Electronic Version

About WMRC's Electronic Publications:

Hazardous Waste Research and Information Center
One East Hazelwood Drive
Champaign, Illinois 61820

HWRIC RR-073 *$10 00*

Stabilization of Arsenic Wastes

by

Max Taylor and Robert Fuessle
Bradley University

October 1994
Printed on recycled/recyclable paper

Illinois Department of Energy and Natural Resources

HWRIC RR-073

Stabilization of Arsenic Wastes

by

Max Taylor
Dept of Chemistry
and
Robert Fuessle
Dept of Civil Engineering and Construction
Bradley University
Peoria, Illinois

Prepared for
Hazardous Waste Research and Information Center
One East Hazelwood Drive
Champaign, Illinois 61820

HWRIC Project Number HWR 92-095

Printed by Authority of the State of Illinois

94/250

This report is part of HWRIC's Research Report Series Mention of trade names or commercial products does not constitute endorsement or recommendation for use.

ACKNOWLEDGMENTS

The investigators are thankful to many people for their help during this project. These people and their contributions are: Dr. Ron Alderfer, Mr. John LaPayne, and Ms. Carrie Eastburg of PDC Laboratories, Inc. for chemical analyses of TCLP extracts and digestates; Dr. Marvin Piwoni, Dr. Aaron Weiss and Ms. Teresa Chow of HML Laboratories in Champaign, IL., for arsenic speciation analyses; Mr. Norm Peters of the Center for Electron Microscopy at the University of Ilinois, Urbana, for SEM analyses of stabilized samples; Dr. Amir Al-Khafaji and Dr. Glover, our chairmen at Bradley University for release time; Sonal Desai, Sarandeep Dhillon, Sunil Kulkarni, Krishna Yerraguntla, and Hui Zhou, our students for all the hours in the laboratory, and Ms. Pamela P. Tazik, our HWRIC Research Project Officer, for her helpful suggestions.

CONTENTS

PAGE

Chapter Four: EXPERIMENTAL DESIGN

Chapter Five: RESULTS AND DISCUSSION

TABLES

FIGURES

ABBREVIATIONS

BDAT	Best demonstrated available technology
B/W; B/HW	Binder to hazardous waste mass ratio
CH	Calcium hydroxide structure in stabilized matrix
CSH	Calcium silicate hydrate structure in stabilized matrix
DI H_2O	De-ionized water
ICAP	Inductively Coupled Argon Plasma Spectrophotometer
K_{sp}	Solubility product
K	Equilibrium constant
SEM	Scanning Electron Microscopy
S/S	Stabilization/Solidification
TCLP	Toxicity Characteristic Leaching Procedure
XRD	X-ray Diffraction

Sample Names	(see Chapter 4 for discussion)
Aij	Stabilization samples with aluminum sulfate; mix number i and sample j corresponding to a cure time
Fij	Stabilization samples with ferric sulfate; mix number i with cure time j
FAij	Stabilization of synthetic arsenate waste with ferric sulfate; mix i with cure time j
FBij	Stabilization of synthetic arsenite waste with ferric sulfate; mix i with cure time j
IAij	Stabilization of D004/D005 waste with iron acetate; mix number i with cure time j
SEMi	Sample for scanning electron microscopy
SSij	Stabilization of D004/D005 waste with sodium sulfate; mix number i with cure time j
USij	Stabilization samples with ferrous sulfate; mix number i with cure time j
USAij	Stabilization of synthetic arsenate waste with ferrous sulfate; mix i with cure time j
USBij	Stabilization of synthetic arsenite waste with ferrous sulfate; mix i with cure time j

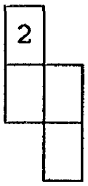

This mix design matrix appears in Table 4.2 through 4.4. A "2" in any one box refers to the use of ferrous sulfate corresponding to a mix design described in Table 4.2. A "3" in any one box refers to the use of ferric sulfate corresponding to a mix design described in Table 4.3.

Elements

As	Arsenic	Fe	Iron
B	Boron	S	Sulfur
Ba	Barium	Zn	Zinc
Ca	Calcium		

ABSTRACT

Arsenic and barium in an actual D004/D005 waste was stabilized for up to 540 days, the duration of project experimentation. Various stabilization designs were used to define a range of designs that are effective over the long term for a wide range of binder and waste compositions. This robust design is essential for practical stabilization because of the nonhomogeneity of industrial hazardous wastes.

The effectiveness of stabilization designs was determined primarily by TCLP. Dynamic column leaching, scanning electron microscopy, and calorimetry were also performed and reinforce conclusions. Data analyses included mass balance and correlation studies among the metal concentrations that permit a characterization of elements leaching from the binders and/or waste.

Ferrous sulfate was the stabilization reagent preferred over ferric sulfate and aluminum sulfate. Excessive sulfate did appear to slow down cement hydration with possible deleterious effects over the long term. Arsenate stabilization was more easily accomplished compared to arsenite. Aeration and/or chemical oxidation may be used to oxidize arsenite to arsenate for improved stabilization.

STABILIZATION OF ARSENIC WASTES

CHAPTER ONE
INTRODUCTION

1.1 Recent Legislation and a Need

In 1984, the Hazardous and Solid Waste Amendments to RCRA were signed into law. These amendments require EPA to promulgate regulations for the treatment of hazardous wastes before land disposal. Congress set deadlines for developing standards for wastes containing solvents and dioxins, for wastes containing constituents from the "California List", and all remaining hazardous wastes. The remaining hazardous wastes were ranked and partitioned into thirds according to volume and toxicity. In 1990, EPA promulgated the final rule for treatment requirements of the third one-third (Third Third) of scheduled wastes (Federal Register, 1990).

Treatment standards are based on performance of best demonstrated available technology (BDAT) which is a commercially available or leasable technology that yields statistically better treatment results than other treatment technologies. Treatment standards may be specified either by a required technology or by concentration standards for the leachant. EPA has elected to specify concentration standards for the leachant based on BDAT. Other treatment technologies may be used if these concentration standards are satisfied.

Arsenic wastes are included in the Third Third of scheduled wastes and are classified by several codes: D004, K031, K101, K102, P010, P011, P012, P036, P038, and U136, according to their origin and/or chemical form. In 1988, most of the arsenic waste generated in Illinois was coded D004 and amounted to 109,872 gallons. The total RCRA D004 waste treated, stored, or disposed in Illinois during 1988 was 20,949,963 gallons. This amount is 1.3 times the amount of all types of waste handled by the largest treatment/ storage/disposal facility in Illinois (Illinois EPA, 1990).

The focus of this research report is the development and understanding of a promising treatment technology for arsenic wastes that are nonwastewaters. Nonwastewaters are defined by having either greater than 1% total suspended solids or 1% total organic carbon. In this report, arsenic wastes will mean arsenic nonwastewaters.

1.2 Basis for Legislation

In 1990, EPA solicited comments for the treatment of arsenic wastes. The responses and the rationale for the final EPA ruling (Federal Register, 1990) included a discussion of the treatment technologies of stabilization and vitrification. Stabilization (S/S) involves chemical bonding of the waste with binders and proprietary compounds. A variety of binders were used including asphalt, cement, fly ash, and cement kiln dust. Vitrification involves the application of heat generated by electrodes or direct flame to a mixture of waste and glass-forming compounds. The cooled solid matrix is a glass/slag matrix. The intense heat of 1200-1500 degrees Celsius will destroy any organics present.

For stabilization of arsenic nonwastewaters, data reported to the EPA (Federal Register, 1990) are summarized in Table 1-1. The first observation is that stabilization appears to have potential for D004 arsenic wastes but not for K031 wastes. According to the EPA, the data are inconclusive for the following reasons: 1) the possible presence of organic interferences with the stabilization processes were not investigated; 2) the data did not include QA/QC data; and 3) the binder/waste ratio was not always stated or was too high. A high binder/waste ratio indicates more dilution and less treatment. Furthermore, the effect of cure time on treatment effectiveness has not been investigated.

There is some debate among commentors whether vitrifica-tion is "available" and "demonstrated". Nevertheless, based on 14 data points for a variety of wastes having 0.3%-23.5% arsenic, EP Toxicity Leaching of vitrified wastes yielded 0.007 to 1.8 mg/L arsenic. Neither QA/QC data nor volume increases were furnished. Furthermore, commentors expressed concerns about air emissions. EPA's response is that emissions from the vitrification process will be governed by current air quality regulations, and "a special furnace configuration with a recycling vapor scrubbing system is being investigated" and is "currently under development" (Federal Register, 1990).

Although the data are "equivocal", EPA decided that vitrification is BDAT because it appears to treat a variety of arsenic wastes based on current information. Since the data were for EP toxicity leaching, EPA expressed a concentration standard of 5.0 mg/L arsenic for EP leachate. If the arsenic in the extract from the toxicity characteristic leaching procedure (TCLP) is 5 mg/L or less, the treatment of arsenic satisfies treatment standards (Federal Register, 1990). EPA states that stabilization may be considered for certain arsenic wastes on a case-by-case basis. EPA issued a variance for the treatment of arsenic nonwastewaters until May, 8, 1992. Apparently, vitrification capacity and/or capability (e.g. air quality concerns) need to be addressed.

Although EPA declared vitrification as BDAT for arsenic wastes in general, research for effective arsenic stabilization is worthwhile for several reasons: 1) certain arsenic wastes, especially D004 which Illinois has the most of, may be stabilized effectively on a case-by-case basis, according to the EPA (Federal Register, 1990); 2) vitrification is costly; assuming a contaminated soil amenable to both vitrification and stabilization, and a specific gravity of 2.6 for soil, vitrification costs are $150-$220/cubic meter whereas stabilization is $92/cubic meter (Cullinane, 1985 and Pacific Northwest Laboratories, 1986); 3) vitrification may have air quality impacts; and 4) the proposed stabilization methodology allows an improved binder/hazardous waste ratio, i.e. more treatment and less dilution.

Table 1-1. Summary of Stabilization Data Submitted to EPA[1]

Waste Type	WASTE Untreated Leachant Conc. or [As Concentration]	WASTE Treated Leachant Conc.	Treatment Technology	EPA Comments
D004	41 mg/L (EP Tox.)	1.7 mg/L	asphalt	
D004	[73,000 ppm]	2.7 mg/L	Chemfix	no binder/ waste ratio no QA/QC organic interferences?
D004	409 mg/L (TCLP)	2.27 mg/L	proprietary stabilization	binder/ waste=1
D004	[35,000 ppm]	0.08 mg/L	proprietary stabilization	no QA/QC no binder/ waste ratio organic interference
D004	[750,000 ppm]	0.75 mg/L	American Nukem	high binder/ waste ratio high sludge production
K031	533 mg/L (EP Tox.)	25.3 mg/L	asphalt	
K031	5930 mg/L (TCLP)	10% inc.	cement	
K031	5930 mg/L (TCLP)	4687 mg/L	fly-ash	

1. Federal Register, 1990.

1.3 Objectives

1.3.1 Volume Efficiency, Treatment Effectiveness and Endurance

The goals of the research were to determine if S/S is a treatment for arsenic nonwastewaters that is cost-effective and volume-efficient. Satisfactory stabilization entails compliance with treatment standards for all time. Stabilization that is cost-effective will make it preferable to the costly and energy-intensive vitrification process with attending potential air emission problems. Volume efficiency, indicated by the volumetric ratio of untreated arsenic waste to treated arsenic waste, is important in that a waste is not really stabilized if it has been diluted greatly to decrease leachant concentrations. Furthermore, volume efficiency is important for the limited capacity of hazardous waste landfills. Finally, stabilization treatment must endure through time to avoid the potential migration of arsenic into the groundwater.

1.3.2 Development of Stabilization Technology

The investigators have stabilized a D004/D005 waste containing arsenic and barium. The stabilization included two steps: 1) a chemical pretreatment of arsenic using ferrous sulfate, ferric sulfate or aluminum sulfate; 2) stabilization with fly ash cement. This stabilization with pretreatment is promising because of the precipitation of barium sulfate and iron-arsenic compounds. This chemistry has been used for arsenic removal in the treatment of wastewaters. The precipitates may be encapsulated within or adsorbed onto the cement matrix.

This research was conducted to understand and develop this promising stabilization process. The mechanism of stabilization and its treatment effectiveness was investigated.

Research with a variety of pretreatment reagents, binders, and pozzolans was conducted on actual D004/D005 arsenic wastes from a glass manufacturer. This development includes a determination of the type and amount of pretreatment, binder, and pozzolan required for a lasting, satisfactory stabilization of arsenic. Ferrous sulfate and other pretreatment reagents were selected for their capacity to immobilize arsenic. Excessive amounts of these reagents and other waste components may be detrimental to the development of the cement matrix. For example, excess sulfate is deleterious to cement matrix development by reacting with hydrous or anhydrous calcium aluminate to form a crystalline ettringite structure. Cracking of the cement paste will occur if too much ettringite is formed (Mindess, 1981). There are types of cements and fly ash that minimize the impact of excess sulfate on the development of the cement matrix (Mehta, 1986; Mindess, 1981; Odler, 1988).

1.3.3 More Fundamental Understanding of Arsenic Stabilization

EPA has suggested that stabilization of certain arsenic wastes may be considered on a case-by-case basis. This project addresses a research need by developing a deeper microchemical/microstructural understanding of why stabilization works in some cases and not in others and by comparing methods of pretreatment to eliminate or minimize interferences. A more fundamental understanding of arsenic stabilization will aid in the characterization of those arsenic wastes amenable to stabilization. Furthermore, a deeper understanding of the microstructure and chemistry of arsenic stabilization is necessary to predict whether the treatment is lasting or not.

1.3.4 Development of Guidelines

Guidelines and recommendations for the stabilization of arsenic nonwastewaters have been developed. The guidelines aid in the decision as to which arsenic wastes are amenable to stabilization. The recommendations include pretreatment dosages and mix design parameters. These guidelines are intended to improve the design and operation of commercial arsenic stabilization processes.

1.4 Report Organization

A review of stabilization, arsenic chemistry, and treatment is provided in Chapter 2. Experimental methods and procedures are described in Chapter 3. Chapter 4 contains a description of the experimental design, and results are discussed in Chapter 5. Sections in Chapters 4 and 5 are written in parallel so the reader may follow the design and results of any part of the project without any loss of continuity. Stabilization mix design critical to understanding the results is found in Tables 4-2 to 4-4 on pages 52 to 54. These tables are repeated in Appendix A for convenience. Notations for mix designs are defined in the list of abbreviations and in Section 5.1 of Chapter 5. Chapter 6 provides a final summary and recommendations. Appendix B contains the analytical data for TCLP extractions of samples discussed in the report.

CHAPTER TWO
STABILIZATION AND TREATMENT OF ARSENIC AND BARIUM

2.1 Introduction

After a brief introduction to occurrences and sources of arsenic and barium, the relevant chemistries of these elements are discussed in sections 2.2 through 2.5. The hydration and chemical microstructure of cement is reviewed in section 2.6. A literature review of arsenic stabilization is presented followed by a discussion of arsenic adsorption and precipitation from wastewaters and natural waters. Adsorption and precipitation are reviewed since they may be important in stabilization.

2.2 Sources and Occurrences of Arsenic

Arsenic is an ubiquitous element occurring in land, air, and natural waters. The average arsenic content in the soil is 5-6 ppm (NAS, 1977) and may range from 1 ppm to 6000 ppm depending on the type of soil or rock (Gulledge and O'Connor, 1973). Arsenic occurs in about 100 different minerals such as arsenopyrite (FeAsS) and realgar (AsS). Nearby industrial sources such as smelters or the use of arsenical agricultural products may increase natural soil concentrations.

Arsenic residues enter natural waters by the weathering of rocks and soils and by runoff from decaying vegetation containing arsenic. Concentrations in the water are generally low. Seawater concentrations range from 1-8 ppb with sediments at 2-20 ppm (Penrose, 1974). Inorganic arsenic exists in several oxidation states and forms in water depending on pH and Eh. Arsenic may be metabolized by anaerobes to methylated forms that may bioaccumulate in certain seafoods.

Primary industrial contributions of arsenic to the environment are by-products of the smelting of non-ferrous metal ores, primarily copper with minor contributions by lead, zinc, and gold (NAS, 1977). Arsenic has also been used in agricultural herbicides, insecticides, and feed additives. In the 1940's and 50's, inorganic arsenic such as lead arsenate and calcium arsenate were used for herbicides. The development of organic arsenicals in the 60's replaced the inorganic forms for herbicidal use. Arsenic also enters the environment by accompanying phosphates in fertilizers and detergents.

Other industrial uses for arsenic include: wood preservation by zinc and chromium arsenates, additives in metallurgical applications and glass production, and catalysis in manufacturing processes. Arsenic trioxide is added to molten glass to coalesce air bubbles which can then rise out of the glass. The arsenic trioxide is captured in the flue as a tan colored dust. This hazardous waste, coded as D004/D005, must be treated before land disposal.

2.3 Arsenic Chemistry

The chemistry of stabilization is a very complex process. Arsenic stabilization, in particular, is currently not well characterized in the literature. In order to begin a study of arsenic stabilization, it is helpful to review the chemistry of arsenic in simple systems.

2.3.1 Oxidation States, Equilibrium, and Adsorption on Iron

The chemistry of arsenic in the condensed phase is primarily that of the +3 and +5 oxidation states. Unless insoluble sulfide compounds are formed, the normal forms found are the arsenite, AsO_2^-, the arsenate, AsO_4^{3-}, and their protonated species. $AsCl_3$ and $AsCl_5$ hydrolyze rapidly in water to form HCl(aq) and the corresponding arsenic acid.

Metallic arsenic (oxidation state 0) is a facile reducing agent, reducing solutions of $CuSO_4$, $Hg_2(NO_3)_2$, $FeCl_3$, $KMnO_4$, and $PtCl_4$. The other common oxidation state of arsenic (-3) is normally found only in the highly toxic compound $AsH_3(g)$, formed by reduction with nascent hydrogen.

Equilibrium constants for arsenic compounds are difficult to find in the literature, and various sources disagree significantly due to the difficulties of measurement and correction for solution nonidealities. In general, it is quite common to find reported values of ionization and solubility equilibrium constants varying over a one or two order-of-magnitude range. Several values for equilibrium constants from primary and secondary literature sources are listed in Table 2-1. Because iron(III) hydroxide is extremely insoluble ($K_{sp} = 4 \times 10^{-38}$), iron arsenate and arsenite are reported to be soluble in basic solutions. It is reported that $FeAsO_4$ dissolves completely and quickly in concentrated ammonia to form a blood-red solution (H. Metzke, 1899). An examination of the solubility product of $Al(OH)_3$ ($K_{sp} = 1.3 \times 10^{-33}$) indicates that aluminum arsenate should also be soluble in strong bases.

As(III) in aqueous solution behaves as a monobasic acid, while As(V) is a tribasic acid in aqueous solution. All known soluble As(III) compounds reduce nitric acid and decolorize $Br_2(aq)$, with the subsequent oxidation of As(III) to As(V). Strong solutions of H_2O_2 will oxidize As(III) to As(V) in acidic solution.

G. Lockemann (1911) found that arsenic is strongly adsorbed onto the surface of freshly precipitated $Fe(OH)_3$. This was used as an antidote for arsenic poisoning during the early part of the twentieth century. The process was shown to be a reversible adsorption reaction, not the formation of a basic arsenate precipitate. Because As(III) is oxidized to As(V) by the presence of Fe(III), the adsorption process takes place with arsenate or arsenite in solution. The amount of $Fe(OH)_3$ necessary for the

Table 2-1. Arsenic Equilibrium Constants

Dissociation of arsenous acid:

$HAsO_2(aq) \text{ ----> } H^+(aq) + AsO_2^-(aq) \quad K = 2.1\times10^{-9}$

Dissociation of arsenic acid:

$H_3AsO_4(aq) \text{ ----> } H+(aq) + H_2AsO_4^-(aq) \quad K_1 = 5.0\times10^{-3}$

$H_2AsO_4^-(aq) \text{ ----> } H^+(aq) + HAsO_4^{2-}(aq) \quad K_2 = 8.3\times10^{-6}$

$HAsO_4^{2-}(aq) \text{ ----> } H^+(aq) + AsO_4^{3-}(aq) \quad K_3 = 6.0\times10^{-10}$

Solubility products:

Ag_3AsO_3	1.2×10^{-17}	
Ag_3AsO_4	3.1×10^{-18}	(brownish-red)
$AlAsO_4$	1.6×10^{-16}	
$Al_2(HAsO_4)_3$	1.7×10^{-17}	
As_2S_3	4.4×10^{-27}	(yellow)
$Ba_3(AsO_4)_2$	8.0×10^{-51}	
$BiAsO_4$	4.4×10^{-10}	
$Ca_3(AsO_4)_2$	6.8×10^{-19}	
$FeAsO_4(s)$	5.7×10^{-21}	(red or yellow)
$Mg_3(AsO_4)_2$	2.1×10^{-20}	

complete adsorption of arsenic is given by the formula

$$E = k\ A^{0.57}$$

where E is the milligrams of $Fe(OH)_3$ in 100 mL of solution containing A milligrams of As. The constant k varies with temperature:

t, °C:	0	25	80
k :	70	90	130

W. Blitz (1904) found that the amount of As_2O_3 adsorbed from aqueous solution by $Al(OH)_3$ is very small and is practically independent of the As_2O_3 concentration.

In the sulfide qualitative analysis scheme used by Sorum (1960) and Hogness & Johnson (1954) arsenic appears in the acid sulfide group, being precipitated as the sulfide from a solution ranging from 0.2 M to 2 M HCl saturated with $H_2S(g)$. As(III) is precipitated as $As_2S_3(s)$ while As(V) is both reduced by the H_2S to As(III) and precipitated as $As_2S_5(s)$.

From the chemical background above we can conclude that the predominant forms of arsenic in any waste to be stabilized are the AsO_2^- or AsO_4^{3-} anions in various stages of protonation. The most common of the simple chemical models of the concrete matrix is that of an anionic silicate-aluminate lattice with cations bound to lattice sites by ionic attraction. The amorphous, water-rich regions of the matrix are at very high pH values. In order to hold an anionic material in the matrix, the stabilization process must provide either covalent bonding into the matrix during the curing of the matrix or formation of insoluble compounds inside the matrix. Previous work (Akhter, 1990) indicates that incorporation of the arsenic anions into the silicate-aluminate backbone is not likely. Therefore, the most obvious mechanism for stabilizing arsenic is to form insoluble compounds with iron(II), iron(III), or aluminum(III) incorporated in the concrete.

Both iron(III) and aluminum(III) stabilizations appear to be difficult because the solubility of the arsenates should increase with increasing pH. The reactions supporting this argument are:

$$FeAsO_4(s) + 3\ OH^-(aq) \text{ -----> } Fe(OH)_3(s) + AsO_4^{3-}(aq) \qquad (1)$$

$$K = K_{sp}[FeAsO_4] \ / \ K_{sp}[Fe(OH)_3] = 5\times10^{+15}$$

and

$$AlAsO_4(s) + 3\ OH^-(aq) \text{ -----> } Al(OH)_3(s) + AsO_4^{3-}(aq) \qquad (2)$$

$$K = K_{sp}[AlAsO_4] \ / \ K_{sp}[Al(OH)_3] = 1\times10^{+17}$$

Accordingly, in order to keep the concentration of the arsenate ion low enough to meet TCLP standards, the solution must have a very low concentration of hydroxide ion ($pH < 7$). This observation may explain why arsenic stabilization fails in a cement only matrix.

This argument is too simplistic in this form, because we have not considered the fraction of the total arsenate in the solution which is actually present as the AsO_4^{3-} ion. The TCLP protocol is based on the total arsenic in the leachate from the sample. At pH = 7, only 0.6% of the total arsenic in solution is present as the AsO_4^{3-} ion, due to the weak acid character of H_3AsO_4. After we take the hydrolysis of arsenate anions into account we find the requirement that the pH must be below 5.5 to meet the TCLP standard from $AlAsO_4$ or $FeAsO_4$ for stabilization by simple precipitation. In the dynamics of a TCLP leaching procedure, it is unlikely that the equilibrium concentrations calculated would be reached because the surface of particles of $FeAsO_4(s)$ would be coated with a gelatinous precipitate of $Fe(OH)_3(s)$, slowing the rate of dissolution.

The weak acid character of the arsenate and arsenite anions indicates that the solubility of most arsenite and arsenate precipitates should increase markedly in acidic solution. If the pH becomes too low, the hydrolysis of the anion in the precipitate could lead to solubilization of the arsenic precipitate. The reaction to be considered is:

$$FeAsO_4(s) + H^+(aq) \text{ -----> } Fe^{3+}(aq) + HAsO_4^{2-}(aq) \qquad (3)$$

$$K = K_{sp}[FeAsO_4] \; / \; K_3[H_3AsO_4] = 1.1x10^{-18}$$

The total concentration of arsenic expected from this process is below 6 mg/L at pH = 1.0, indicating that it is unlikely to find much dissolution of the precipitate in acidic solutions.

The weak acid nature of H_3AsO_4 complicates any equilibrium discussions due to ionization and hydrolysis of the ions involved. Using the ionization constants reported in Table 2-1, the distribution of total arsenate in solution among the various species can be calculated, assuming ideal solution behavior. The results are presented in Figure 2-1. Examining these results, one notices that in solutions near pH 2, if the total concentration of As(V) is below the TCLP 5.0 mg/L standard (equal to $6.67x10^{-5}M$), then the concentration of AsO_4^{3-} anion, which is controlled by the solubility of $FeAsO_4$, must be below $1.1x10^{-15}M$.

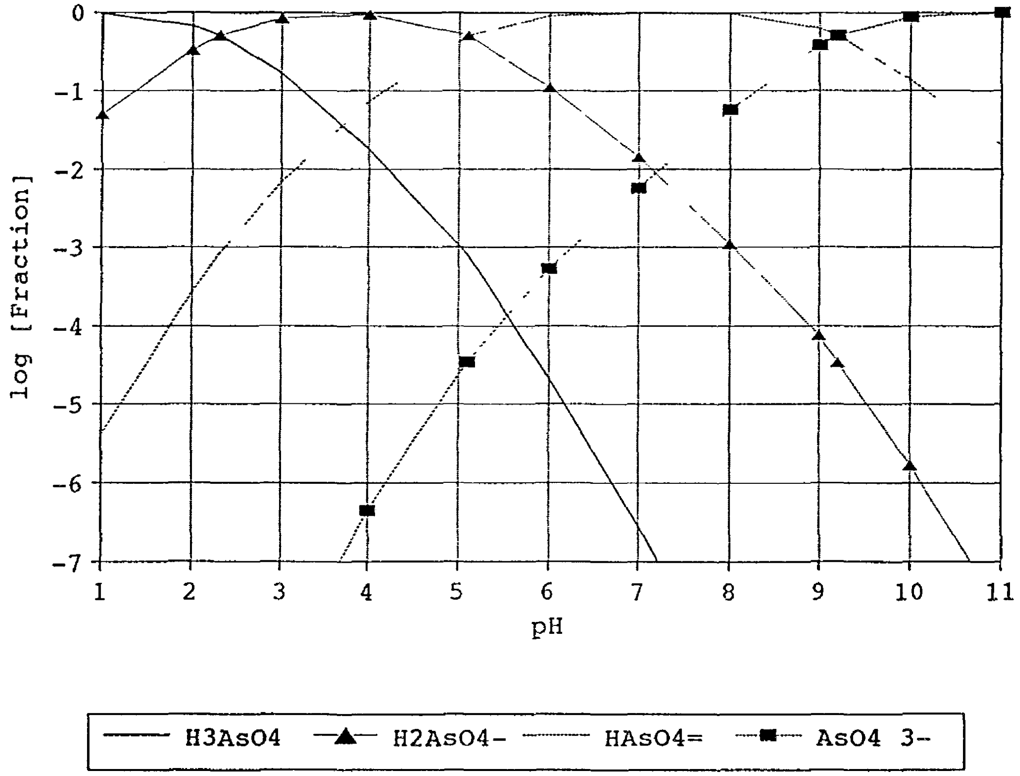

Figure 2-1. Principal Species Analysis for Arsenic Acid

$FeAsO_4(s)$ is a very insoluble material, with $K_{sp} = 5.7 \times 10^{-21}$. The solubility of $FeAsO_4$ is complicated by the fact that AsO_4^{3-} is the anion of a very weak acid. When we look at the solution properties, we should keep in mind the strong similarities between H_3AsO_4 and H_3PO_4. Another complicating factor is the extreme insolubility of $Fe(OH)_3(s)$, with $K_{sp} = 4 \times 10^{-38}$.

When appropriate solubility products and physical properties are collected, we note that comprehensive handbooks do not list nor contain properties for intermediate iron hydrogen arsenates or iron hydrogen phosphates.

In the simplest case, $FeAsO_4$ solubility is not affected by the pH of the solution. In this case the equilibrium is

$$FeAsO_4(s) \rightleftharpoons Fe^{3+}(aq) + AsO_4^{3-}(aq) \qquad (4)$$

If we consider only the dissolving of $FeAsO_4(s)$, then $[Fe^{3+}] = [AsO_4^{3-}]$ and

$$[AsO_4^{3-}] = (5.7 \times 10^{-21})^{1/2} = 7.5 \times 10^{-11}\ M = 5.6 \times 10^{-6}\ mg\ As/L$$

This very small value, when compared to experimental results, appears to be unrealistic. Therefore we must consider the effect of pH on the solubility.

As seen in Figure 2-1, in mildly acidic solutions the arsenate anion is often at least monoprotonated, and in some cases multiply protonated at equilibrium. In this case, the major equilibrium to be considered is:

$$FeAsO_4(s) + H^+(aq) \rightleftharpoons Fe^{3+}(aq) + HAsO_4^{2-}(aq) \qquad (5)$$

The equilibrium constant for this process is the solubility product for $FeAsO_4(s)$ divided by K_3 for arsenic acid. If we consider the process to be dissolving $FeAsO_4(s)$, then the concentration of $Fe^{3+}(aq)$ is equal to the concentration of $HAsO_4^{2-}(aq)$ and

$$[HAsO_4^{2-}] = \{[H^+] \times 1.80 \times 10^{-9}\}^{1/2}$$

Using this equation produces the expected concentrations of arsenic shown in Table 2-2. It has been assumed that no protonation of the arsenic anion occurs beyond the monohydrogenarsenate form. This oversimplification predict solubilities that are too small when the pH is below 4. In any case, note that the concentration of arsenic from the dissolution of $FeAsO_4(s)$ becomes significant only in the pH range below 3.

When the system has appreciable hydroxide ion concentrations, then another complication can arise from the competition of hydroxide ion for the iron(III) species. The extreme insolubility of $Fe(OH)_3(s)$ provides a large driving force for this competition.

Table 2-2. Solubility of Ferric Arsenate in Acidic Solutions

pH	3.0	4.0	5.0	6.0	7.0
$[HAsO_4^{2-}]$, M	1.3E-6	4.2E-7	1.3E-7	4.3E-8	1.3E-8
conc As, mg/L	0.10	0.03	0.01	0.003	.001

The relevant main equilibrium reaction now becomes

$$FeAsO_4(s) + 3\ OH^-(aq) \rightleftharpoons Fe(OH)_3(s) + AsO_4^{3-}(aq) \qquad (6)$$

The equilibrium constant for this reaction is

$$K_{sp}(FeAsO_4)/K_{sp}(Fe(OH)_3) = 1.4\times10^{+17}$$

which indicates that the reaction should lie far to the right. Our only hope of maintaining low arsenic concentrations is to keep the solution acidic enough so that the concentration of hydroxide ion is very low. We can calculate the concentration of dissolved arsenic using the equilibrium expression:

$$[AsO_4^{3-}] = [OH^-]^3 \times 1.4 \times 10^{+17}$$

This equation leads to the results in Table 2-3. It should be noted that iron(III) is not useful for precipitation of arsenate at pH levels above 7.0

Table 2-3. Estimated Solubilities of Ferric Arsenate in Weakly Basic Solutions

pH	6.0	6.5	7.0	7.25	7.5	8.0
$[AsO_4^{3-}]$, M	1.4E-7	4.5E-6	1.4E-4	8.0E-4	4.5E-3	0.14
conc As, mg/L	0.01	0.34	1.1	6.0	34.	1100.

When dealing with simple precipitates of $FeAsO_4(s)$, one can conclude that the pH must be kept in the range of 3.0 to 7.0 in order for arsenic to be effectively immobilized. The system is much more sensitive on the basic side than on the acidic side. This result is verified by column leaching results discussed in Section 5.3.

2.3.2 Implications for Stabilization in a Concrete Matrix.

This brings up the question, "How does the presence of ferric sulfate improve the stabilization of arsenate wastes in a basic cement matrix?" There are several possible explanations to be considered: First, the Fe^{3+} ions may be serving as bridges between the arsenate anions and the silicate matrix. The geometry of the silicate oxygen atoms around the ferric ion could be quite similar to that of the oxygen atoms around the ferric ion in ferric hydroxide gel. If this were true, then hydroxide ions could not compete as effectively for ferric ion sites. Second, the concentration of free hydroxide ions in the cement matrix decreases as the matrix hardens. Most of the hydroxide has been immobilized by reaction with calcium and other species. This immobility reduces the ability of hydroxide ions to compete with arsenic for iron sites. Third, the ferric arsenate is physically protected from the leachant by the low diffusion rates in the cement matrix. If this is the case, then the amount of arsenic release should be related to the amount of cement matrix broken down by the leaching process.

Several methods for helping to distinguish between the possibilities were tried. Correlation of arsenic release with calcium and zinc release from the cement matrix during TCLP and column leaching tests allows the estimation of the contribution of the third case. Using atomic spectroscopy in the scanning electron microscope enabled us to look at the spatial arrangement of iron and arsenic. If the arsenic is bound to the lattice through iron, then the arsenic should be fairly evenly distributed. If the arsenic is immobilized through the physical encapsulation of ferric arsenate precipitate particles, then the arsenic should be found as separated clumps and correlate highly with the iron distribution.

As the problem of arsenic stabilization equilibria was investigated further, it was decided to consider the possibility of using a stabilizing agent such as Fe(II) to immobilize arsenic. Because the value of the K_{sp} for $Fe(OH)_2$ is larger than that for the tri-hydroxides, the solubility of iron-arsenate precipitates should be less in basic solutions. Quantitative calculations could not be attempted because not enough applicable equilibrium constants could be found in the literature.

2.4 Sources and Occurrences of Barium

Barium, a very reactive member of the alkaline earth family, is widely distributed over the earth's crust, mostly in conjunction with calcium. Barium ores include baryites ($BaSO_4$) and witherite ($BaCO_3$). In addition to the barium mined as the major product of an operation, barium is found in the tailings of lead, zinc, silver, fluorite and rare-earth mines. The metal is used as a sealed-tube vacuum system getter for residual gases and to deoxidize steel and other metals. Over 90% of the over one-million tons of barium used annually is as $BaSO_4$. The major use of this insoluble compound is in the petroleum industry as high-density well-drilling muds. $BaSO_4$ is also used as an extender in automotive paints and a rubber and plastics filler, particularly for sound-deadening applications.

Barium sulfate is used in the glass industry as a flux to promote melting of the glass at a lower temperature and thus to increase the production rate, reduce seed imperfections, and reduce annealing time. As a glass additive, barium sulfate increases the refractive index of the glass and thus its brilliance.

About ten thousand tons of barium carbonate are used annually by the U.S. glass industry as a flux to decrease melting temperatures, and as an additive to increase durability, add weight and density, increase refractive index and increase x-ray absorption. The more expensive barium carbonate is often preferred over barium sulfate in glass melting because the dense carbonate doesn't become airborne when furnaces are charged. Other uses of barium carbonate include brick and tile glazes, ferrite molded and flexible magnets, and photographic papers.

2.5 Chemistry of Barium

Barium is being stabilized in a cement lattice using an additive such as iron(II) sulfate, iron(III) sulfate or aluminum sulfate in this project. The most probable mechanism for this stabilization process involves the precipitation of barium as barium sulfate and the mechanical incorporation of this solid into the cement lattice. In considering the concentration of barium to be expected in TCLP or column extracts, chemical principles can provide some guidelines.

Because barium sulfate is the insoluble precipitate formed from the interaction of a strong base and a strong acid, its solubility in aqueous systems is independent of the pH of the solution. The only effect which is expected to change the solubility of $BaSO_4$ is the activity coefficient correction due to the total ionic strength of the solution. Taking the solubility reaction to be

$$BaSO_4(s) \rightleftharpoons Ba^{2+}(aq) + SO_4{}^{2-}(aq) \qquad (7)$$

the solubility product constant expression is

$$K_{sp} = [Ba^{2+}][SO_4{}^{2-}] = 1.1 \times 10^{-10}$$

If solid $BaSO_4$ is dissolved in pure water, the equilibrium concentration of Ba^{2+} is equal to the concentration of $SO_4{}^{2-}$. The equilibrium concentration of barium in pure water will be

$$[Ba^{2+}] = (1.1 \times 10^{-10})^{1/2} = 1.05 \times 10^{-5}M = 1.4 \text{ mg/L} \qquad (8)$$

if the solution is ideal.

In a real solution, activity coefficients must be taken into account. The Debye-Huckel theory can provide correction factors which are accurate enough for our purposes. Debye-Huckel activity coefficients are determined by the total ionic strength of the solution. In the case above, the ionic strength, I, is given by

$$I = 0.5 \{[Ba^{2+}](+2)^2 + [SO_4{}^{2-}](-2)^2\} = 2.1\text{x}10^{-5}M$$

In these rather dilute ionic environments, we can substitute concentrations in molarity for concentrations in molality with enough accuracy for our purposes. The Debye-Huckel limiting law defines the mean ionic activity coefficient, y, by:

$$\log(y) = 0.509(+2)(-2)(I)^{1/2} = -0.00933 \qquad (9)$$

which implies that $y = 0.979$. The corrected solubility is the ideal solubility (8) divided by the activity coefficient y (9), or 1.47 mg/L. Table 2-4 relates ionic strengths, activity coefficients, and expected solubilities.

Table 2-4. Barium Sulfate Solubility

Ionic Strength M	Activity Coefficient	Ba^{2+} Solubility mg/L	
0	1	1.4	
$2\text{x}10^{-5}$	0.98	1.4	
$1\text{x}10^{-3}$	0.86	1.7	(pH 3 extract)
$1\text{x}10^{-2}$	0.63	2.3	
$2\text{x}10^{-2}$	0.52	2.8	
$5\text{x}10^{-2}$	0.35	4.1	(pH 8.5 extract)
$1\text{x}10^{-1}$	0.23	6.3	

The pH 3 extract solution is $5\text{x}10^{-2}M$ acetic acid.
The pH 8.5 extract solution is $5\text{x}10^{-2}M$ sodium acetate.

If the concentration of free sulfate ion is different from the concentration of barium in an extract fluid, the solubility of barium can be affected. When the barium concentration is 1.4 mg/L ($1\text{x}10^{-5}M$), the equivalent sulfate concentration is 0.3 mg/L. Because the barium concentration is inversely proportional to the sulfate concentration, when the sulfur concentration is larger than 0.3 mg/L in an extract fluid (working with the reasonable assumption that the predominant sulfur species is sulfate) then the barium concentration should be smaller than that calculated above.

2.6 Chemistry of Cement

2.6.1 Manufacture of Cement

Raw materials for the manufacture of portland cement consist of calcium carbonates such as limestone, chalk, and shell deposits and iron-bearing aluminosilicates such as clays, silts, and shales. These materials are ground and conveyed through a kiln with zones of increasing temperatures. The initial zone drives off moisture and makes the materials reactive. In the calcination zone at about 1200 deg. C, calcium aluminates and ferrites are formed. Calcium silicates are formed in the liquid form of the charge in the clinkering zone at 1400 - 1600 deg. C. The material from the kiln is known as clinker which is mixed with a small amount of gypsum to make portland cement. The gypsum is necessary to prevent a flash set of the cement as explained in Section 2.6.3.

2.6.2 Chemical Composition of Cement

Based on the mix and type of raw materials as well as the operation of the kiln, the exact chemical composition of portland cement may vary. Approximate compositional formulae and abbreviations are shown in Table 2-5.

The proportions of the various components may be controlled to yield five different types of portland cement as shown in Table 2-5. Type I is used for most construction purposes where no special properties are required. If a more rapid set is required, then C_3S may be increased to yield Type III cement. A more rapid set may also be accomplished by grinding the cement to finer particles. The heat liberated during cement hydration may cause tensile cracking due to thermal stresses developing during cool-down periods. Thermal cracking is especially problematic with larger concrete placements. A decrease in C_3S and C_3A provides Type IV cement with a lower heat of liberation and longer set times. The exposure of concrete to sulfates (e.g. seawater) can cause cement deterioration. The replacement of C_3A with C_4AF yields a sulfate-resistant Type V cement.

2.6.3 Cement Hydration

All chemical reactions are written in a shorthand notation that is commonly used in the study of concrete chemistry. These notations are defined in Table 2-6.

The hydration of portland cement can be described by a series of consecutive and interacting reactions between clinker materials and water. As shown in Table 2-5, the general rates of hydration proceed in the approximate order: $C_3A > C_3S > C_4AF > C_2S$ although there may be considerable overlapping of reactions. The reactivities of the various compounds are affected by differences

Table 2-5. Principal Compounds of Portland Cement and Their Characteristics

Approximate Composition	$3CaO \cdot SiO_2$	$B2CaO \cdot SiO_2$	$3CaO \cdot Al_2O_3$	$4CaO \cdot Al_2O_3 \cdot Fe_2O_3$
Abbreviated formula	C_3S	BC_2S	C_3A	C_4AF
Common name	Alite	Belite		Ferrite Phase, Fss
Principal impurities	MgO, Al_2O_3, Fe_2O_3	MgO, Al_2O_3, Fe_2O_3	SiO_2, MgO, alkalies	SiO_2, MgO
Common crystalline form	Monoclinic	Monoclinic	Cubic, orthorhombic	Orthorhombic
Proportion present (%)	35 - 65	10 - 40	0 - 15	5 - 15
Average in Type:				
I	50	25	12	8
II	45	30	7	12
III	60	15	10	8
IV	40	40	4	10
Rate of reaction with H_2O	Medium	Slow	Fast	Medium
Contribution to strength:				
Early age	Good	Low	Good	Good
Ultimate	Good	High	Medium	Medium
Typical heat of hydration (cal/g)	Medium 120	Low 60	High 320	Medium 100

Refs: Jones, 1990; Mindess and Young, 1981.

Table 2-6. Cement Chemistry Notations

Abbreviation	Chemical Formula
C	CaO
S	SiO_2
H	H_2O
C_2S	$2CaO \cdot SiO_2$
C_3S	$3CaO \cdot SiO_2$
$C\bar{S}H_2$	$CaSO_4 \cdot 2H_2O$
C_3A	$3CaO \cdot Al_2O_3$
C_4AF	$4CaO \cdot Al_2O_3 \cdot Fe_2O_3$

in particle size and the presence of impurities. Cement hydration initially yields dramatic chemical and structural changes with smaller changes continuing for a period of years. The chemical reactions describing the hydration of cement compounds have been studied by investigating the hydration of each compound separately; this assumes that the hydration of each compound is independent of the hydration of other compounds. This pragmatic assumption is considered reasonable although there is some interaction among hydration reactions.

The exothermic reactions yield a rate of heat evolution curve as shown in Figure 2-2 for portland cement. The general shape of two heat peaks is determined by individual contributions of a similar shape from C_3A and C_3S as shown in Figures 2-3 and 2-4, respectively.

Within a few minutes of cement hydration, C_3A reacts with gypsum according to reaction (10) to form ettringite in the form of long slender prismatic needles growing into capillary pores between cement grains.

$$\underset{\substack{\text{tricalcium}\\\text{aluminate}}}{C_3A} + \underset{\text{gypsum}}{3C\bar{S}H_2} + \underset{\text{water}}{26H} \text{------>} \underset{\text{ettringite}}{C_6A\bar{S}_3H_{32}} \qquad (10)$$

C_3A is highly reactive; if gypsum is not available, C_3A reacts with the sulfate in ettringite according to reaction (11) to form monosulfoaluminates which are thin hexagonal plates set in an irregular cluster. The formation of ettringite slows down the hydration of C_3A by creating a diffusive barrier. This barrier may be removed as the ettringite is converted to monosulfoaluminate. The first heat peak occurs within 10-15 minutes and the second occurs within 12-36 hours depending on the

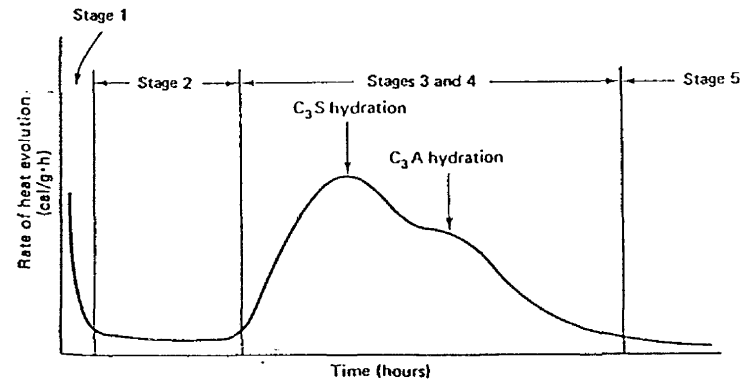

Figure 2-2. Rate of Heat Evolution During the Hydration of Portland Cement. (Mindness and Young, 1981)

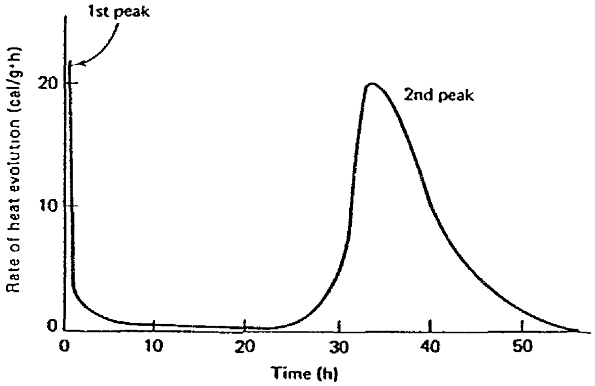

Figure 2-3. Rate of Heat Evolution During the Hydration of Tricalcium Aluminate with Gypsum. (Mindness and Young, 1981)

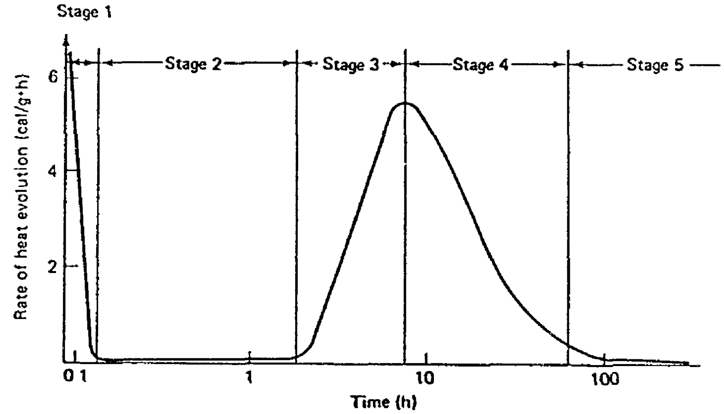

Figure 2-4. Rate of Heat Evolution during the Hydration of Tricalcium Silicate with Gypsum. (Mindness and Young, 1981)

amount of gypsum available. More gypsum prolongs the occurrence of a second heat peak and allows ettringite to remain stable.

$$\underset{\substack{\text{tricalcium}\\ \text{aluminate}}}{2C_3A} + \underset{\text{ettringite}}{C_6A\bar{S}_3H_{32}} + \underset{\text{water}}{4H} \text{------>} \underset{\substack{\text{tetracalcium aluminate}\\ \text{mono-sulfate-12-hydrate}\\ \text{"monosulfoaluminate"}}}{3C_4A\bar{S}H_{12}} \tag{11}$$

The formation of monosulfoaluminate in reaction (11) occurs because of an apparent deficiency of sulfate ions. If a new source of sulfate appears, ettringite can be formed again according to reaction (12).

$$\underset{\text{monosulfoaluminate}}{C_4A\bar{S}H_{12}} + \underset{\substack{\text{new sulfur}\\ \text{source}}}{2C\bar{S}H_2} + \underset{\text{water}}{16H} \text{---->} \underset{\text{ettringite}}{C_6A\bar{S}_3H_{32}} \tag{12}$$

The reaction of sulfate with calcium hydroxide and the formation of ettringite after initial stages of cement hydration are the cause of cement deterioration due to excessive exposure to sulfates. The volume expansion of the paste accompanying these reactions creates internal stresses that ultimately lead to cracking.

To a lesser extent, the absence of sulfate may also lead to the formation of hydrogarnet according to reactions (13) and (14).

$$\underset{\substack{\text{tricalcium}\\ \text{aluminate}}}{C_3A} + \underset{\text{water}}{21\ H} \text{----->} \underbrace{C_4AH_{13} + C_2AH_8}_{\text{calcium aluminate hydrates}} \tag{13}$$

$$\underbrace{C_4AH_{13} + C_2AH_8}_{\text{calcium aluminate hydrates}} \text{----->} \underset{\text{hydrogarnet}}{2C_3AH_6} + 9H \tag{14}$$

The heat curve consisting of two peaks also describes the exothermic reactions of the calcium silicates as shown in Figure 2-4. As indicated in reactions (15) and (16), the reactions of the two calcium silicates are very similar, differing only in the amount of calcium hydroxide formed. The principal product, calcium silicate hydrate (C-S-H), has an approximate formula because its composition may vary. C_2S hydrates in a similar manner to C_3S but is much slower with less heat of evolution. A discussion of C_3S follows.

$$\underset{\substack{\text{tricalcium}\\ \text{silicate}}}{2C_3S} + \underset{\text{water}}{6H} \text{------>} \underset{\text{C-S-H}}{C_3S_2H_3} + \underset{\substack{\text{calcium}\\ \text{hydroxide}}}{3CH} \tag{15}$$

$$\underset{\substack{\text{dicalcium}\\ \text{silicate}}}{2C_2S} + \underset{\text{water}}{4H} \text{------>} \underset{\text{C-S-H}}{C_3S_2H_3} + \underset{\substack{\text{calcium}\\ \text{hydroxide}}}{CH} \tag{16}$$

During stage I, the initial hydrolysis of C_3S yields a rapid heat of evolution with the dissolution of various ions such as calcium and hydroxyl ion into the surrounding pore water. At the end of stage I, an insulating rind of C-S-H about 10 nm thick surrounds the C_3S particle. In stage II, a dormant period of relative inactivity occurs because of the diffusive control of calcium hydroxide through the C-S-H rind. Relative inactivity also occurs because concentrations of calcium hydroxide in the pore water have not reached limits necessary for the initial formation of crystal nuclei.

During stage III, C-S-H continues to develop from the particle surface growing outward to form a coating around the grain. The spinal morphology on the surface is various: pointed, blunt, flat, long, and thin. The presence of admixtures and impurities influences the morphology. The principal growth of C-S-H occurs in the underlying layer that surrounds the cement grain. When C-S-H surfaces expand and contact other C-S-H surfaces, the spines intermesh and a solid bond continues to develop as hydration proceeds.

At the same time, calcium hydroxide crystallizes from solution. Calcium hydroxide is a highly crystalline material with dimensions on the order of 0.01 to 0.1 mm. It occupies approximately 20-25% of the volume of a fully developed paste. Calcium hydroxide crystals grow toward free spaces within the capillary pore space. They stop growing at points of contact with other crystals or cement grains. They may grow around and occlude cement grains. Calcium hydroxide morphology depends on admixtures, impurities, and temperature of hydration. Increasing the thickness of the C-S-H layer presents an increasing barrier for ionic diffusion necessary for calcium hydroxide growth, so hydration approaches completion asymptotically as indicated by the heat of evolution for stages 4 and 5 in Figure 2-2.

The development of C-S-H and calcium hydroxide is shown schematically in Figure 2-5. The initial unreacted cement grains and water are shown in Figure 2-5a. The growth of C-S-H around cement particles is indicated in Figure 2-5b. The pore space is occupied by calcium hydroxide and water. In Figure 2-5c, the C-S-H occupies more and more volume as about 50-60% of a well-developed paste is C-S-H by volume. The remaining pore space is occupied mostly by calcium hydroxide with a small amount of pore water indicated.

C_4AF reacts slower with less heat of evolution. Gypsum retards these reactions more than C_3A. An increase of iron content slows the rate of hydration. As seen in reactions (17) and (18), the presence of gypsum affects the end products.

$$C_4AF + 3C\bar{S}H_2 + 21H \text{ ----> } C_6(A,F)\bar{S}_3H_{32} + (A,F)H_3 \qquad (17)$$

$$C_4AF + C_6(A,F)\bar{S}_3H_{32} + 7H \text{ ----> } 3C_4(A,F)\bar{S}H_{12} + (A,F)H_3 \qquad (18)$$

The term (A,F) indicates that iron oxide and alumina occur interchangeably in the compound.

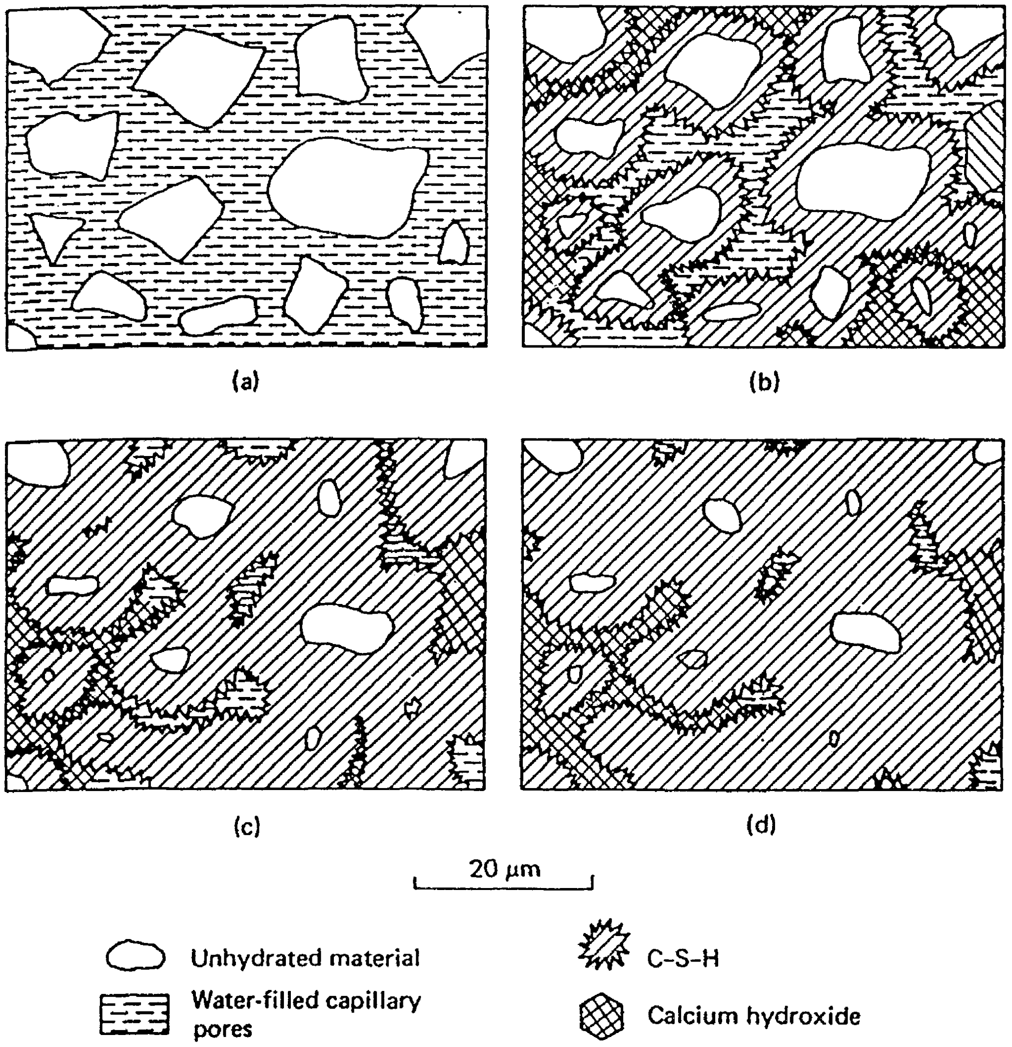

Figure 2-5. Schematic Outline of Microstructural Development of Portland Cement Paste. (Calcium Sulfoaluminates are included as part of C-S-H although they crystalize as separate phases.) (a) Initial (b) 7 days (c) 28 days (d) 90 days (Mindness and Young, 1981)

As cement paste hydration continues, the composition and pore structure continually changes. In a fully hydrated paste, 50-60% of the volume is occupied by C-S-H. The voids within the C-S-H structure are about 0.5 to 2.5 nm in diameter and account for about 25-30% of the C-S-H porosity. These voids have little effect on strength and permeability but appear to be important for drying shrinkage and creep.

Capillary voids are larger spaces not filled by solid components. In well-hydrated, low water/cement ratio mixes, voids range from 10 - 50 nm. In higher water/cement mixes, these voids may be 3000 - 5000 nm. Figures 2-6 and 2-7 illustrate how hydration time and water/cement ratio affect the amount of capillary space. Capillary voids larger than 50 nm are thought to be detrimental to strength and porosity.

2.7 Stabilization of Arsenic

In U.S. Patent 4,118,243 Sandesara (1978) stated that mixing a source of iron(II) with $Ca(OH)_2$ and sulfuric acid with an aqueous arsenic product led to a set-up matrix containing the arsenic. Arsenate ion is reduced to arsenite by the ferrous ion, and the precipitated arsenic is in the form of insoluble ferric arsenite after iron air oxidation.

In U.S. Patent 4,142,912 Young (1979) stated that combining arsenic wastes with water, portland cement, sand and "one or more water-soluble manganese and alkaline earth metal compounds" produced a solid that was "completely impervious" to arsenic leaching after a curing time of about 2 days. Leaching studies were done with a simulated oil well brine, providing a less stringent test than the TCLP procedure. Effective mole ratios of transition metals to arsenic were in the 2 to 12 range.

In a 2-year dynamic leaching study of cement-based solidified wastes using distilled water, Cote (1987) observed that arsenite anion was much more leachable than cadmium, chromium, or lead cations. Leachate pH varied from 11.5 to 9.0 during the study on several different matrices. With about 3000 mg/L As in the stabilized waste form, from 4.0% to 15% of the As was leached from the stabilized form over a 2-year period. Leaching percents for cadmium, chromium and lead ranged from 0.03% to 0.9% in the study. Arsenic was found to be present as $Ca(AsO_2)_2 \cdot Ca(OH)_2$ which had a leaching rate linear with time. The mechanism of leaching was inferred to be limited by the amount of CO_2 available. $CO_2(aq)$ reacts with basic calcium arsenite to form the more soluble calcium arsenite, $Ca(AsO_2)_2$. The water used in the leaching experiments was saturated with air. A mass balance of the dissolved $CO_2(aq)$ with the total As liberated was successful.

Sakata (1987) noted a high correlation between the adsorption of arsenic(III) on soil and the dithionite-extractable iron content. This correlation implies that arsenic(III) adsorption is

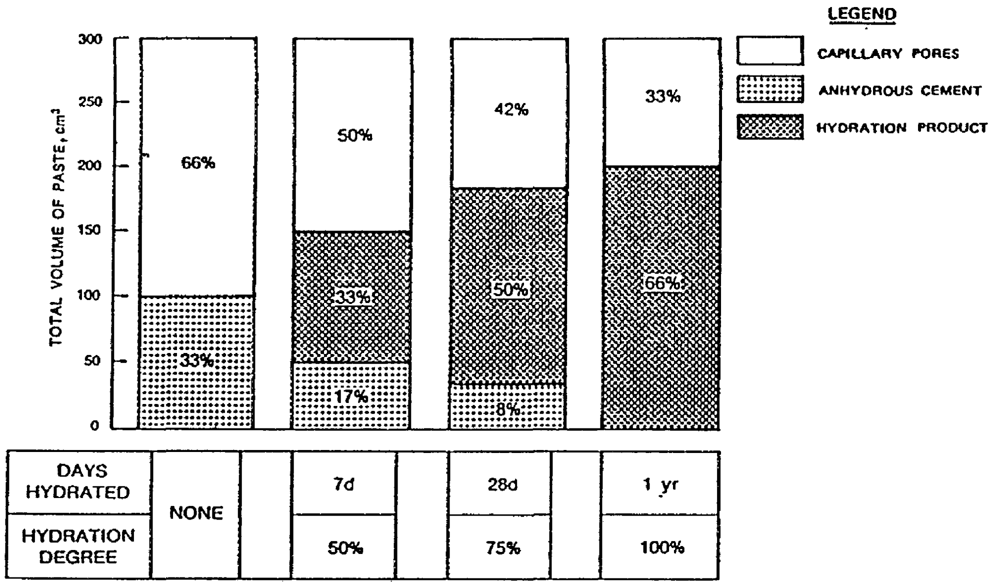

Figure 2-6. Changes in Capillary Pore Sapce with the Degree of Hydration for a Cement Paste with Water/Cement = 0.66 (Mehta, 1987)

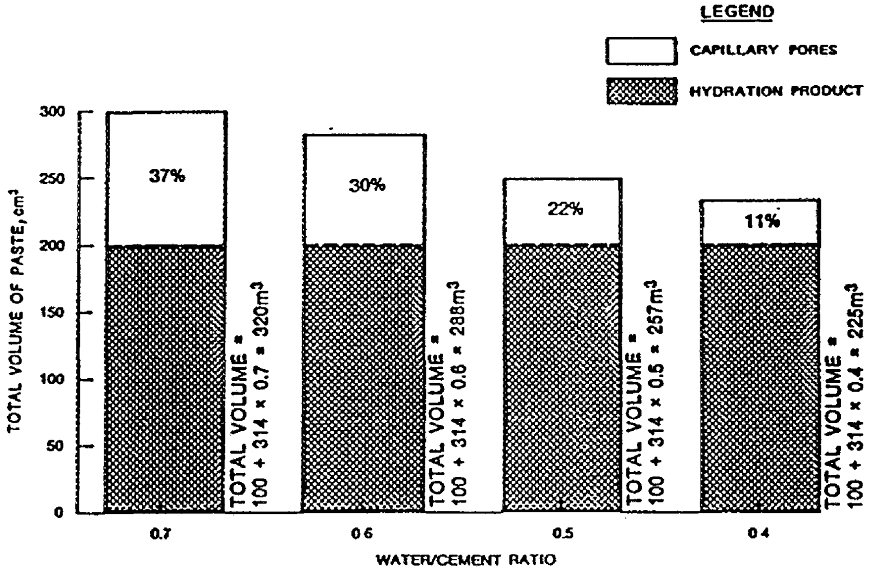

Figure 2-7. Changes in Capillary Pore Space for a Fully Hydrated Cement Paste with Variable Water/Cement Ratios, Based on Equal Amounts of Portland Cement. (Mehta, 1987)

controlled mainly by levels of amorphous iron oxides and hydroxides.

In a model study of soils contaminated with 12,200 mg/L of sodium arsenite, Akhter, et. al., (1990) found that cement or pozzolanic fixing agents were largely ineffective in immobilizing the arsenite. The study concluded that arsenic was probably immobilized in a cement-based binding system primarily through encapsulation. The soil matrix was a Mississippi Loess with a 2% organic content. Additions of type-F fly ash, blast furnace slag, and lime worsened or did not improve stabilization of arsenite. Silica fume provided only a marginal improvement in stabilization. The only formulation which was able to meet the 5 mg/L As TCLP standard was 44 parts cement in 100 parts contaminated soil.

Artiola et. al., (1990) treated arsenic-contaminated soils with iron oxides, ferrous sulfate, ferric sulfate, gypsum, and ferrous carbonate. Ferric and ferrous sulfate provided over 95% stabilization of the arsenic according to the EP toxicity test. All other treatments provided little or no treatment.

In a study of leaching models, Batchelor (1990) developed values for a leachability index for various contaminants. Increases in this parameter measure the degree of chemical or physical immobilization of a contaminant in a stabilization matrix. The leachability index for arsenic was determined to be 11.9. Nitrate anion has a value of 10.7 and nonreactive sodium ion has a value of 8.3.

A series of studies by Ortego (1990) has provided a better understanding of the chemical environment of cationic metals in a portland-cement matrix. The presence of barium or other sulfate-insoluble ions reduces the effectiveness of gypsum ($CaSO_4$) added as a "flash-set" inhibitor. Many metal ions enhance the formation of carbonate in the hardened cement. This series of studies used the TCLP procedure and a modification in which the pH of the leachant was kept near 5.0 Dramatic differences in metal ion extractabilities were found (Table 2-7). Additional work is being done in an attempt to understand these results. In the TCLP procedure the sample was treated with 0.040 M acetic acid in a 50:1 solvent-to-solid ratio. The pH 5.0 buffer was constructed from acetic acid and sodium acetate. Metal ions could be

Table 2-7. Weight Percent Metal Extracted (Ortego, 1990)

Metal	TCLP	Final pH	pH 5.0 buffer
Cd	6.20 %	7.7	16.84 %
Cr	0.12 %	9.5	62.99 %
Cu	4.36 %	9.9	92.43 %
Pb	0.004%	11.0	69.35 %
Ni	0.21 %	9.9	48.16 %
Zn	3.16 %	10.5	48.44 %

effectively prevented from leaching by coupling the portland cement treatment with the addition of an anion which forms a precipitate insoluble in dilute acetic acid (e.g. cadmium sulfide, lead phosphate).

Chu et al, 1991, conducted a study comparing fixation techniques for soil containing inorganic arsenic at concentrations ranging from 1200-2100 mg/kg. The TCLP of untreated soil yielded 22 mg/L arsenic. At least one of three tests: Extraction Procedure Toxicity, TCLP, or California Waste Extraction Test were performed on three types of treated samples. The first treatment used ferric chloride and aluminum sulfate with calcium carbonate for neutralization. The pH was important for the effectiveness of this treatment. The second treatment involved S/S with fly ash and Portland cement. The third treatment used calcium aluminate silicates with a proprietary cementitious mixture. The latter treatment appeared to be most effective, but conclusions are difficult when binder/waste ratios are not reported and some mix designs are proprietary.

U.S. EPA, 1992, contains several articles on the supply and demand, chemistry, industrial use, stabilization, and recovery of arsenic compounds. Cartledge (1992) and Connor (1990) present a summary of arsenic stabilization. Both arsenate and arsenite were stabilized using a binder/arsenic weight ratio of ten percent. Cartledge has observed that the percent hydration of the cement silicate phase is significantly retarded by arsenate and more so by arsenite. After one year of curing, both salts greatly retarded silicate polymerization. Also, a new crystalline material, $NaCaAsO_4 \cdot 7.5H_2O$ was found depending on the amounts of sodium and calcium available. In normal fly ash-Portland cement development, Cartledge also observed that the aluminate phase converts from tetrahedral to octahedral forms for up to 28 days. After 28 days, the conversion slowly reverts itself. Arsenic compounds appeared to catalyze the reversion process and current research is investigating the long-term effects on arsenic S/S. Table 2-8 presents a summary of data reported by Cartledge showing the degradation of some stabilization maxtures over curing times up to one year.

In a study of the bioavailability of arsenic and lead from soils, Davis (1992) found that the kinetics of dissolution or extraction of metals from soils in simulated pH 1.3 gastric acids could be quite slow. While enough pure sodium arsenite dissolved under the experimental conditions in about one hour to reach a concentration of 100 mg/L As, with soil present the concentration of As took 4 hours to reach 12 mg/L, and did not achieve higher concentrations after 30 hours. The arsenic species in the soil were identified to be enargite (85%) (Cu_3AsS_4) with impure arsenopyrite (FeAsS) and tennentite ($Cu_{10}(Cu\text{-}Fe)_2As_4S_{13}$). The total arsenic content of the soil was 1400 mg/L. These mineral species are quite insoluble in aqueous media, with only limited solubility in dilute acids. Further studies with rabbits indicated that As(III) in soils is less labile than As(V) compounds, as determined from fecal concentrations. The study

Table 2-8. TCLP Leachate Concentration from S/S Waste with 1 Year or (28 days) of Curing[1]

	Leachate Concentration (mg/L)				
Binder[2]	As(III)[3]	As(V)	Pb(II)	Cr(III)	Cr(VI)
OPC	1.7(2.1)	1.4(1.7)	35(48)	0.4(0.4)	2500(1400)
OPC,no gyp.	3.1(2.7)		43(2.2)		3200(2400)
1/1OPC,FFA	430(540)	94(7.9)	0.9(0.3)	0.7(0.2)	2900(1600)
20/1OPC,SiO2	2.3(2.4)		25(24)		2500(1600)
20/1OPC with Na_2SiO_3	2.0(3.5)	0.4(0.1)	28(1.8)	0.5(0.2)	2500(1800)
10/1OPC with Betonite	2.4(30)		46(1.4)		2400(1700)
10/1OPC with Organoclay	1.1(3.0)		40(16)		2800(2400)
20/1 TypeIA SiO_2	2.5(3.1)	0.4(0.1)	41(5.2)	0.2(0.2)	2800(1900)
White	0.9(1.7)	10(3.6)	54(1.0)	0.4(0.2)	2900(2000)
20/1 White Na_2SiO_3	1.0(2.5)	15(8.0)	38(6.0)	0.8(0.2)	2800(2000)
Luminite	240(140)		4(400)		3700(2300)
Refcon	190(150)		190(680)		3600(1900)
Pyrament	47	4.4	1.7	1.4	2800

1. After Cartledge (1992).
2. OPC = Type I portland cement; FA = fly ash; SiO_2 silica fume; Na_2SiO_3 = Type N soluble sodium silicate; White = portland cement with low iron content; Luminite and Refcon are specialty cements that are for refractory applications and high in alumina content. The water to binder weight ratio is 0.5 and the metal to binder ratio is 0.1.
3. The salts are $Pb(NO_3)_2$, $NaAsO_2$, $Na_2HAsO_4 \cdot 7H_2O$, $Cr(NO_3)_3 \cdot 9H_2O$, and $Na_2CrO_4 \cdot 4H_2O$.

concluded that the use of soluble arsenic compounds to model the bioavailability of soil arsenic seriously overestimates the amount of arsenic liberated.

Cheng and Bishop (1992a) used synthetic metal sludge generated from 0.01 molar solutions of cadmium nitrate, lead nitrate, and sodium arsenite with the pH adjusted to 8.5 using 6.0 molar sodium hydroxide. These metal sludges served as the only water source for the hydration of type I portland cement with water/cement mixtures of 0.4, 0.6, and 0.75. Curing was performed in spherical molds for at least 78 days at 100% humidity. Static leaching tests with periodic leachant renewal was performed with various acetic acid solutions. After leaching, the surface layer of the leached samples was removed from the unleached sphere, "kernel", with a knife. SEM/X-ray and wet digestion/AA analyses of the leached surface layer and kernel were performed. The AA analyses indicated that heavy metals were released only in the surface layer and not the kernel. SEM/X-ray indicated a sharp change in heavy metal content and calcium at the leaching boundary. Calcium appeared to leach most easily while silicon, iron, and aluminum appeared to remain in the leached layer. The authors suggest that the leached layer may create a resistant barrier to slow down the acid attack on the waste form.

Cheng and Bishop (1992b) used a modified Generalized Acid Neutralizing Capacity Test (Isenburg and Moore, 1992) which is similar to the Acid Neutralization Capacity test (Environmental Canada and Alberta Environmental Center, 1986) with acetic acid leachant instead of nitric acid. The test is a single-batch leaching procedure that utilizes a series of dried crushed samples extracted in parallel with increasing acidic leachant. Metal concentrations in leachates permit development of a relationship between leached metal concentrations and pH. Approximately 100% of Ca, 90% of Cd, 70% of Pb, and 60% of As were desorbed in acetic acid solutions of pH = 5. Dissolved metal concentrations decreased with increasing pH. If the pH of the pore water in the cement-based form remained above 9, the desorption process of most heavy metals did not occur to any large extent. The amphoteric nature of certain metals was not evident. The authors suggest that these metals were adsorbed on solid surfaces since these surfaces are negatively charged under alkaline conditions. They assert that the silicon-rich leached layer has lost most of its calcium hydroxide and adsorbs like an amorphous silica gel. This leached layer provides some adsorption capacity and provides a barrier to diffusing metals leaching out and acid leaching in. As evidence of this fact, they provide a comparison of adsorption profiles as a function of pH for the leached layer and silicon material.

2.8 Treatment of Arsenic in Waters

A limited literature review is presented that includes arsenic treatment in waters and solids. An exhaustive review is beyond the scope of this report. The chemistry and treatment processes may be pertinent to the stabilization of arsenic nonwastewaters.

Gulledge and O'Connor (1973) simulated coagulation, flocculation, sedimentation, and filtration for arsenic removal by alum and ferric sulfate. Ferric sulfate was more effective with 90-100% removal at doses of 10 mg/L to 50 mg/L over the tested pH range of 5-8. Alum was less effective and could only compare to that of ferric sulfate at a lower pH of 5 or 6 with a higher concentration of 30-50 mg/L.

Gupta, et. al., (1978) studied arsenic adsorption on activated alumina, activated carbon, and activated bauxite. Adsorption was carried out in fresh water, diluted seawater,

seawater, and sodium chloride. Activated alumina adsorbed more and was faster than other adsorbents. The rate of arsenic(V) adsorption was greater than that for arsenic(III). A ranking of adsorption capacity was: alumina first, bauxite a close second, and activated carbon a distant third. Arsenic(V) adsorption by activated alumina or bauxite decreases above pH = 7. Activated carbon adsorbs arsenic(V) better in the 3-5 pH range. Increasing the ionic strength by using seawater decreased the adsorption of arsenic significantly.

Bhattacharyya, et. al., (1980) observed that metal sulfide precipitation is attractive over a broad pH range because of the high reactivity of sulfides (S^{2-}, HS^- , H_2S) with heavy metal ions and the low solubilities of heavy metal sulfides. Using Na_2S and NaHS with heavy metal and arsenic wastes, the extent of metal sulfide precipitation is a function of pH, type of metal, sulfide dosage, and interfering ions. At a pH of 8, heavy metals were 98-99.6% removed with a dosage of 0.6 mole sulfide to mole metal. Arsenic removal was not effective unless ferric iron was added at a Fe/As mole ratio of 2.

Schlicher and Ghosh (1985) investigated ion exchange, activated carbon, activated alumina, and air flotation with the goal of less expensive arsenic removal with less sludge production. For ion exchange, they used a strong base anionic resin but the resin reached exhaustion quickly with 100% arsenates removal and only 50% arsenite removal. They estimated a selectivity sequence of common ions by strong base anionic resin by the similarity between arsenic and phosphate chemistry. Therefore:

known sequence: $SO_4^{2-} > HPO_4^{2-} > NO_3^- > Cl^- > HCO_3^- > H_2PO_4^-$

estimated: $SO_4^{2-} > HAsO_4^{2-} > NO_3^- > Cl^- > HCO_3^- > H_2AsO_4^-$

Adsorbing colloid flotation for metal removal has been widely studied. The process consists of adding a flocc-forming substance such as ferric chloride or alum to collect metals by adsorption or coprecipitation on metal hydroxides formed by addition of a base. The floccs are removed by flotation using a surfactant, e.g. sodium lauryl sulfate (NLS). Arsenates are highly removed but arsenites are not. The optimum pH for arsenate removal was 5-6 with alum as the coagulant. The rate of adsorption on activated alumina was faster than that for activated carbon. Also, the adsorption capacity of activated alumina was greater than that for activated carbon.

Egawa, et. al., (1985) manufactured a macroreticular chelating resin containing mercapto groups. Three resins were used in batch and column experiments to determine the adsorption rate and capacity of three different resins. One of the resins appeared to be successful in removing As(III) in columns and batches. They also showed that the resin was selective for As in the presence of other ions such as Ca and Na.

Ghosh and Teoh (1985) studied adsorption kinetics and capacity for arsenites and arsenates on activated alumina. The rate of arsenate adsorption varied significantly with pH. The rate of arsenite adsorption increased slightly with increasing pH. Arsenate adsorption was described by the Langmuir isotherm. Fixed bed column studies showed the effect of mass loading and empty bed contact time on the breakthrough curve. Competitive adsorption by bicarbonate, sulfate, and silicate yielded an earlier breakthrough of arsenic species.

Sen and De (1987) used coal fly ash and powdered activated carbon in batch adsorption studies of As(III) and As(V). Adsorption rates and capacities were studied. Fly ash was adsorbed at a slower rate than activated carbon but in the end it was comparable in capacity. The optimal adsorption pH for both activated carbon and fly ash was about 3-4. The solutions were 0.9 mg/L in As(III) and As(V). The fly ash dose was varied from 0.35 g to 1.4 g, the adsorption of arsenic increased up to about 1.0 g/50 mL and became constant after that. Various diverse ions showed no effect on the adsorption of arsenic on fly ash. Data was fit to the Freundlich isotherm.

Wagemann (1978) investigated four metals: Ba, Cr, Fe, and Ca as controlling factors on solubility of metal arsenates in freshwater systems. Barium at typical concentrations in freshwaters was found to be most likely to limit the solubility of arsenate. He developed an Eh-pH diagram which summarizes a theoretical As speciation in freshwater environments.

Harper and Kingham (1992) were concerned with the treatment of contaminated water generated from cleanup activities at a former pesticide facility. Initial laboratory treatment studies included chemical precipitation using either alum, Na_2S, or $FeCl_3$ as a coagulant with pH adjustment by hydrated lime. The initial arsenic concentration was 9.8 mg/L and coagulant doses were 500 to 1000 mg/L. $FeCl_3$ with hydrated lime was the most successful coagulant with 98-99% removal. In another sample having 31 mg/L As, dosages of $FeCl_3$ ranging from 200 mg/L - 1000 mg/L resulted in As removals of 86-93%. Multiple doses of coagulants in series did not improve results significantly. Filtration of the treated wastewater did not yield significant improvements.

Brewster (1992) describes a process for arsenic removal from wastewaters. The wastewater passes through an electrochemical cell where ferrous ions and hydroxyl ions are generated at the anode and cathode, respectively. Hydrogen peroxide is added to the wastewater in an ensuing reactor tank where the ferrous hydroxide is oxidized to its ferric form. Hydrogen peroxide also oxidizes any arsenite to arsenate. The pH is maintained at 6.5 for optimum ferric arsenate precipitation and maximum adsorption. Small amounts of polymers are added between the reactor tank and clarifier to improve settling characteristics.

If arsenic is the only contaminant of concern and proper pH levels are maintained, a 5:1 iron to arsenic ratio can reduce residual arsenic to near or below analytical detection limits. If other metals are to be removed and different pH levels are necessary, then higher amounts of iron are required.

Process advantages are: low dissolved solids since the added ferrous and hydroxyl ions are removed by precipitation; the sludge is stable since arsenic concentrations in TCLP extracts are less than standards; low residual As concentrations; low sludge production rate; and low operating cost.

Brewster (1992) explains the process chemistry with reference to common arsenic removal mechanisms: the addition of the counter ion to form an insoluble precipitate; surface complexation; and electrostatic attractions. Ferric ion is effective to remove arsenate by forming ferric arsenate precipitate with a residual of 7.5 mg/L of dissolved arsenic. Ferric ion is not effective for arsenite precipitation, hence the need for hydrogen peroxide.

Surface complexation is also important for arsenic removal. The addition of ferric iron results in the formation of hydrous ferric oxide [FeO(OH)] with ferric arsenate. If undissociated arsenic acid donates a proton to the hydroxyl group of the hydrous ferric oxide to form water, surface complexation may occur with the arsenate ion taking the place of the hydroxyl group. Surface complexation is more favorable at low pH because of the greater potential for proton donation by arsenic acid. As the pH is increased, the potential for proton donation decreases and surface complexation is less important. Therefore, at higher pH values, the iron to arsenic ratio must be increased for effective arsenic removal. After surface complexation, electrostatic attractions may occur between complexes.

Arsenate removal is approximately 50% greater than arsenite for two reasons: ferric arsenate is less soluble than ferric arsenite and arsenous acid does not readily lose its protons. Other anions such as sulfates, chlorides, and nitrates can hinder treatment by directly occupying adsorption sites or orienting around positively charged sites.

CHAPTER THREE
METHODS AND MATERIALS

3.1 Sample Collection and Composition of Wastes, Binders, and Reagents

Approximately 70 pounds of D004/D005 waste were collected at one time from Peoria Disposal Company. This amount was sufficient for the project duration. A chemical analysis is provided in Table 3-1.

Table 3-1. Chemical Composition of D004/D005[1] Waste

Metal	Average Concentration[2] (grams /kilogram of waste)	TCLP Concentration (mg/L)
Aluminum	8.0	.03
Antimony	0.3	7.7
Arsenic	6.0	280
Barium	133.	3350
Boron	29.4	5560
Cadmium	0.003	0.015
Calcium	2.3	16.
Chromium	0.009	0.015
Copper	0.03	0.093
Iron	2.7	0.6
Lead	0.10	0.13
Magnesium	0.65	1.2
Manganese	0.17	0.021
Nickel	0.012	0.057
Phosphorus	<0.05	0.21
Potassium	2.0	94.
Sodium	2.1	81.
Sulfur	0.37	0.29
Zinc	0.95	0.57

1. Density = 0.116 g/cc; moisture content = 9.0%
2. Average concentration based on three samples; nitric acid digestion followed by chemical analysis with an inductively coupled plasma emission spectrometer (USEPA, 1986, Method 6010).

Arsenic valence speciation was carried out using the Dionex Ion Chromatograph at the Hazardous Materials Laboratory of HWRIC. An anion column was used with 120 mM NaOH eluant. Arsenic(III) was detected using a pulsed amperometric detector and was quantitated as AsO_2^-. Arsenic(V) was detected with a conductivity detector and was quantitated as AsO_4^{3-}. TCLP extracts were diluted 1:15 to match the dynamic range of the ion chromatograph detector system as well as to prevent column flooding.

The arsenic in distilled-water extracts of D004/D005 waste extracted under a N_2 blanket was up to 15% arsenic(III). If a TCLP extraction with acetic acid was performed, with or without a N_2 blanket, less than 5% of the arsenic was present as As(III).

Arsenic(III) is easily oxidized in diute aqueous solution to form arsenic(V). Fifty mg/L aqueous laboratory standards were approximately half oxidized in two to three days.

X-ray diffraction is nearly the only tool suitable for determining the compound composition of an inorganic material. Other inorganic analysis techniques identify elemental or ionic compositions, but do not enable the identification of compounds as such. In order for x-ray diffraction to be useful, the sample must be crystalline in nature, with particle sizes over the micrometer range. Highly mechanically-distorted components, glasses, and amorphous materials do not produce analytically useful diffraction patterns.

An x-ray diffraction powder pattern was obtained on a sample of the D004/D005 waste using a Phillips Automated Diffractometer. The diffraction pattern obtained is shown in Figure 3-1. Manual analysis of the major peaks of the diffraction pattern indicated high confidence matches for $Ba(OH)_2$ and BPO_4 (ASTM patterns 1-0630 and 11-237) (ASTM, 1965), in addition to several polymorphs of silica, SiO2. By no means have all the major line intensities been accounted for, but no other matches which agree with Table 3-1 have been identified. A second, insoluble compound of barium was not identified in the x-ray diffraction pattern to account for the half of the Ba that is not extractable from the raw waste by TCLP. X-ray diffraction only characterizes crystalline components, while glasses and other phases of low crystallinity do not produce strong diffraction lines.

Sufficient amounts of binders were stocked and homogenized before beginning this project. Two bags of Type I Portland Cement, manufactured by Continental Cement Company were used. Class C fly ash from Davenport Cement Company was used. Table 3-2 provides information on the binder chemical compositions provided by the suppliers. Table 3-3 presents an ICAP analysis of nitric acid digestates.

3.2 Stabilization Procedures

Mixing was performed in a kitchen mixer with an acid-rinsed stainless steel bowl and stainless steel wire impeller. All the dry materials including pozzolan, cement, and hazardous waste were mixed thoroughly before water was added. Various additives such as ferrous sulfate, ferric sulfate, sodium sulfate, or iron acetate were dissolved in the water prior to mixing with the binders (see Chapter 4). The purpose of this mixing procedure is to ensure a consistent application of water and additive to dry materials from one mix to another. Four hundred to nine hundred grams were mixed at one time for at least one minute. Consistent results were obtained with mix durations of at least one minute (Bayasi, 1992). The sample was partitioned into approximately 110-gram samples and cured. Since at least 100 grams are required for the TCLP, the additional 10 grams allows for moisture loss during curing. If more weight was lost, then like samples were

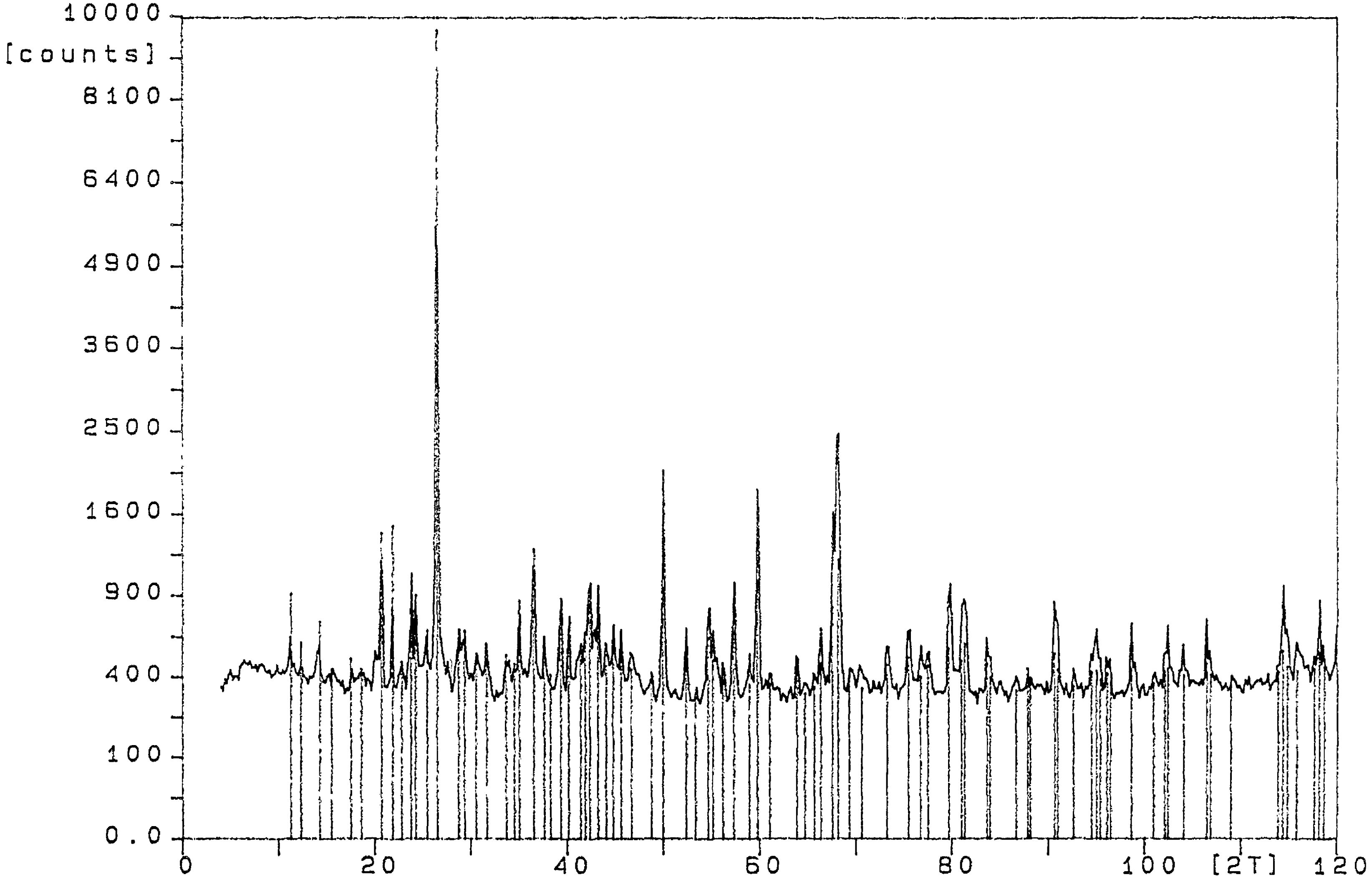

Figure 3-1. X-Ray Diffraction Pattern of D004/D005 Waste

Table 3-2. Manufacturers' Composition of Binders
Fraction of Total Mass (%)

Compound	Portland Cement[1]	Class C Fly Ash[2]
SiO_2	20.80	33.55
Al_2O_3	4.10	18.95
Fe_2O_3	2.78	6.35
SO_3	2.60	1.87
CaO	63.90	27.25
MgO	4.50	3.88
Na_2O		1.73
K_2O		0.35
C		0.20

1. Loss in ignition 1.80%. Insoluble residue 0.15%.
2. Particles greater than No. 325 sieve (45 microns = 0.018 in.) = 18%. Specific gravity = 2.72.

Table 3-3. Chemical Composition of Binders

Metal	Cement[1] Total (mg/kg binder)	Cement TCLP (mg/L)	Fly Ash[1] Total (mg/kg binder)	Fly Ash TCLP (mg/L)
Arsenic	1.	0.13	24.	0.14
Barium	170	0.30	5742	0.32
Cadmium	3.4	0.02	8.3	0.02
Chromium	170	1.2	57.	0.26
Lead	8.5	0.13	19.	0.14
Nickel	40.	0.05	53.	0.05
Calcium	381,000	3120	180,000	1490
Iron	14,600	0.10	34,100	0.10
Copper	24.	0.021	140	0.14
Potassium	2820	53	1560	1.7
Magnesium	22,700	0.16	30,300	52.
Manganese	910	0.015	202	0.02
Sodium	815	8.4	9560	36.
Sulfur	10,200	204	11,300	160
Zinc	207	0.33	237	0.21

1. Nitric acid digestion followed by chemical analysis with an inductively coupled plasma emission spectrometer. (USEPA, 1986, Method 6010).

combined to satisfy the 100-grams requirement.

Stabilization (S/S) forms were cured with air. Air curing of small samples in acid-rinsed plastic cups took place within the protection of a lab cabinet which reduced any air-borne dust deposition on the sample. Air curing provides samples that are similar to surface samples taken from a stockpile of treated waste awaiting treatment verification before landfilling. Cure times of 2 days were selected to model common industrial practice. Longer cure times were studied to assess S/S durability.

3.3 Leaching Procedures

3.3.1 TCLP

The TCLP (USEPA, 1986, Method 1311) is recognized by the U.S. EPA as the standard method for measuring treatment effectiveness of S/S. The TCLP is a batch procedure with a leaching duration of 18 hours ± 2 hours. Information pertaining to the time and sequence of metals leached cannnot be obtained by the TCLP so a dynamic leaching procedure was also used. Equipment and procedures for both leaching tests are described below.

Standard equipment for TCLP testing were used (Code of Federal Regulations, 1987). These include: a) Model DC-18 rotary agitator from Analytical Testing and Consulting Services, Inc.; b) type 316, stainless steel, 142 mm (5.6 in) filter holder from Fisher Scientific; c) borosilicate glass fiber filters (GF/F Whatman Grade) with a 0.7 micrometer effective pore size; d) high-density polyethylene bottles for agitation and for sample storage which were obtained from Crown Glass Corporation; and e) pH meter with a relative accuracy and repeatability of 0.01 pH.

Standard TCLP procedures were used. Pertinent to the inorganic hazardous waste used in this research, a brief, nontechnical summary of the TCLP procedure follows (Code of Federal Regulations, 1987): One hundred grams of stabilized waste were ground with mortar and pestle to pass a 9.5 mm standard sieve. The waste was put into a 2000-cc bottle containing 2.000 kg of an extraction fluid consisting of diluted glacial acetic acid. Although the bottle size is designated as 2000-cc, sufficient headspace was available for fluid agitation. Extraction fluid type 2 (pH = 2.88 ± 0.05) was selected on the basis of EPA-specified test procedures. The mixture of S/S form and extraction fluid was agitated end-over-end for 18 ± 2 hours. The fluid was extracted from the solids by means of positive pressure filtration through a 0.7 micron borosilicate fiber filter. The pH and alkalinity of the extract were measured. Alkalinity was measured by the amount of 1.00N sulfuric acid necessary to decrease the pH to 4.5. Fluid samples were preserved by acidification to pH < 2 with nitric acid and stored at 4 degrees C prior to chemical analysis.

In addition to standard procedures, the following precautions were taken in order to achieve consistent high-quality data. First, nitrogen was the pressuring gas. Second, approximately 2000-cc of extract were obtained during the extraction which takes 5-20 minutes. In initial TCLP tests, the pH and possibly the chemical composition of the extraction fluid varied depending on whether the fluid passed the filter earlier or later during the extraction process. Therefore, the 2000-cc of extract were well-mixed to obtain a representative sample for preservation and chemical analysis. Third, new acid-rinsed bottles were used for agitation and for storage of the TCLP extract.

3.3.2 Column Leaching

For dynamic leaching, a vertical glass column 47 cm long and 1.6 cm in diameter, was used. Perpendicular tapered glass connections at the bottom and top allow the introduction and exit of extraction fluid. A 3.0 mL/min flow from bottom to top of the column was driven by a peristaltic pump using 0.8 mm (inner diameter) Norprene tubing. Openings at the top and bottom of the glass column allowed easy filling and removal of waste samples from the column. During the leaching process, the open ends were plugged with stoppers covered with Parafilm.

During the column leaching experiment, effluent samples were collected at time intervals given by the empty bed detention time which equals the column volume divided by the leachant flowrate. The effluents were first tested for pH and acid neutralization capacity followed by preservation with nitric acid to $pH < 2$. The analyses of samples collected over time allows the observation of relative leaching rates for various metals.

Three different leachants: DI water, 0.10 M glacial acetic acid (pH = 3.0), and 0.10 M sodium acetate (pH = 8.7) solutions were used to observe the effects of leachant pH on metal leaching rates. Fresh leachant was continuously fed to the column in each case.

3.4 Chemical Analyses

All extracts and solid digestates were analyzed with an inductively coupled argon plasma (ICAP) emission spectrophotometer, Model ICAP 61 made by Thermo Jarrel Ash Corporation. This is a simultaneous vacuum spectrophotometer with a 23-element configuration. A standard cross-flow nebulizer is used to atomize the extract or digestate into a plasma emission source. The intensity and wavelength of the photon emissions resulting from orbital transitions of excited electrons are determined. A number of orbital transitions are possible for a given element leading to a number of possible emission lines for the element. The excitation energy is provided by the high temperature of the inductively coupled plasma, a largely ionized gas in an oscillating magnetic field.

After the temperature of the plasma has equilibrated after startup, a mercury vapor lamp is used to precisely align the optics of the instrument. Instrument calibration follows by using three points plus a blank for each element. This calibration is confirmed by verification measurements that must be within ± 10% of their known concentration value for the initial calibration to be considered valid. These calibration and verification procedures are repeated after the analysis of every ten samples.

If an element could not be calibrated properly, that data were flagged and samples were rerun at a later date. Samples with questionably extreme values were typically rerun.

For each element, the calibration and verification standards, detection limits for TCLP and solid measurements, and analytical ranges are provided in Tables 3-4 and 3-5. The acid-preserved TCLP extracts were routinely diluted ten-fold to avoid emission interference by the high levels of calcium present in the extracts.

Table 3-4. Standards and Detection Limits for ICAP

Element	Calibration Standard (mg/L)	Calibration Verification (mg/L)	Instrumental Detection Limits[2] (mg/L)	Project Detection Limits[1] TCLP (mg/L)	Project Detection Limits[1] Solids (mg/kg)
Aluminum	10	1	0.02	0.20	1.0
Antimony	10	1	0.05	0.50	2.5
Arsenic	10	1	0.025	0.25	1.25
Barium	10	1	0.002	0.02	0.1
Beryllium	10	1	0.001	0.01	0.05
Boron	10	1	0.04	0.4	2.0
Cadmium	10	1	0.003	0.03	0.15
Calcium	100	10	0.01	0.10	0.5
Chromium	10	1	0.003	0.03	0.15
Cobalt	10	1	0.003	0.03	0.15
Copper	10	1	0.003	0.03	0.15
Iron	10	1	0.02	0.20	1.0
Lead	10	1	0.025	0.25	1.25
Magnesium	100	10	0.02	0.20	1.0
Manganese	10	1	0.003	0.03	0.15
Nickel	10	1	0.007	0.07	0.35
Phosphorus	10	1	0.06	0.60	3.0
Potassium	100	10	0.15	1.5	7.5
Selenium	10	1	0.04	0.40	2.0
Silver	10	1	0.005	0.05	0.25
Sodium	100	10	0.02	0.20	1.0
Sulfur	10	1	0.05	0.50	2.5
Vanadium	10	1	0.002	0.02	0.1
Zinc	10	1	0.005	0.05	0.25

1. Project detection limits for TCLP extracts and solids are respectively 10 and 50 times the instrumental detection limits.
2. Instrumental detection limits according to USEPA, 1990b.

3.5 Digestion Studies

TCLP extracts were not routinely digested because there is no significant difference observed in the chemical analyses of digested and undigested TCLP extracts. This conclusion has been verified by independent testing performed by PDC Laboratories,

Table 3-5. ICAP Analytical Range[1] for Elements

Element	Analytical Range (mg/L)
Aluminum	0.025-500
Antimony	0.05-1000
Arsenic	0.050-500
Barium	0.001-100
Beryllium	0.001-100
Boron	0.006-500
Cadmium	0.004-200
Calcium	0.01-1000
Chromium	0.005-500
Cobalt	0.003-300
Copper	0.002-200
Iron	0.005-500
Lead	0.025-1000
Magnesium	0.015-1000
Manganese	0.001-100
Nickel	0.01-500
Phosphorus	0.06-1000
Potassium	0.3-1500
Selenium	0.05-1000
Silver	0.003-300
Sodium	0.01-500
Sulfur	0.08-1000
Vanadium	0.002-200
Zinc	0.004-200

1. Supplied by manufacturer.

Inc. and by studies conducted during earlier research in this laboratory (Bayasi, 1992). Twelve TCLP extracts were selected from S/S with K061 waste; six from fly ash S/S and six from silica fume S/S. Within each set of six samples, three were from S/S with one-day curing and three were from samples that had cured 11 months before TCLP. These samples provide a wide range of concentration values ranging from detection level to 3100 mg/L.

Table 3-6 presents the results for six metals. Cadmium, chromium, lead, and nickel were selected for presentation because they are regulated metals for K061 waste used in the earlier project (Bayasi, 1992). Calcium was selected because it occurs in high concentrations since it is a significant component of cement and fly ash. Zinc was selected because its concentration values were most variable and are not highly correlated with the regulated metals.

An inspection of Table 3-6 shows that the correlation between chemical analyses of TCLP extracts with and without digestion is significantly high. This high degree of correlation is reasonable because the extracts have been filtered through a 0.7 micron filter and stored at a pH < 2. Furthermore, extracts were shaken just before injection to the ICAP to suspend any small particles that might have passed a 0.7 micron filter. With the high energy levels of ICAP, metals in these particles would be measured.

Table 3-6. Correlations Between Digestates and Extracts

Metal	Silica Fume Samples	Fly Ash Samples
Cadmium	1.00	1.00
Chromium	0.959	0.995
Lead	1.00	0.999
Nickel	0.841	0.903
Calcium	0.998	0.989
Zinc	1.00	0.999

3.6 Spike Recovery

Two sample digestates with relatively high concentrations of calcium, lead, nickel, chromium and cadmium were matrix spiked to show that instrumental interference effects are minimal for these samples. Five milliliters of these standard solutions: 2500 mg/L barium, 500 mg/L arsenic, 500 mg/L chromium, 500 mg/L lead, 100 mg/L cadmium, and 500 mg/L nickel were added to 50 milliliter samples. TCLP results of the digestates and the spiked samples are presented in Table 3-7 along with spike recoveries. All spike recoveries are within a reasonable range of 75% to 125%.

Table 3-7. TCLP of Spiked Digestates

	SAMPLE MEASUREMENTS[1]					
Metal	1	2	3	4	5	6
Arsenic	<0.13	<0.13	5.5 (120%)	0.04	0.10	5.0 (108%)
Barium	0.29	0.31	27.5 (120%)	0.84	0.84	25.5 (108%)
Cadmium	<0.02	<0.02	1.04 (115%)	6.47	6.46	7.29 (91%)
Calcium	1030	1070		4020	4010	
Chromium	1.58	1.66	6.77 (113%)	0.14	0.14	4.68 (100%)
Lead	<0.14	<0.14	5.09 (110%)	10.7	10.6	14.7 (90%)
Nickel	<0.04	<0.04	5.04 (112%)	0.52	0.52	4.97 (98%)

1. Measurements 1 and 2 are duplicate digestates of the same sample; matrix spike results are shown under measurement 3. Measurements 4 and 5 are duplicate digestates of the same sample; matrix spike results are shown under measurement 6. Spike recoveries are indicated as percentages in parenthesis.

3.7 Error Analysis

In considering the potential sources of variability in the concentrations found for a TCLP extract of a stabilized waste mix, the following factors can be identified: (1) composition of stabilized waste mix, (2) mixing parameters, (3) TCLP leaching procedure, (4) storage of extracts, (5) analysis of TCLP extracts by ICAP, and (6) data reduction. Each factor will be discussed below and its contribution to the overall uncertainty estimated.

3.7.1 Composition of Stabilized Waste Mix.

A stabilized waste mix is assembled from five components, each weighed to the nearest 0.1 gram. The range of masses used for a single 110-gram TCLP mix is from 5 grams to 100 grams, with the smallest component being the stabilization additive. The stabilization additive (ferrous sulfate, ferric sulfate or aluminum sulfate) is an ACS reagent-grade material and should make no contribution to the hazardous trace metal content of the TCLP extract. These chemicals are used in the form of soluble crystalline powders and are expected to be uniformly distributed in the final mixed sample. The water used is deionized, and does not contribute to the concentrations of metals in the extracts. The composition of cement and fly ash are given in Table 3-3. A quantity of these raw materials sufficient for the project duration was thoroughly mixed before being stocked in the laboratory.

The D004/D005 hazardous waste used is the most inhomogeneous of the raw materials. Although the bulk of the industrial waste is a fine powder, a visual examination shows pieces of broken glass up to several millimeters across and variations in apparent color in different regions. The waste used was mixed in a bulk mixer and then stored for laboratory use. Table 3-8 presents results of triplicate nitric acid digestion analyses and TCLP extraction procedures on 100.0-gram samples of this mixed D004/D005 waste. An examination of the data for zinc in Table 3-8 shows the variability of industrial wastes. This variability is why practical S/S research must be done with actual waste materials. Variations in regulated as well as non-regulated components of the wastes being treated require the development and use of very robust treatment procedures.

Examination of the compositions of the raw materials given in Table 3-3 indicates that following concentrations of the trace metal zinc can give us information on the cement and fly ash binder variability in the samples. The elements arsenic, barium and boron can be used as indicators of waste content in samples.

The variability of the analytical results in Table 3-8 indicates that the composition of industrial hazardous wastes is not uniform. The relative error in the composition of the stabilized mixtures is about 10% for arsenic and barium as a result of waste nonuniformity. One result of this is that any treatment procedures must be very well-designed so that variations in the waste will not cause treatment procedures to fail.

Table 3-8. Untreated D004/D005 Waste Variability

Concentration (mg/kg) in Nitric Acid Digest

Metal	Sample 1	Sample 2	Sample 3	Average	Std. Dev.
Arsenic	6220	5520	6200	5980	6.7%
Barium	131500	128600	140000	13340	4.4%
Calcium	3740	1260	1970	2323	55.0%
Iron	4540	2420	1000	2653	67.1%
Magnesium	1160	267	520	649	70.9%
Potassium	1930	1860	2110	1967	6.6%
Sodium	2360	1740	2180	2093	15.2%
Sulfur	620	110	380	370	69.0%
Zinc	2630	98	120	949	153. %

Concentration (mg/L) in TCLP Extract

Metal	Sample 1	Sample 2	Sample 3	Average	Std. Dev.
Arsenic	296	295	247	279	10.0%
Barium	2790	2890	4370	3350	26.4%
Calcium	15.4	18.2	15.0	16.2	10.8%
Iron	0.10	0.19	1.5	0.60	131. %
Magnesium	0.83	0.93	1.9	1.22	48.4%
Potassium	126	120	35	93.7	54.3%
Sodium	105	101	38	81.3	46.2%
Sulfur	0.42	0.71	0.58	0.57	25.4%

3.7.2 Mixing Parameters

These include the type of mixer used in the laboratory, the speed of mixing, the time of mixing, and the order of addition of components to the mix. Mix homogeneity has been a concern in the past (USEPA, 1990a). The same mixer was used as in previous projects (Bayasi, 1992) and the speed of mixing was kept constant throughout the study. As shown in previous studies (Bayasi, 1992) , mixing intensities longer than one minute at 140 rpm do not contribute to an improved consistency of results. The order of mixing, whenever experimentally possible, included thorough mixing of dry components before adding water, so that uniform wetting of the solid is possible. When cured stabilized waste mix forms are broken up for TCLP analysis, non-wetted zones or large inhomogenieties (with the exception of glass cullet) are not observed visually.

3.7.3 TCLP Leaching

The TCLP leaching procedure involves several steps: crushing the stabilized-waste form, extraction of the crushed material with the extraction fluid for 18 ± 2 hours, and filtration to separate the leachant from unreacted material. In the sample preparation stage, 100.0 grams of sample were used to minimize effects of inhomogeniety. Care was taken during the crushing operation to not lose fine material which might have a different composition than coarser particles. The 2.000 kilograms of extraction fluid was measured to a precision of 0.05% and care was taken to avoid leakage during the 24-hour extraction period. The small particle size of the sample coupled with the long time of extraction serves to minimize effects due to diffusion within particles as well as surface sealing in the curing of S/S waste forms.

The filtration step is potentially the greatest source of error in the TCLP extraction process. Some materials, e.g. $BaSO_4$, produce very fine, chemically inert precipitates. The particle size of precipitated $BaSO_4$ is easily small enough to pass through the filter specified for the TCLP process (Koltoff, 1969). If a fine solid were suspended in the extract, it would produce a false reading in the ICAP experiment. This potential problem was not judged to be severe because a visual spot check of several extracts showed very little turbidity. Also, normal operating procedures for ICAP used the average and standard deviation of three repeated aspirations for each sample and our relative standard deviation for barium was judged to be sufficiently small after taking waste inhomogeniety into account. Even though ICAP determinations of samples with small particles may be reproducible, particulate penetration of the filter may not be reproducible or controllable. One consequence of this is that the variance in barium determinations can be larger than other elements.

3.7.4. Extract Storage

TCLP extracts were acidified with nitric acid to below pH 2 before storage at $4^{o}C$, following recommended EPA procedures. EPA recommendations are that samples stored in this manner should yield satisfactory results for storage periods up to six months. In a few instances in this study, samples were reanalyzed after interim storage for periods of several weeks with comparable results, indicating that no severe changes were taking place during the storage process.

3.7.5 Analysis of Extracts

The analysis of TCLP extracts by ICAP was carried out following the standard quality control procedures of the US EPA. Samples were diluted 1:10 before analysis to extend the linear range while still maintaining sufficient sensitivity to meet TCLP standards. The instrument was standardized with three sets of standard solutions with concentration ratios in 1:10:100 ratios before and after samples were analyzed. Standards agreement before and after samples are required to meet instrument manufacturer's specifications for the data to be considered valid.

Samples were analyzed three times with blanks aspirated between to prevent sample cross-talk in the ICAP torch. A percent relative standard deviation was calculated for the three sample determinations and reported along with the mean of the values. Because the sources of instrumental noise are varied, the precision of determinations often is best understood as a function of the concentration being determined. In this project the detection limit for such a determination is defined as the concentration where the noise is 100% of the analytical signal. Figure 3-2 presents plots showing the instrumental relative standard deviation for elements important in this project versus concentration for 24 representative samples.

The instrumental precision at the TCLP standard limit of 5 mg/L for As is better than 5%, at the 100 mg/L limit for Ba the precision is about 1%, at the average concentration in the project for iron of about 40 mg/L the precision is better than 1%, and at the average sulfur concentration of 150 mg/L the instrumental precision is better than 2%. For calcium the concentration in the TCLP extracts is between 1000 and 3000 mg/L and the relative precision observed is 0.6% on the average. In summary, we can assume that instrumental precision is always better than 5% in this project, justifying the use of at least 2 significant figures.

3.7.6 Data Entry and Reduction

Data entry and reduction is also a possible source of error. Notebook protocols for laboratory personnel were constructed to ensure complete records. When large amounts of data were to be entered into a computer, the data entered was proofed by more than one person.

3.7.7 Error Analysis Summary

The overall error associated with the TCLP process can be considered using a propagation of errors approach. This method of error estimation will provide a very pessimistic view of the overall error associated with an experimental result. The TCLP concentration is written as a function of the independent variables:

TCLP(mix composition, mix parameters, extract analysis)

and the derivative is taken. Assuming linear behavior for the independent variables and stochastic independence, the maximal estimated relative error in the final TCLP extracts can be written

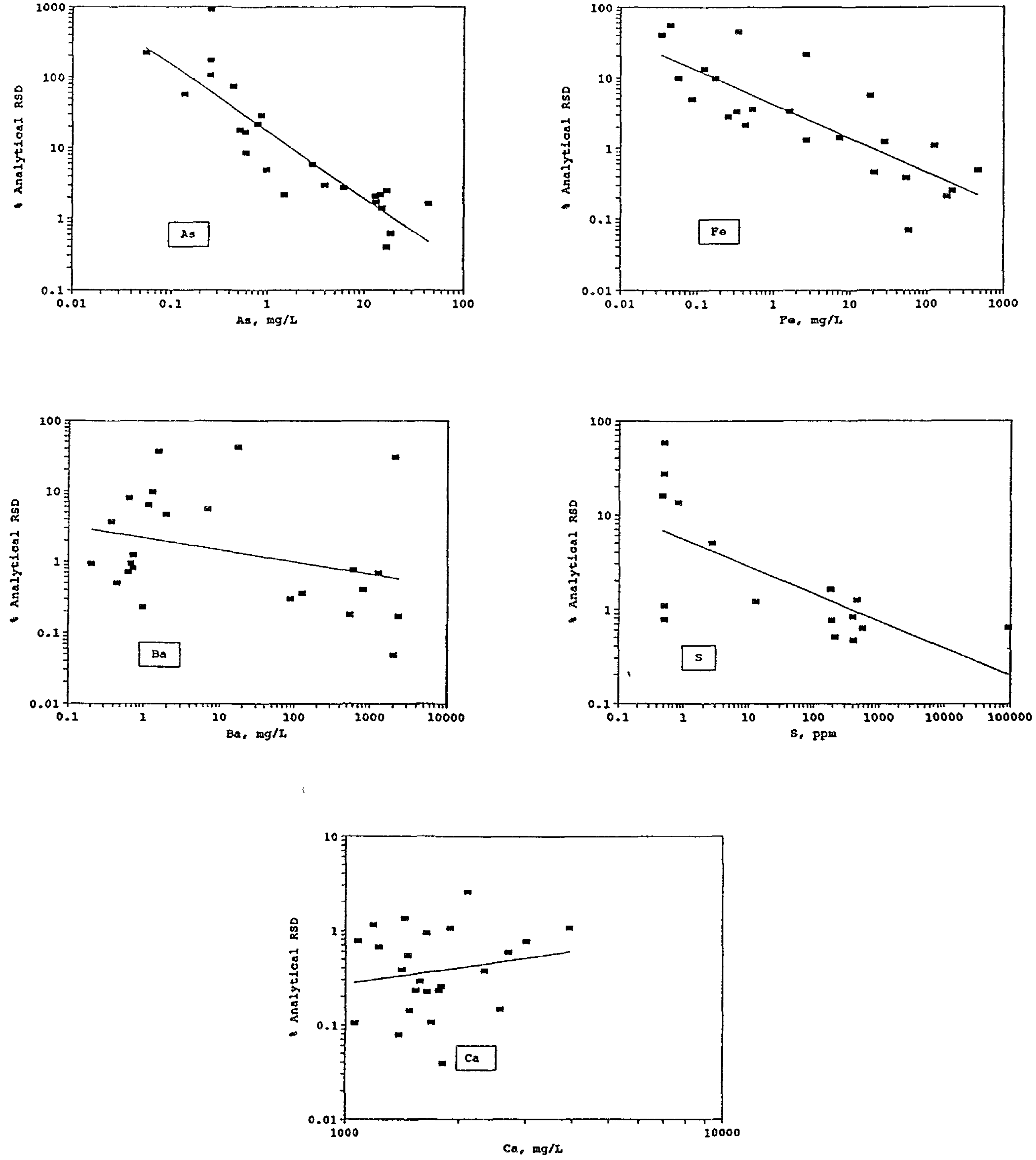

Figure 3-2. ICAP Replicate Relative Standard Deviation as a Function of Concentration with Regression Lines.

as

$$\frac{\text{TCLP error}}{\text{TCLP}} = \frac{\text{comp error}}{\text{comp}} + \frac{\text{mix error}}{\text{mix}} + \frac{\text{anal error}}{\text{anal result}}$$

In this case, following the discussion above, the relative error in the composition of the stabilized mixtures is about 10% for arsenic and barium. The uncertainties found in the mixing study in previous projects were 10% or less for elements of interest (Bayasi, 1992) and probably are insignificant compared to the variability in composition of the raw waste because waste variabilities are folded into the mixing experiment design. As discussed above, a conservative estimate for analytical precision is 5%, so that the overall uncertainty in the TCLP results expected is about 15%.

As a check on this, two mixes with large masses were prepared of the same nominal composition. The composition of these mixes was designed to produce a poor stabilization of the waste so that measurable concentrations may be compared. After suitable curing, these large masses were crushed and partitioned into 4 aliquots for separate TCLP extractions. Each TCLP extract was analyzed independently. The results are shown in Table 3-9 and Figure 3-3.

Table 3-9. TCLP Precision Results

Metal	Sample A Avg mg/L	Sample A % Std Dev	Sample B Avg mg/L	Sample B % Std Dev	All Data Avg mg/L	All Data % Std Dev
Arsenic	48.3	0.7	28.8	15.8	38.5	26.8
Barium	3623	5.7	3638	7.9	3630	6.9
Boron	1242	4.7	1053	7.0	1147	10.0
Calcium	992	3.8	930	7.3	961	6.6
Magnesium	58.9	3.0	59.4	9.4	59.2	14.2
Manganese	1.11	9.0	1.21	10.7	1.16	11.2
Average % RSD		4.5%		9.7		12.6

The average standard deviations among the TCLP extracts of each S/S mix are within the expected uncertainties for the TCLP extraction and instrumental analysis components being tested. The larger uncertainty found when both S/S mixes are compared ("All Data") indicates the variation from inhomogeniety of the raw waste. Examination of the data in Table 3-10 for iron and sulfur sheds light on the problems of mixing of samples of this type.

Even though the samples appeared homogeneous to the eye and uniform in color, some sections had higher concentrations of iron and sulfur from the addition of ferrous sulfate as a stabilizing additive. With all the data included, the iron results have a 105% relative standard deviation. If sample B3 is discarded, the

Table 3-10. TCLP Repeatability Data for Iron and Sulfur

Sample	Fe, ppm	% RSD	S, ppm	% RSD
A1	0.3	6.1	**24.9**	9.4
A2	0.1	20.	**30.7**	14.
A3	0.06	21.	0.5	29.
A4	0.05	9.4	0.8	13.
B1	0.06	53.	0.3	34.
B2	0.12	11.	8.5	3.4
B3	**0.63**	8.2	**59.2**	8.0
B4	0.07	7.8	4.8	7.5

relative standard deviation is 8.8%. In a conventional analytical chemistry laboratory, one would consider discarding sample B3 via a traditional mechanism such as a Q test. However, when the large value for sulfur is also noted, it seems that an explanation more likely than an analytical error is a volume of incomplete mixing which contains excess levels of ferrous sulfate additive.

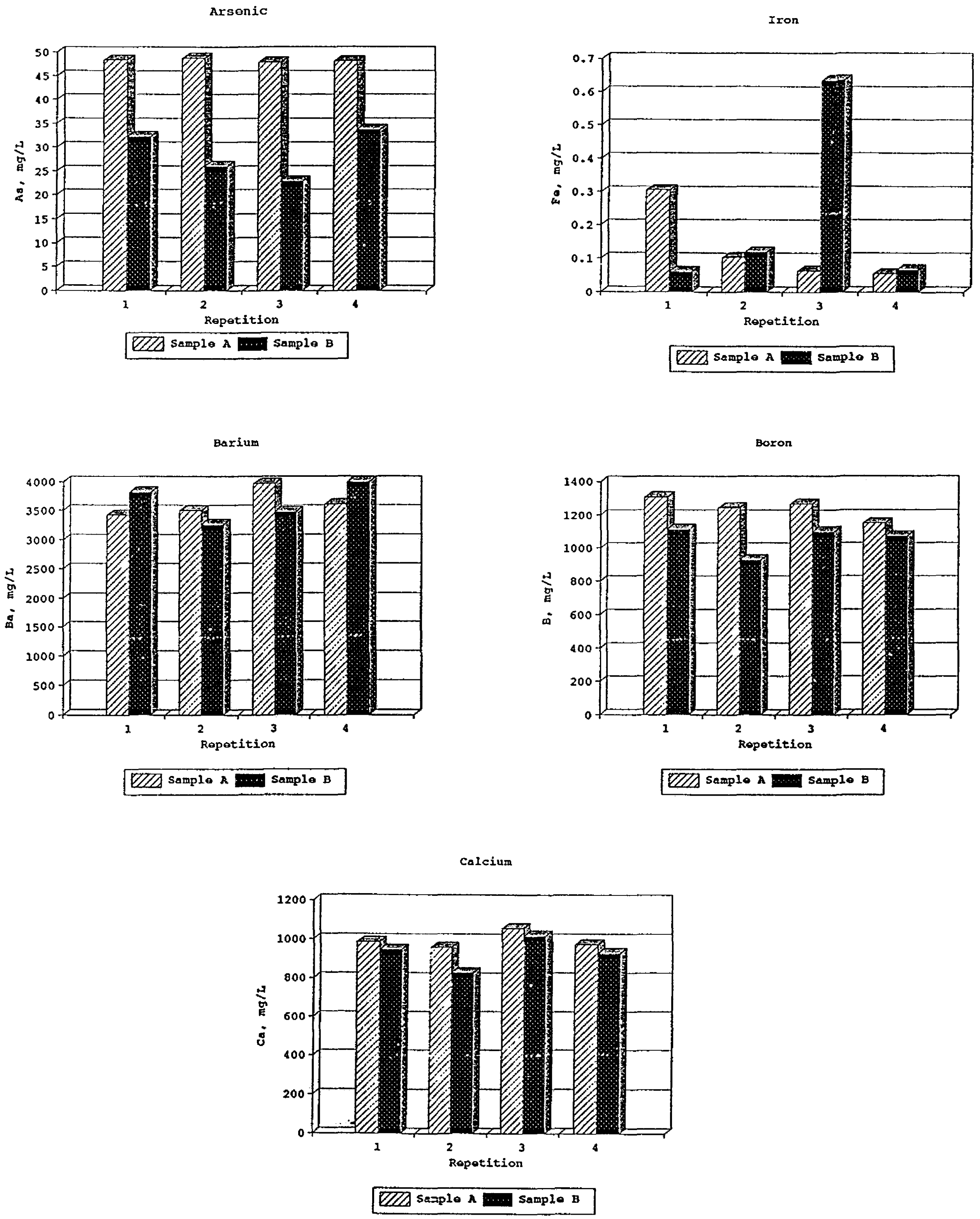

Figure 3-3. TCLP Repeatability Replication Study

CHAPTER FOUR
EXPERIMENTAL DESIGN

4.1 TCLP Experimentation for Arsenic and Barium Stabilization

Arsenic and barium are the primary contaminants of concern in the D004/D005 waste generated by a glass manufacturer. Stabilization mixes were prepared using portland cement and either silica fume or fly ash. Numerous experiments were conducted, but no treatment designs were effective, and no significant differences between silica fume and fly ash were discovered. Table 4-1 shows two typical results from these stabilization efforts. The mix designs use comparable amounts of the pozzolan, and both arsenic and barium TCLP standards are exceeded with no significant difference between treatments. The mix design parameters were: water/binder = 0.87; binder/D-waste = 0.40, silica fume/binder = 0.30, and fly ash/binder = 0.40. These results were for samples cured for seven days. Other data showed that curing time did not appear to improve treatment effectiveness.

Table 4-1. TCLP Results with D004/D005 Waste

Stabilization	Arsenic (mg/L)		Barium (mg/L)	
Method	Sample 1	Sample 2	Sample 1	Sample 2
Silica Fume	48.6	50.1	528	548
Fly Ash	66.3	66.2	565	565
Untreated Waste	296	295	2790	2890
TCLP Standard	5.0		100.	

An hypothesis for effective S/S was to precipitate the barium with sulfate and to precipitate or change the oxidation state of arsenic. Therefore, ferrous sulfate was added to both silica fume and fly ash S/S designs at dosages measured as grams of ferrous sulfate per gram of water. Other mix design parameters were: water + ferrous sulfate solution/binder = 2.3, binder/D-waste = 0.40, silica fume/binder = 0.30, and fly ash/binder = 0.40.

The TCLP concentrations for arsenic and barium are presented in Figures 4-1 and 4-2, respectively. Increasing amounts of ferrous sulfate up to 60 grams ferrous sulfate/100 grams of water decrease both arsenic and barium TCLP concentrations. Arsenic appears to decrease more rapidly with fly ash S/S. More effective arsenic stabilization with fly ash may be because of the adsorptive capability of fly ash (Sen and De, 1987). On the other hand, barium stabilization is more effective with silica fume S/S.

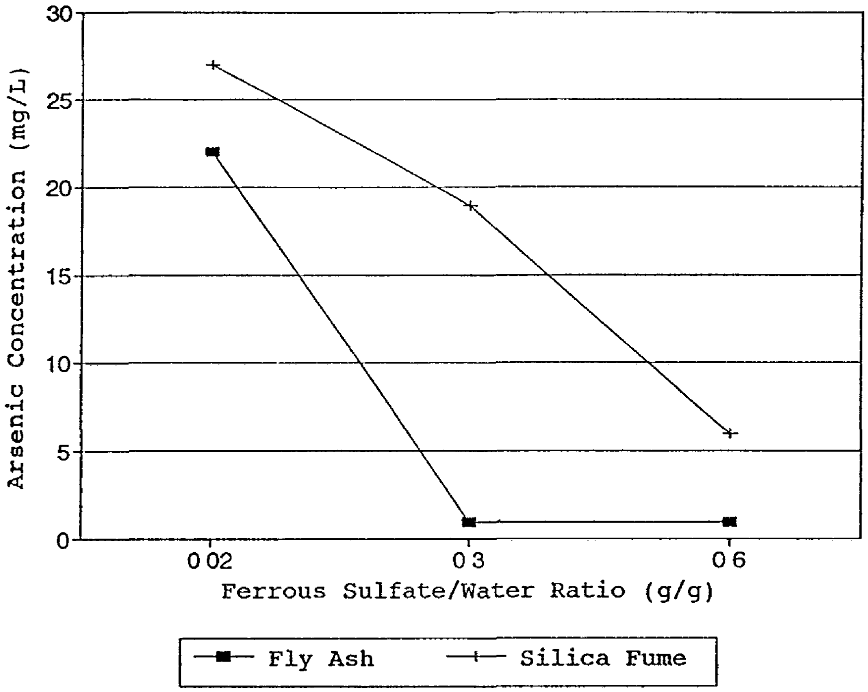

Figure 4-1. TCLP Results for Arsenic

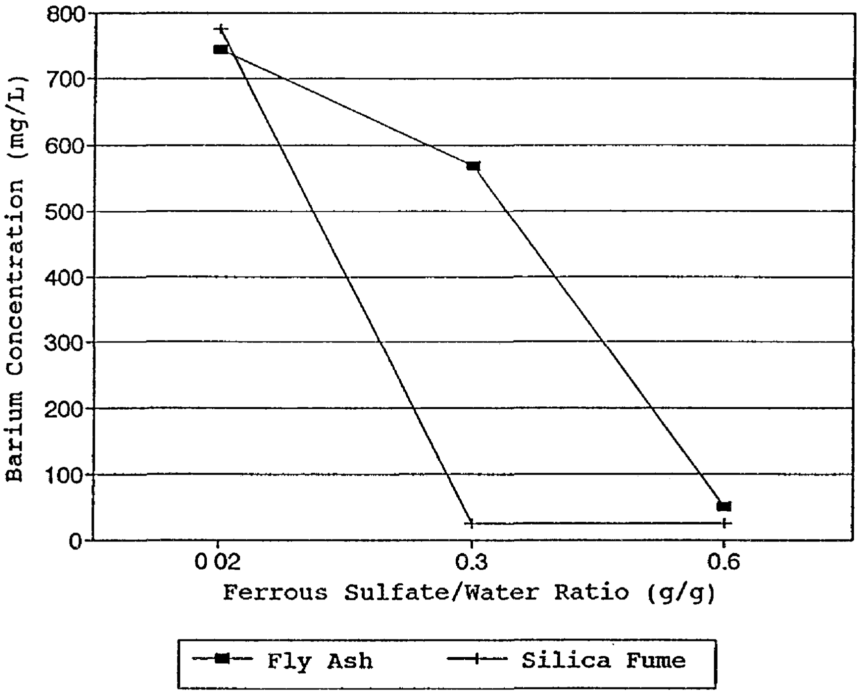

Figure 4-2. TCLP Results for Barium

Barium sulfate is a very fine precipitate, and its more effective encapsulation by silica fume may indicate the improved impermeability of silica fume cement paste.

4.2 Stabilization Mix Designs

Based on this preliminary work, a matrix of mix designs for stabilization treatments using ferric sulfate, ferrous sulfate, and aluminum sulfate are presented in Tables 4-2 through 4-4 respectively. In the top line of each box, each mix design is named with a prefix US, F, or A for ferrous sulfate, ferric sulfate, and aluminum sulfate, respectively. The first number in the mix name refers to a series of stabilizations with an additive, and the second number is a sample number that is associated with a particular length of curing before undergoing TCLP. Samples one through four of each mix have undergone TCLP after 2, 60, 360, and 540 days of cure, respectively.

Each matrix in Tables 4-2 through 4-4 consists of four mix designs set out in two columns and three rows. For each mix design, the mass of each component and important ratios are provided. Mix designs in a column have the same binder/waste mass ratio; those in the left column have binder/waste mass ratios of 0.15, and those in the right column have ratios of 0.40. Binders are defined to be cement and fly ash. The lower ratio is more volume efficient.

Mix designs in each row are characterized by comparable mole ratios of additive to waste in terms of iron/arsenic and sulfur/barium. The amounts of arsenic and barium in these ratios are the moles of arsenic and barium leached during the TCLP of the raw waste. The water/binder mass ratio was constant at 1.6 for all these designs. Thirty percent of the total binder was fly ash.

Mix design parameters were chosen to produce a workable wet mix that would set up into a monolithic solid. These solids generally had sufficient mechanical integrity to require crushing before TCLP extraction.

These mix designs were selected for preparation in a random order to confound any systematic error. Replicate studies were performed on comparable mix designs and results are discussed in Section 3.5.

4.3 Column Leaching

The use of column leaching procedures provides different information from the TCLP. The TCLP is designed as an exhaustive leaching procedure. With a column leaching procedure, data can be obtained on the relative rates of leaching of various components of the stabilized matrix. It is to be expected that the

Table 4-2. MATRIX OF MIX DESIGNS FOR FERRIC SULFATE STABILIZATION OF D004/D005 WASTE

F1x Series

Component per 100.0 g waste	Mass g
Water	24.0
Cement	9.0
Fly Ash	6.0
$Fe_2(SO_4)_3 \cdot 9H_2O$	4.8

Important ratios:

Binder/Waste	0.15	g/g
Binder/H_2O	0.59	g/g
Fe^{3+}/binder	0.063	g/g
Fe^{3+}/As	2.1	mol/mol
SO_4^{2-}/binder	0.16	g/g
SO_4^{2-}/Ba^{2+}	0.53	mol/mol

F2x Series

Component per 100.0 g waste	Mass g
Water	24.0
Cement	9.0
Fly Ash	6.0
$Fe_2(SO_4)_3 \cdot 9H_2O$	14.4

Important ratios:

Binder/Waste	0.15	g/g
Binder/H_2O	0.53	g/g
Fe^{3+}/binder	0.19	g/g
Fe^{3+}/As	6.4	mol/mol
SO_4^{2-}/binder	0.49	g/g
SO_4^{2-}/Ba^{2+}	1.6	mol/mol

F3x Series

Component per 100.0 g waste	Mass g
Water	64.0
Cement	24.0
Fly Ash	16.0
$Fe_2(SO_4)_3 \cdot 9H_2O$	12.8

Important ratios:

Binder/Waste	0.40	g/g
Binder/H_2O	0.59	g/g
Fe^{3+}/binder	0.064	g/g
Fe^{3+}/As	5.7	mol/mol
SO_4^{2-}/binder	0.16	g/g
SO_4^{2-}/Ba^{2+}	1.4	mol/mol

F4x Series

Component per 100.0 g waste	Mass g
Water	64.0
Cement	24.0
Fly Ash	16.0
$Fe_2(SO_4)_3 \cdot 9H_2O$	38.4

Important ratios:

Binder/Waste	0.40	g/g
Binder/H_2O	0.53	g/g
Fe^{3+}/binder	0.19	g/g
Fe^{3+}/As	17.	mol/mol
SO_4^{2-}/binder	0.49	g/g
SO_4^{2-}/Ba^{2+}	4.2	mol/mol

Notes:

1. Water of hydration is taken into account in Binder/H_2O ratio.
2. 100 g waste contains 0.060 g Arsenic.
3. 100 g waste contains 13.3 g Barium of which 43% is found to be extractable in TCLP.
4. Assume 50% of Ba in waste is available for reaction in ratios calculated.

Table 4-3. MATRIX OF MIX DESIGNS FOR FERROUS SULFATE STABILIZATION OF D004/D005 WASTE

US1x Series

Component per 100.0 g waste	Mass g
Water	24.0
Cement	9.0
Fly Ash	6.0
$FeSO_4 \cdot 7H_2O$	4.8

Important ratios:

Binder/Waste	0.15	g/g
Binder/H_2O	0.57	g/g
Fe^{2+}/binder	0.064	g/g
Fe^{2+}/As	2.2	mol/mol
SO_4^{2-}/binder	0.11	g/g
SO_4^{2-}/Ba^{2+}	0.36	mol/mol

US2x Series

Component per 100.0 g waste	Mass g
Water	24.0
Cement	9.0
Fly Ash	6.0
$FeSO_4 \cdot 7H_2O$	14.4

Important ratios:

Binder/Waste	0.15	g/g
Binder/H_2O	0.49	g/g
Fe^{2+}/binder	0.19	g/g
Fe^{2+}/As	6.5	mol/mol
SO_4^{2-}/binder	0.33	g/g
SO_4^{2-}/Ba^{2+}	1.1	mol/mol

US3x Series

Component per 100.0 g waste	Mass g
Water	64.0
Cement	24.0
Fly Ash	16.0
$FeSO_4 \cdot 7H_2O$	12.8

Important ratios:

Binder/Waste	0.40	g/g
Binder/H_2O	0.57	g/g
Fe^{2+}/binder	0.064	g/g
Fe^{2+}/As	5.7	mol/mol
SO_4^{2-}/binder	0.11	g/g
SO_4^{2-}/Ba^{2+}	0.95	mol/mol

US4x Series

Component per 100.0 g waste	Mass g
Water	64.0
Cement	24.0
Fly Ash	16.0
$FeSO_4 \cdot 7H_2O$	38.4

Important ratios:

Binder/Waste	0.40	g/g
Binder/H_2O	0.49	g/g
Fe^{2+}/binder	0.19	g/g
Fe^{2+}/As	17.	mol/mol
SO_4^{2-}/binder	0.33	g/g
SO_4^{2-}/Ba^{2+}	2.9	mol/mol

Notes:

1. Water of hydration is taken into account in Binder/H_2O ratio.
2. 100 g waste contains 0.060 g Arsenic.
3. 100 g waste contains 13.3 g Barium of which 43% is found to be extractable in TCLP.
4. Assume 50% of Ba in waste is available for reaction in ratios calculated.

Table 4-4. MATRIX OF MIX DESIGNS FOR ALUMINUM SULFATE STABILIZATION OF D004/D005 WASTE

A1x Series

Component per 100.0 g waste	Mass g
Water	24.0
Cement	9.0
Fly Ash	6.0
$Al_2(SO_4)\cdot 18H_2O$	4.8

Important ratios:

Binder/Waste	0.15 g/g
Binder/H_2O	0.57 g/g
Al^{3+}/binder	0.026g/g
Al^{3+}/As	1.8 mol/mol
SO_4^{2-}/binder	0.14 g/g
SO_4^{2-}/Ba^{2+}	0.45 mol/mol

A2x Series

Component per 100.0 g waste	Mass g
Water	24.0
Cement	9.0
Fly Ash	6.0
$Al_2(SO_4)\cdot 18H_2O$	14.4

Important ratios:

Binder/Waste	0.15 g/g
Binder/H_2O	0.48 g/g
Al^{3+}/binder	0.078g/g
Al^{3+}/As	5.4 mol/mol
SO_4^{2-}/binder	0.42 g/g
SO_4^{2-}/Ba^{2+}	1.3 mol/mol

A3x Series

Component per 100.0 g waste	Mass g
Water	64.0
Cement	24.0
Fly Ash	16.0
$Al_2(SO_4)\cdot 18H_2O$	12.8

Important ratios:

Binder/Waste	0.40 g/g
Binder/H_2O	0.57 g/g
Al^{3+}/binder	0.026g/g
Al^{3+}/As	4.8 mol/mol
SO_4^{2-}/binder	0.14 g/g
SO_4^{2-}/Ba^{2+}	1.2 mol/mol

A4x Series

Component per 100.0 g waste	Mass g
Water	64.0
Cement	24.0
Fly Ash	16.0
$Al_2(SO_4)\cdot 18H_2O$	38.4

Important ratios:

Binder/Waste	0.40 g/g
Binder/H_2O	2.1 g/g
Al^{3+}/binder	0. 79g/g
Al^{3+}/As	14. mol/mol
SO_4^{2-}/binder	0.42 g/g
SO_4^{2-}/Ba^{2+}	3.6 mol/mol

Notes:

1. Water of hydration is taken into account in Binder/H_2O ratio.
2. 100 g waste contains 0.060 g Arsenic.
3. 100 g waste contains 13.3 g Barium of which 43% is found to be extractable in TCLP.
4. Assume 50% of Ba in waste is available for reaction in ratios calculated.

leachabiity rate of different metals depends on the matrix surrounding each metal.

Mix design numbers US1 and US4 shown in Table 4-2 have undergone column leaching so that TCLP results can be compared with dynamic leaching results.

4.4 Calorimetric Analyses of Hydration Reactions

The objective of this series of experiments was to determine the adiabatic temperature of the cement hydration reactions in a waste stabilization process. This information should be useful in determining the rates of the hydration reactions and the relative completion of the hydration reaction processes.

Thermal isolation was achieved by placing the reacting sample in a styrene foam cup inside a glass dewar insulating flask with a foam lid. The sample cup was supported inside the dewar flask on thin insulating legs to reduce conductive heat transfer to the glass (Figure 4-3). Two matching samples and dewars were run simultaneously inside a foamed styrene isolation container.

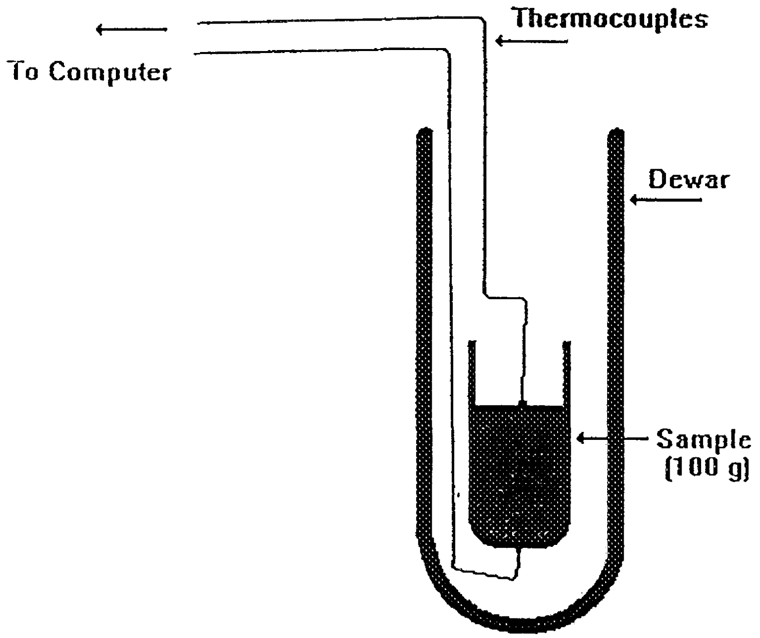

Figure 4-3. Calorimetric Heat of Hydration Apparatus

Temperatures were determined with ASTM Type E chromel-constantan thermocouples, inserted in the top and the bottom of each reaction mass. Another thermocouple was used to determine the background temperature in the outer isolation container. The output voltages of the thermocouples were determined using a MINI-16 analog-to-digital interface board manufactured by Industrial Computer Source (4837 Mercury Street, San Diego, CA 92111). A ± 50-millivolt range was used with 16-bit analog-to-digital resolution. After conversion to temperature, a relative precision of ± 0.01°C was obtained. The offset voltages of the individual thermocouples were made internally consistent by forcing the temperatures determined from all thermocouples to be the same when the measuring junctions of the thermocouples were in the same stirred thermal bath. The agreement between the temperatures indicated by the thermocouples and a laboratory thermometer was better than ± 0.1°C in the 20 to 35°C temperature range used in the experiment.

Temperature data were acquired from all measuring junctions at 1800-second intervals to provide sufficient data to allow smoothing while keeping the data file size manageable during the 3000-minute reaction time. Data presented in Section 5.3 are the averages of the top and bottom temperatures which was then smoothed with a 3- or 5-point moving average low-pass data filter.

A three-point moving average low-pass data filter is calculated using the formula

$$\overline{x}_i = (x_{i-1} + x_i + x_{i+1}) / 3$$

where $\overline{x}_i$ = filtered i-th data point
x_{i-1}, x_i and x_{i+1} = i-th and surrounding data points.

A five-point moving average filter is calculated similarly. In principle, any odd number of terms can be used in a moving average filter. For these experiments, the response time of the apparatus becomes too slow and the data features hard to distinguish when more than 7-point smoothing is used. The data presented has been subjected to three-point smoothing for graphical purposes.

Samples for calorimetric analysis were prepared following the procedures outlined above. Samples were dry-mixed and then water was added. The data acquisition time clock was started when the water was added. As soon as the mixture appeared to be consistent, the 100.0 g sample was placed in the calorimeter cup, the thermocouples inserted, and the thermal isolation put in place. Data logging of sample temperatures was continuous for periods of about two days after mixing. Reactions with the waste replaced by an equal mass of sand were used for baseline comparisons.

4.5 Arsenite Stabilization

4.5.1 Ferrous and Ferric Sulfate Stabilization

As shown in Table 4-5, a study was designed to compare arsenate and arsenite stabilization with either ferrous sulfate or ferric sulfate. A synthetic but realistic waste was made by adding sodium arsenite to a F006 waste (which has very little arsenic) so that the total arsenic was comparable to that of the project waste. Other synthetic waste samples were made using sodium arsenate for comparison. The arsenic compounds were added to the F006 waste according to the mole ratios in the left column. The binder/waste ratios were either 0.15 or 0.40 as shown in the top row. Two samples for each possible mix design in Table 4-5 underwent TCLP after 2 and 60 days of cure.

Table 4-5. Matrix of Mix Designs for the Stabilization of Arsenite and Arsenate

Binder/F Waste (doped with arsenic)

Mole Ratio	0.15		0.40	
	USA2x (USB2x series)		**USA4x (USB4x series)**	
$\frac{Fe^{2+}}{As}$ 2.0	Component per 100.0 g waste	Mass (g)	Component per 100.0 g waste	Mass (g)
	Na_2HAsO_4 or	2.50	Na_2HAsO_4 or	2.50
	$NaAsO_2$	1.04	$NaAsO_2$	1.04
	Water	24.	Water	64.
	Binder	21.	Binder	56.
	$FeSO_4 \cdot 7H_2O$	4.5	$FeSO_4 \cdot 7H_2O$	4.5
	FA1x (FB1x series)		**FA3x (FB3x series)**	
$\frac{Fe^{3+}}{As}$ 1.1	Component per 100.0 g waste	Mass (g)	Component per 100.0 g waste	Mass (g)
	Na_2HAsO_4 or	2.50	Na_2HAsO_4 or	2.50
	$NaAsO_2$	1.04	$NaAsO_2$	1.04
	Water	24.	Water	64.
	Binder	21.	Binder	56.
	$Fe_2(SO_4)_3 \cdot 9H_2O$	2.4	$Fe_2(SO_4)_3 \cdot 9H_2O$	2.4

4.5.2 Pretreatment with Oxidation

Results of the study shown in Table 4-5 indicated that stabilization of arsenite was less effective than arsenate. Another study using arsenite waste was designed to evaluate pre-treatments that oxidize arsenite to arsenate making the waste more amenable to effective stabilization. A synthetic waste was made with a similar arsenic/waste mass fraction as the actual D004/D005 waste used in the project. For 100 grams of F006 waste, either 1.04 grams of sodium arsenite or 2.50 grams of sodium arsenate were added to the F006 waste by first dissolving the arsenic compound in 1.0 M NaOH prior to mixing it with the F006 waste.

Two pretreatments of the arsenite waste were investigated as shown in the experimental design in Table 4-6. Oxidation of arsenite was attempted with either air entrainment by intense mixing or with compressed air diffusion. Chemical oxidation with hydrogen peroxide was also used at H_2O_2/AsO_3^{3-} mole ratios of 0.5 and 1.0.

Table 4-6. Pretreatment and Stabilization of Synthetic Arsenite Waste

Pre-treatment	Binder/F Waste (doped with arsenic)			
	0.15		0.40	
	USB1x		**USB2x**	
	Component per 100.0 g waste	Mass (g)	Component per 100.0 g waste	Mass (g)
Aeration 11 min. 200 rpm	$NaAsO_2$	0.72	$NaAsO_2$	0.496
	Water	16.28	Water	30.45
	Binder	10.35	Binder	19.1
	$FeSO_4 \cdot 7H_2O$ or	3.1	$FeSO_4 \cdot 7H_2O$ or	2.15
	$Fe_2(SO_4)_3 \cdot 9H_2O$	1.68	$Fe_2(SO_4)_3 \cdot 9H_2O$	1.15
	USBP1x		**USBP2x**	
	Component per 100.0 g waste	Mass (g)	Component per 100.0 g waste	Mass (g)
Hydrogen Peroxide Oxidation	$NaAsO_2$	0.72	$NaAsO_2$	0.496
	Water	12.83	Water	27.95
	Binder	10.35	Binder	19.08
	$FeSO_4 \cdot 7H_2O$ or	3.12	$FeSO_4 \cdot 7H_2O$ or	2.15
	$Fe_2(SO_4)_3 \cdot 9H_2O$	1.75	$Fe_2(SO_4)_3 \cdot 9H_2O$	1.15
	H_2O_2 (5% or 2%)	3.75	H_2O_2 (5% or 2%)	2.58

4.6 Individual Ion Study

This study was designed to investigate the effect of sulfate and the binder/waste ratio on the early curing of the cement matrix. The effect of iron and sulfate on stabilization can be isolated by the selection and individual application of iron acetate and sodium sulfate as additives. The use of iron acetate will treat the arsenic in the same way as ferrous sulfate without the sulfate. On the other hand, sodium sulfate will precipitate the barium in the same way as ferrous sulfate without arsenic stabilization. The experimental design is presented in Tables 4-7 and 4-8.

Table 4-7. Stabilization Design Using Ferrous Acetate

Mole Ratio Fe^{2+}/As	Binder/Waste Mass Ratio			
	0.15		0.40	
1.5	**IA1x Series**		**IA3x Series**	
	Component per 100.0 g waste	Mass g	Component per 100.0 g waste	Mass g
	Water	22.5	Water	60.
	Cement	9.	Cement	24.
	Fly Ash	6.	Fly Ash	16.
	$Fe(CH_3CH_2)_2$	2.09	$Fe(CH_3CH_2)_2$	2.09
	Fe/binder	0.045	Fe/binder	0.017
3.0	**IA2x Series**		**IA4x Series**	
	Component per 100.0 g waste	Mass g	Component per 100.0 g waste	Mass g
	Water	22.5	Water	60.
	Cement	9.	Cement	24.
	Fly Ash	6.	Fly Ash	16.
	$Fe(CH_3CH_2)_2$	4.	$Fe(CH_3CH_2)_2$	4.
	Fe/binder	0.086	Fe/binder	0.032

Table 4-8. Stabilization Design Using Sodium Sulfate

Mole Ratio SO_4^{2-}/Ba^{2+}	Binder/Waste Mass Ratio			
	0.15		0.40	
1.0	**SS1x Series**		**SS3x Series**	
	Component per 100.0 g waste	Mass g	Component per 100.0 g waste	Mass g
	Water	22.5	Water	60.
	Cement	9.	Cement	24.
	Fly Ash	6.	Fly Ash	16.
	Na_2SO_4	10.	Na_2SO_4	10.
	SO_4/binder	0.451	SO_4/binder	0.17
2.0	**SS2x series**		**SS4x series**	
	Component per 100.0 g waste	Mass g	Component per 100.0 g waste	Mass g
	Water	22.5	Water	60.
	Cement	9.	Cement	24.
	Fly Ash	6.	Fly Ash	16.
	Na_2SO_4	20.	Na_2SO_4	20.
	SO_4/binder	0.90	SO_4/binder	0.338

4.7 Scanning Electron Microscopy

Scanning electron microscopy with x-ray emission analysis was carried out on a series of samples to enable an understanding of the relationship between the cement lattice structure, waste components and treatment additives. Eight samples were prepared for analysis using the ISI 40 Scanning Electron Microscope (SEM) at the Center for Electron Microscopy of the University of Illinois, Champaign. The composition of the samples is given in Table 4-9.

Table 4-9. Composition Table for SEM Samples

SEM Sample Number	CURE TIME (Days)	RATIO B/HW	MASSES (g):					
			HW	Cement	Fly Ash	Water	Fe	Total
Ferrous Sulfate Additive								
SEM1	2	0.080	100	5.6	2.4	16.0	1.6	125.6
SEM2	60	0.080	100	5.6	2.4	16.0	1.6	125.6
SEM3	365	0.080	100	5.6	2.4	16.0	1.6	125.6
SEM6	60	0.12	100	8.4	3.6	24.0	2.4	138.4
SEM7	60	0.12	100	8.4	3.6	24.0	9.6	145.6
SEM8	2	0.12	100	8.4	3.6	24.0	9.6	145.6
Ferric Sulfate Additive								
SEM4	2	0.40	100	24.0	16.0	64.0	12.8	216.8
SEM5	2	0.40	100	24.0	16.0	64.0	38.4	242.8

Polished flat surfaces were prepared on each sample using techniques normal for cement samples. Samples were chipped with a chisel to form a nearly flat surface with less than one square inch cross-sectional area. Samples were then soaked in 100% ethanol overnight to remove any water and dust particles and to help prevent cracking of samples in the subsequent steps of sample preparation. The alcohol was removed and the sample baked overnight in a 70^{o}C oven.

Samples were then encapsulated in LR White resin from Fullem, Inc. The resin was cured at 70^{o}C overnight. Using a Buehler Minimet polishing apparatus, samples were polished using increasingly finer grades of abrasives with Buehler polishing oil, starting with 200 grit and ending with 600 grit. Finish polishing was done using 3 micron Leco Microid Diamond Paste on a Buehler Polisher Ecomet III grinder.

After cleaning with ethanol, samples were coated with carbon from a carbon string source in a Denton vacuum evaporator. SEM microscopy was carried out using magnifications from 130x to 1000x. Atomic composition analyses of areas under examination were done with electron-induced X-ray emission analysis using a Tracor Northern 2010 energy-dispersive detector. Average concentrations over the area scanned by the electron beam were determined as well as spatial distributions of important elements such as arsenic, barium, iron and sulfur. The SEM results are discussed in Section 5.6.

CHAPTER FIVE
Results and Discussion

5.1 Mix Design Review

In chapter four, a matrix of mix designs for stabilization treatments using ferric sulfate, ferrous sulfate, and aluminum sulfate are presented in Tables 4-2 through 4-4 respectively. These tables are repeated in Appendix A. In the top line of each box, each mix design is named with a prefix US, F, or A for ferrous sulfate, ferric sulfate, and aluminum sulfate, respectively. The first number in the mix name refers to a series of stabilizations with an additive, and the second number is a sample number that is associated with a particular length of curing before undergoing TCLP. Samples one through four of each mix have undergone TCLP after 2, 60, 360, and 540 days of cure, respectively.

Each matrix containing four mix designs consists of two columns and three rows as shown in Figure 5-1a. Mix designs in a column have the same binder/waste mass ratio where binders are defined to be cement and fly ash. Thirty percent of the total binder was fly ash. Those in the left column have binder/waste mass ratios of 0.15, and those in the right column have ratios of 0.40. Mix designs with the lower ratio in the left column are more volume efficient. Mix designs in each row are characterized by comparable mole ratios of additive to waste in terms of iron/arsenic and sulfur/barium. The ratio of additive to waste increases moving downward through the matrix. The water/binder mass ratio was constant at 1.6 for all these designs.

A convenient reference for mix designs in the figures in this chapter is shown in Figures 5-1b and 5-1c. If stabilizations are being compared where only one additive was used, then results of different mix designs are distinguished by a symbol in the corresponding box. For example, the symbol, ▓ , refers to a volume efficient (low binder/waste) mix with a lower amount of additive. If stabilizations are being compared using ferrous and ferric sulfate, then a symbol 2 or 3 in the corresponding box indicates ferrous sulfate and ferric sulfate, respectively. An example is shown in Figure 5-1c.

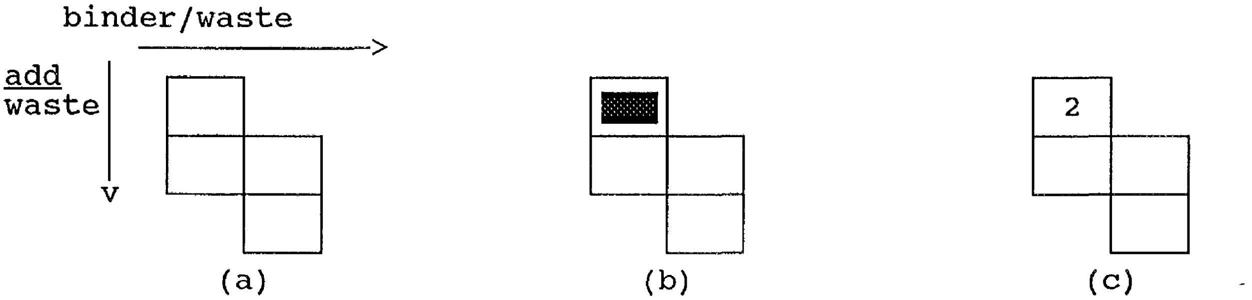

(a) (b) (c)

Figure 5-1. Legend of Mix Designs

5.2 TCLP Results

Analytical results for TCLP extracts of S/S using ferrous sulfate, ferric sulfate or aluminum sulfate additives are presented in Appendix B. Sample numbers used in Appendix B are those used consistently throughout this report.

5.2.1 Stabilization with Ferrous Sulfate

Figure 5-2 presents results of analyses for selected metals in TCLP extracts of waste stabilized with ferrous sulfate. With only two days of curing, arsenic concentrations are predictable according to the iron/arsenic molar ratio of the mix. Design US1 (closed rectangle) has a significantly higher arsenic concentration because its iron/arsenic molar ratio is only 2.16 which is insufficient given the pH conditions and presence of other ions. From the literature survey in Chapter 2, this ratio value was considered too low for arsenic removal from water. For mix design US1, the improvement of arsenic stabilization with curing time is attributed to the more favorable pH conditions for more mature stabilized forms during the TCLP test. As the cement matrix matures, calcium hydroxide becomes less prevalent and calcium silicates more dominant, so the acid neutralization capacity of the stabilized form decreases as indicated by a drop in the extract pH. The pH for extracts of mix US1 at 2, 60, 360, and 540 days was 7.97, 6.86, 5.01, and 4.96, respectively. This pH decrease provided more favorable conditions for the maintenance of the ferrous-arsenate complex.

The significant improvement in arsenic stabilization by mix designs US2, US3, and US4 can be explained by the higher iron/arsenic molar ratio of 6.47, 5.74, and 17.2, respectively. The excess amounts of iron are necessary to maintain the iron/arsenate complex under higher pH conditions during the early cure. However, at longer cure times with more favorable pH conditions, mixes with excess iron leach more arsenic and iron as shown in Figure 5-2.

The barium release in TCLP extracts reflects the amount of sulfate available for precipitation with barium. Mix US1 with a sulfate/binder molar ratio of 0.36 has insufficient sulfate and higher barium concentrations are the result. Mixes US2 and US3 have marginal ratios of 1.07 and 0.95, respectively, and barium concentrations increase moderately with curing age. This increase may be caused by the adsorption of sulfate by the binder to form ettringite. The more porous nature of the cement matrix associated with more ettringite formation is indicated by the higher releases of zinc associated with mixes of higher sulfate/binder mass ratios (mixes US2 and US4).

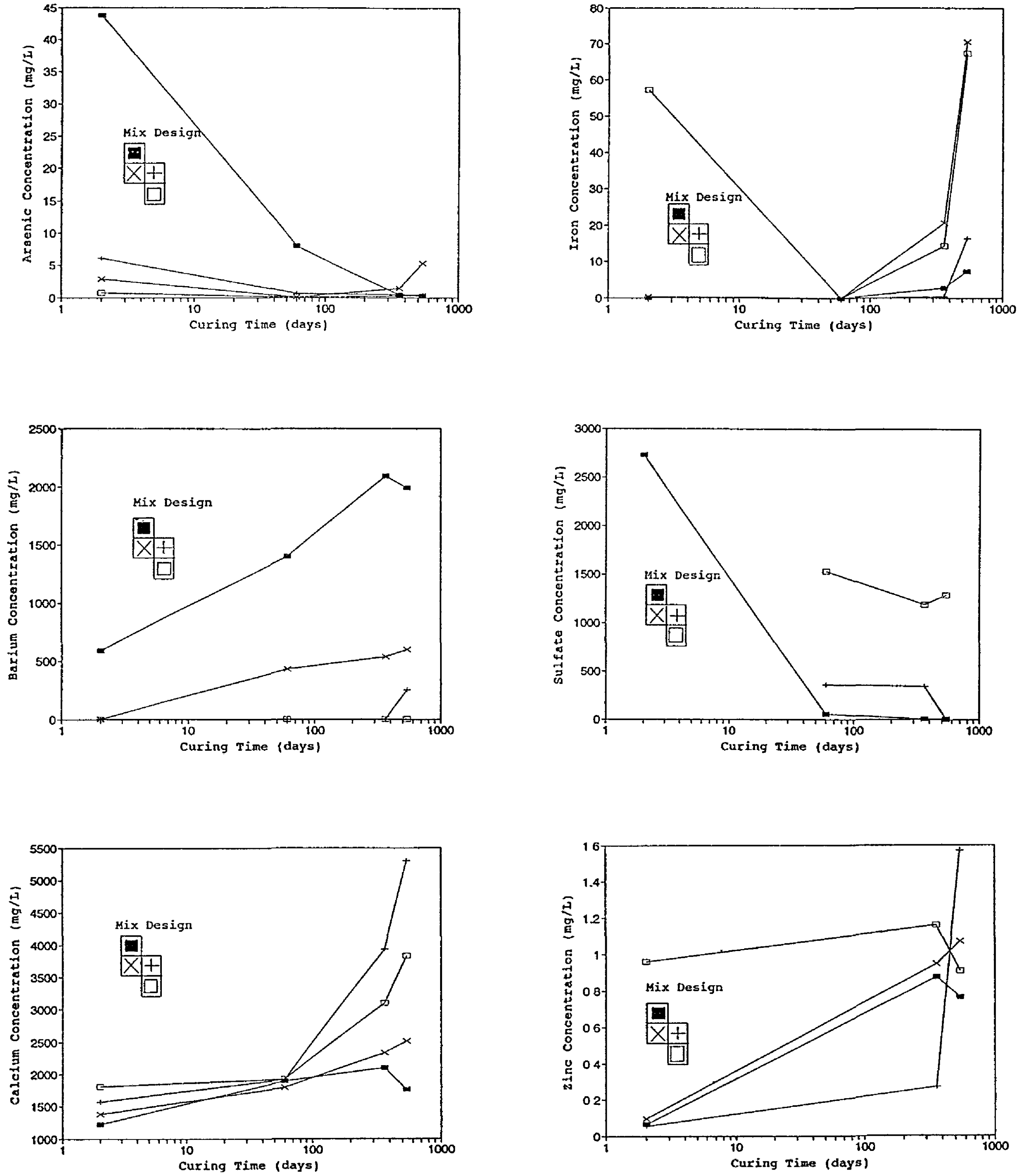

Figure 5-2. **Stabilization with Ferrous Sulfate. Mix designs given in Table 4-2.**

5.2.2 Stabilization with Ferric Sulfate

Samples of stabilized wastes were cured for 2, 60, 360, and 540 days before TCLP. For each curing time, Figure 5-3 presents results of analyses for selected metals in TCLP extracts. The effectiveness of arsenic stabilization changes significantly with curing time. The comparable performance of stabilization designs F1 (closed rectangle) and F3 (plus) in contrast with the comparable performance of design F2 (X) and F4 (open rectangle) can be explained by observing mix design parameters that are equal for comparable designs but different for contrasting designs. One such design parameter is the iron/binder mass ratio which is 0.064 for designs F1 and F3 and is 0.19 for designs F2 and F4. This observation suggests that arsenate and binder compete for iron during the initial curing time when calcium hydroxide is prevalent. A small amount of iron relative to the amount of binder (as in designs F1 and F3) could preclude the complexation of some arsenate with iron. The insufficient amount of iron in mixes F1 and F3 is also indicated by Figure 5-3 by the very low levels of iron in TCLP extracts of mixes F1 and F3 (2 and 60 day curing). Therefore, stabilization designs F1 and F3 perform poorly during initial curing times because the hydroxide phase of the binder reacts with most of the iron leaving an insufficient amount of iron to react with arsenic.

There are other reasons that help explain the success of designs F2 and F4 for short curing times. The larger amounts of iron in these mix designs allow for more fresh ferric hydroxide precipitate which strongly adsorbs arsenic. The high insolubility of ferric hydroxide and the relative abundance of it in mixes F2 and F4 yield lower TCLP pH's of 5.3 and 5.4 in those mixes. In contrast, the TCLP pH of mixes F1 and F3 was 6.8 and 7.6, respectively. The lower pH of mixes F2 and F4 provides more favorable iron-arsenate precipitation and adsorption onto fly ash surfaces (Sen and De, 1987).

Although cement curing is retarded by the presence of the waste, eventually the calcium hydroxide phase becomes less dominant. At extended curing times, another mix parameter provides evidence to explain these results. The sulfate/binder mass ratio is 0.16 for mix designs F1 and F3 and is 0.49 for mix designs F2 and F4. The relative abundance of sulfate in mixes F2 and F4 may lead to more ettringite formation which deteriorates cement by increasing porosity and causing cracking. Roy, et. al., (1992) report that the amount of excess sulfate controls the extent of ettringite formation. Therefore, stabilization designs F2 and F4 perform well early on, but deteriorate later because of a more porous matrix induced by excess sulfate. Additional evidence for the more extensive ettringite (containing aluminum) formation in mixes F2 and F4 is provided by the higher releases of aluminum to the TCLP extract.

The iron/arsenic ratio does not appear to be a critical factor in Figure 5-3. Mix F1 with an iron/arsenic molar ratio of 2.13 performs well with extensive curing. Furthermore, mix F3

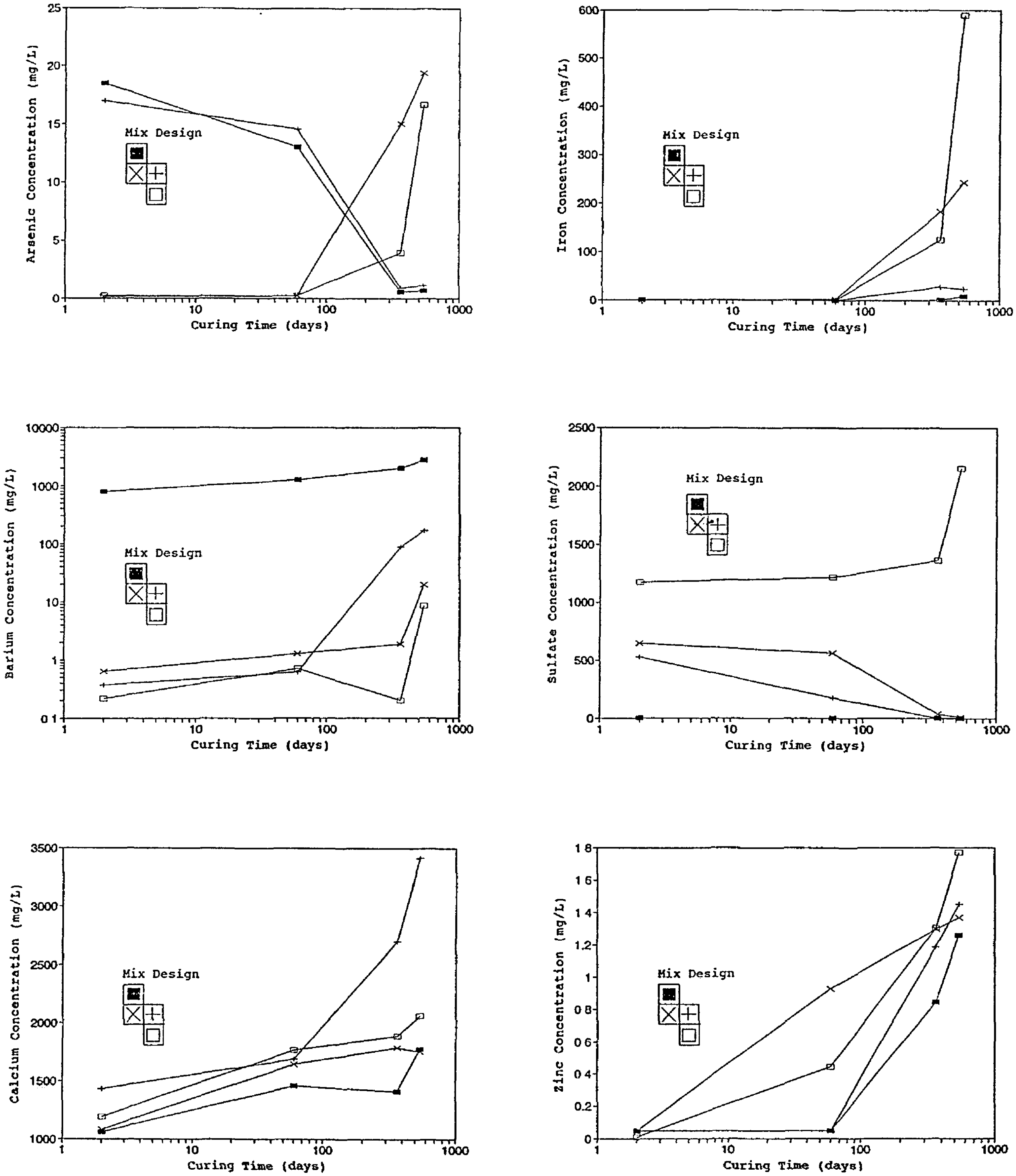

Figure 5-3. TCLP Results for Ferric Sulfate Stabilization. Mix designs defined in Table 4-3.

with an iron/arsenic molar ratio of 5.69 yields results similar to that of mix F1. Stabilization designs F2 and F4 also yield similar results but with iron/arsenic molar ratios of 6.39 and 17.1, respectively.

The barium results can be explained by sulfate/barium molar ratios. Mix F1 with a ratio of 0.45 does not have adequate sulfate to react with the barium as indicated in Figure 5-3 by the high concentrations. At the other extreme, mix F4 with a ratio of 3.6 does have an adequate amount of sulfate. The other two mixes are marginal with a ratio of 1.3. The overall trend of increasing barium concentrations with longer curing times may indicate some consumption of sulfate by the binder to form ettringite. The consumption of sulfate during ettringite formation over the long term is also indicated by Figure 5-3. The sulfate concentrations decrease over longer curing times for 3 of the 4 mixes. Only mix F4 with the highest amount of sulfate shows sulfate release from stabilized forms with longer curing times.

5.2.3 Stabilization with Aluminum Sulfate

Figures 5-4 and 5-5 present a comparison of TCLP results for arsenic and barium respectively, using as additives ferrous sulfate, ferric sulfate, or aluminum sulfate. These three-dimensional bar graphs reflect the experimental designs shown in Tables 4-2 through 4-4 in the horizontal plane with the metal concentration plotted on the vertical axis. The results associated with 60 through 540 days of curing indicate a consistent pattern for the effectiveness of additives. All mix designs at 540 days curing and three of four designs for 60 days curing indicate that the order of effectiveness is $Fe^{2+} > Fe^{3+} > Al^{3+}$. After only two days of curing, either ferrous or ferric sulfate may provide best treatment. The strong affinity of arsenic for freshly precipitated ferric hydroxide may explain why ferric sulfate can be most effective with early curing.

The possibility of long-term sulfate damage to the stabilized form is also evident from Figure 5-4. After two days of curing, more metal addition always means more arsenic removal. In the early curing, the binder succesfully competes for the metal additive. On the other hand after 540 days of curing, more metal addition always results in less arsenic removal in every mix design. This may be the result of excess sulfate.

The consistent pattern of competition of waste and binder for metal during early curing can also be seen by a comparison of mixes two and three with approximately equal metal/arsenic ratios but with a binder/waste ratio of 0.15 and 0.40 respectively. Mix two with the lower amount of binder allows more metal for precipitation of arsenic so arsenic concentrations are predictably lower. After 540 days of curing, mix two has higher arsenic concentrations because of more sulfate damage indicated by the higher sulfate/binder ratio of mix two compared to mix three.

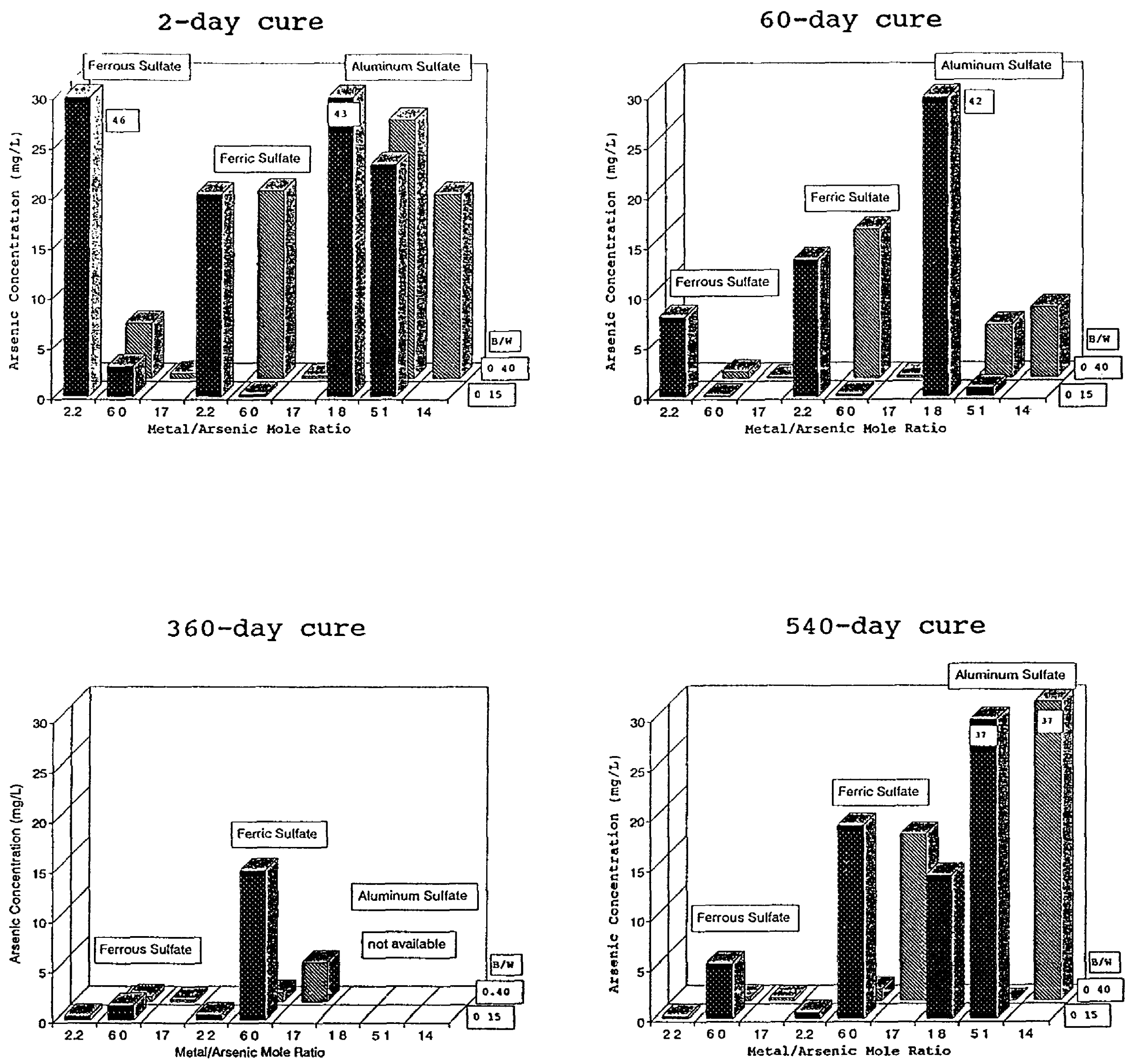

Figure 5-4. Comparison of TCLP Data for Arsenic.

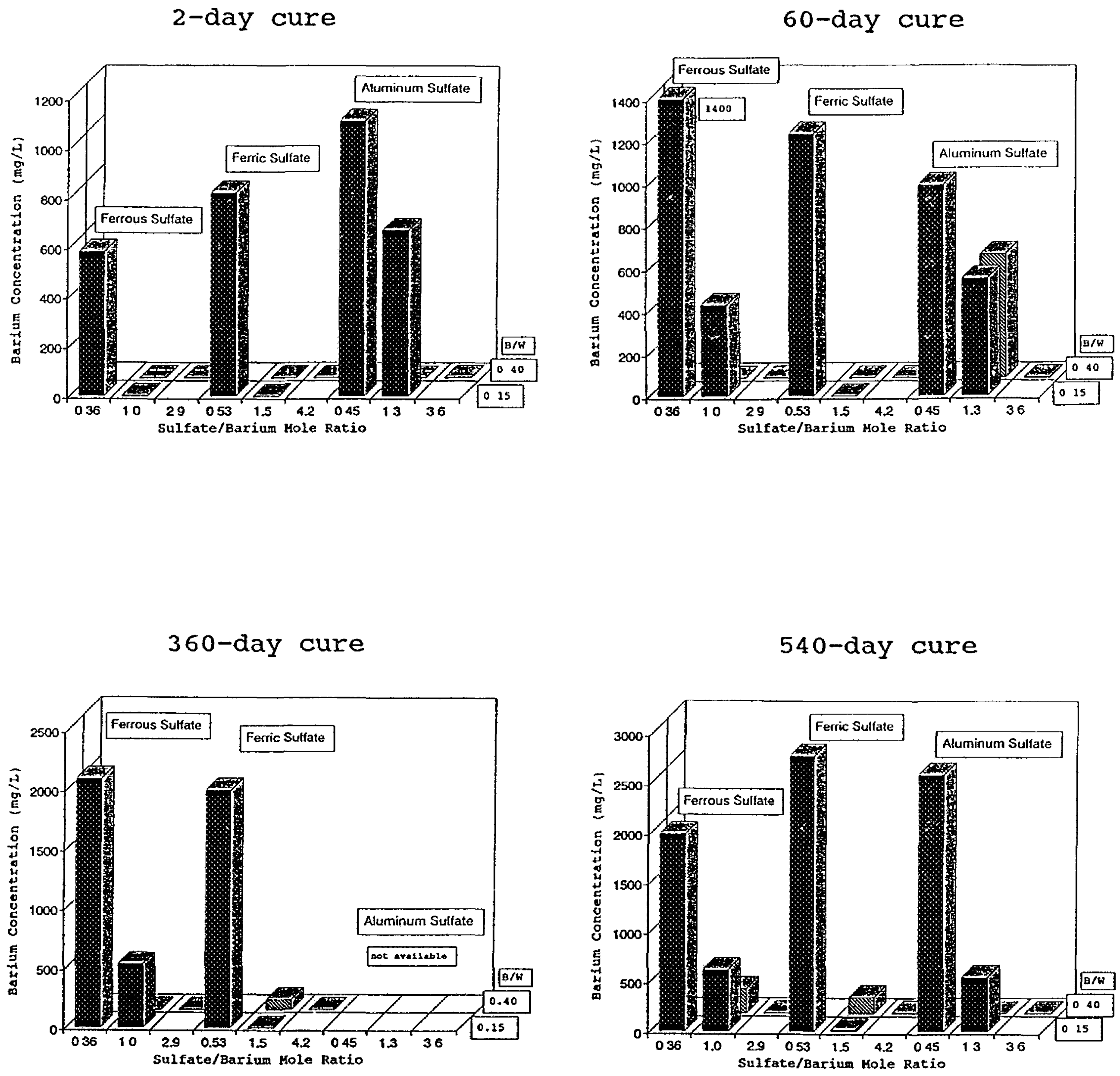

Figure 5-5. Comparison of TCLP Data for Barium.

For barium stabilization, the treatment effectiveness depends only on the amount of sulfate and is independent of the metal counterion used in the additive. This indicates that the removal mechanism is by barium sulfate precipitation.

5.2.4 Percent Retention in TCLP

To investigate the effect of curing of the cement lattice on S/S, a comparison of extractability was made between individual unreacted components and cured S/S mixtures by using a mass balance approach. Retention is defined as the fraction of total metal in the S/S mixture not extracted by TCLP. Percent retention figures were calculated for individual components, ferric sulfate S/S mixes (Table 4-2), and ferrous sulfate S/S mixes (Table 4-3). Using data on the nitric acid digestion of cement, fly ash (Table 3-3) and the D004/D005 waste (Table 3-1), the total amount of each metal was calculated component by component for each S/S mixture. The percent retention of individual S/S components was calculated from the TCLP data of those individual components as reported in Tables 3-1 and 3-3.

The retention percentages for important elements are shown graphically in Figure 5-6 for mixes one and four using ferrous sulfate or ferric sulfate stabilizations. The elements arsenic and barium are primarily found in the waste. Potassium and manganese are found mainly in the cement. Calcium occurs in all components of the S/S mix. The decreasing percent retention for calcium as the S/S mix stabilizes is possible evidence that the cement lattice is degrading as the curing reactions take place. Even when about half the calcium in the S/S mix has been extracted out in the TCLP process, indicating severe destruction of the cement lattice, the elements listed as "Tightly Bound" in Table 5-1 are retained more than 90%. Therefore, we can conclude that "Tightly Bound" elements are bound through different mechanisms than calcium ions.

Using TCLP results on the cured S/S mixture, the effect of the curing reactions of the cement lattice on individual elements could be examined. Table 5-1 lists elements which are tightly bound (>90%) by the cured cement lattice and those which are only loosely bound (<50%). Some elements appear to be more tightly bound at a short 2-day curing time but quite loosely bound at longer 540-day curing times. Arsenic and barium are tightly bound when enough additive is in the S/S mix to ensure reaction. The retention percentage of manganese is very interesting, with low retention in good mixes for arsenic and barium stabilization but high retention in poorer S/S mixtures.

Boron is very extractabile from the raw waste and as well as from S/S mixtures. This can be interpreted by remembering that sodium borates are generally soluble in aqueous matrices. The borate anions are unlikely to be bound to the anionic silicate matrix of the cement lattice.

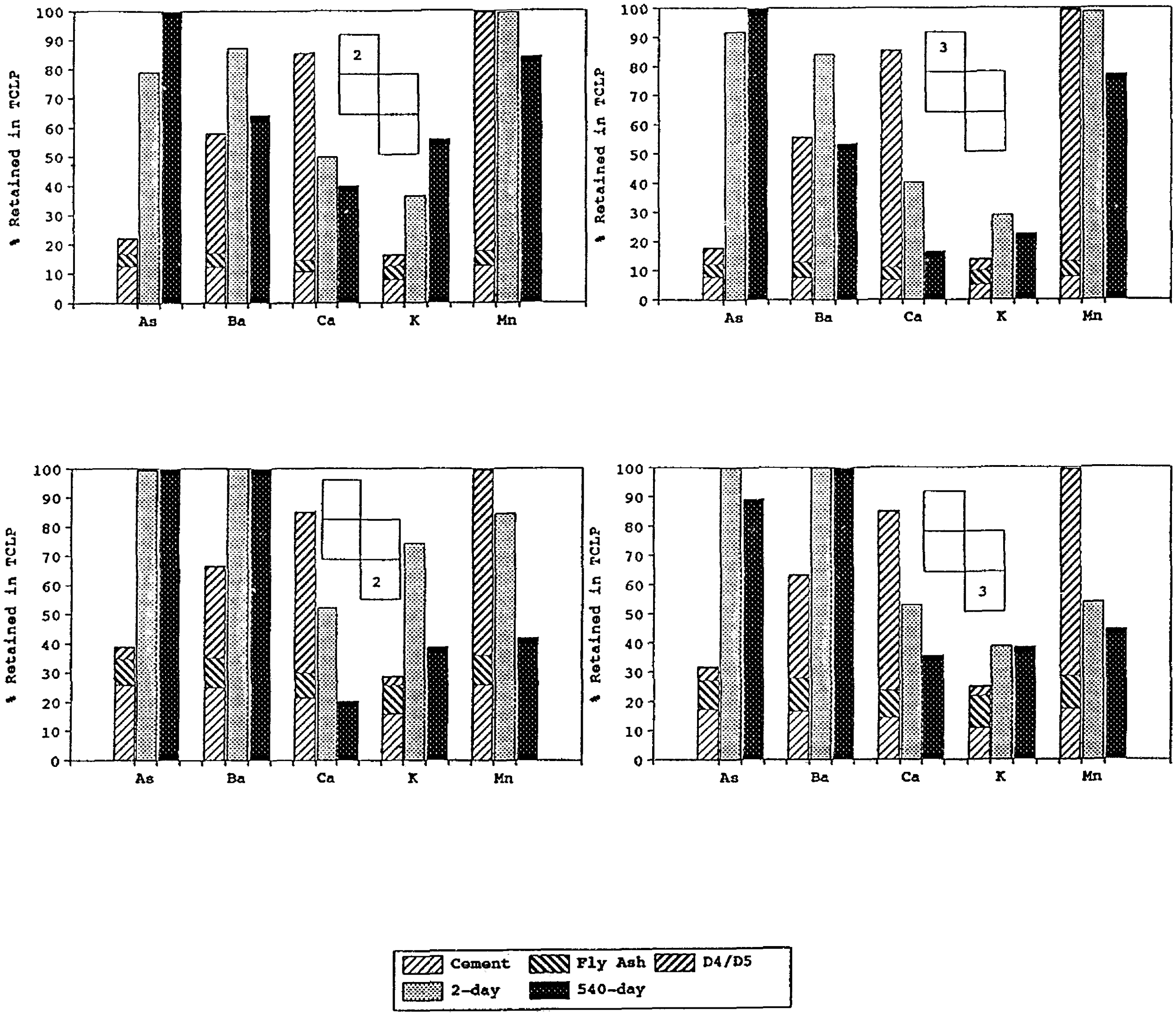

Figure 5-6. Percent Extraction by TCLP

Table 5-1. Classification of Elements by Retention in Cured S/S

Loosely Bound(<50%) in Cured S/S	Tightly Bound(>90%) in Cured S/S	Binding Degrades as S/S Cures
B	As	Al
Ca	Ba	Mn
K	Fe	
Mg	P	
Na	Sb	
	Zn	

5.2.5 Correlation

Another way of viewing the same data presented in Section 5.2 is to correlate "tracer" metals of specific stabilization components with arsenic, barium and each other. Tracer metals are TCLP-leachable metals found principally in one stabilization component but not in others. Accounting for differing amounts of materials in the mix design and using information in Tables 3-1 and 3-2, some tracer metals yield at least three times more leachable metals from a component (e.g. cement, fly ash, waste) compared to others.

Table 5-2 presents correlation matrices for all the data and for ferrous sulfate and ferric sulfate S/S separately. Sodium, potassium, and boron are principally from the waste. Correlations of these elements with arsenic is insignificant which may indicate that arsenic is not uniformly distributed throughout the waste or that arsenic is bound through a different mechanism. It may also be a result of comparing larger amounts of sodium, potassium, and boron with small amounts of arsenic. Barium is present in larger amounts and is moderately correlated with these waste elements. Calcium, a binder and waste component, is not significantly correlated with arsenic or barium.

Table 5-3 presents selected significant correlations of TCLP data from all S/S designs for 2 through 540 days. Iron and arsenic have a low correlation up to 60 days of curing, but significant correlations were found after 365 days. This observation reflects how some short term stabilizations exceed arsenic TCLP standards because of the competition of fresh concrete in binding with iron. With additional curing, arsenic and iron either remain encapsulated or leach out together. If significant iron and arsenic are leaching out, then sulfur also tends to be high as evidenced by the increasing iron-sulfur correlation with more cure time.

Table 5-2. Correlation Matrices for Stabilizations Across All Curing Times

a) Correlation Marix for Ferric Stabilization

	As	Ba	Ca	Fe	Mg	Mn	Na	B	K	S	Zn
As	100										
Ba	-15	100									
Ca	-26	-26	100								
Fe	37	-27	8	100							
Mg	-46	-39	64	41	100						
Mn	-25	-36	27	58	77	100					
Na	7	52	4	3	-27	6	100				
B	12	48	-20	-17	-55	-17	92	100			
K	23	69	-2	-19	-46	-35	83	80	100		
S	-16	-47	-14	41	53	49	-72	-76	-86	100	
Zn	-15	-1	58	61	62	72	44	13	12	1	100

b) Correlation Matrix for Ferrous Stabilization

	As	Ba	Ca	Fe	Mg	Mn	Na	B	K	Zn
As	100									
Ba	8	100								
Ca	-38	-28	100							
Fe	-17	-20	17	100						
Mg	-45	-29	92	25	100					
Mn	-46	-18	77	43	83	100				
Na	18	43	-2	-12	5	6	100			
B	11	52	-9	-10	-2	-3	98	100		
K	42	15	36	-11	25	2	56	50	100	
Zn	-13	-1	-22	-33	-29	0	0	0	-29	100

c) Ferrous Sulfate and Ferric Sulfate S/S

	As	Ba	Ca	Fe	Mg	Mn	Na	B	K	S
As	100									
Ba	6	100								
Ca	-47	-22	100							
Fe	6	-22	1	100						
Mg	-52	-35	76	29	100					
Mn	-50	-26	61	45	80	100				
Na	17	49	-12	8	-16	1	100			
B	22	47	-31	-1	-31	-16	92	100		
K	33	52	5	-10	-21	-21	73	68	100	
S	-5	-36	-26	37	23	22	-39	-32	-67	100

Table 5-3. Correlation of All S/S Data: Selected Curing Times

(a) Two Day Curing Time

	As	Ba	Ca	Fe	Mg	Mn	Na	B	K	S
As	100									
Ba	70	100								
Ca	-38	-66	100							
Fe	-30	-25	67	100						
Mg	-49	-49	5	22	100					
Mn	-53	-37	0	30	92	100				
Na	56	81	-84	-46	-40	-35	100			
B	41	76	-89	-45	-28	-24	92	100		
K	64	85	-45	-26	-73	-59	67	60	100	
S	-26	-38	-20	-10	89	75	-23	-6	-66	100

(b) Sixty Day Curing Time

	As	Ba	Ca	Fe	Mg	Mn	Na	B	K	S
As	100									
Ba	45	100								
Ca	-59	-25	100							
Fe	-7	-26	-6	100						
Mg	-51	-73	48	30	100					
Mn	-71	-39	62	0	51	100				
Na	37	50	-57	6	-60	-35	100			
B	22	38	-48	10	-50	-28	94	100		
K	67	66	-39	-15	-60	-68	73	65	100	
S	-38	-60	12	22	52	46	-65	-54	-83	100

(c) 365 Day Curing Time

	As	Ba	Ca	Fe	Mg	Mn	Na	B	K	S
As	100									
Ba	-33	100								
Ca	-38	-51	100							
Fe	92	-45	-42	100						
Mg	-24	-75	76	-3	100					
Mn	41	-70	9	62	57	100				
Na	60	33	-59	36	-84	-28	100			
B	57	40	-63	33	-88	-39	98	100		
K	25	44	-13	-12	-69	-72	73	77	100	
S	11	-27	-27	48	36	61	-36	-33	-75	100

(d) 540 Day Curing Time

	As	Ba	Ca	Fe	Mg	Mn	Na	B	K	S
As	100									
Ba	-42	100								
Ca	-46	-48	100							
Fe	82	-44	-37	100						
Mg	-19	-66	88	7	100					
Mn	23	-74	58	30	66	100				
Na	21	42	-42	-16	-52	-47	100			
B	23	46	-50	-18	-63	-53	99	100		
K	-10	37	4	-41	-13	-26	84	78	100	
S	52	-27	-27	91	19	17	-32	-36	-48	100

Another significant observation is the increasing calcium-magnesium correlation with cure time. Both calcium and magnesium are principally from the binders as shown in Table 3-3. One explanation for some of the failures in stabilization was matrix deterioration due to sulfate damage. An increasing calcium-magnesium correlation over cure time reinforces that conclusion.

As shown in Table 5.4, column leaching data present many more significant correlations as shown by correlation results using the US1 mix design. Correlation results from the US4 mix design are shown in Table 5-5. These mix designs are defined in Table 4-3. Each mix design underwent leaching with three different leachants after two days of curing. These significant correlations illustrate that the rate of metal release follows a similar pattern in many cases. This result does not necessarily imply that the total amount of metals leached will correlate.

5.3 Column Leaching

5.3.1 Model Development

During column extraction, stabilized waste components located in chemically reactive regions (such as calcium hydroxide, CH) of the S/S matrix are easily mobilized. Initially, the dissolution of the CH phase occurs at the head end of the column and a "front" of CH dissolution proceeds toward the column exit as time progresses. Waste and binder components will transport through this column in two different ways depending on their solubility and molecular size.

If the components are insoluble in the extraction fluid, then components mobilized at the head of the column because of CH dissolution are trapped farther down the column in the undissolved stabilization matrix. As the deterioration of the CH phase proceeds toward the column exit, the exit portion of the column becomes filled to capacity, and breakthrough is observed. Under these conditions the concentration of the component in the column eluant steadily increases similar to an ion exchange breakthrough curve. After breakthrough, concentrations decrease exponentially.

As explained in Chapter Two, the more reactive CH volume will decrease with cure time as the less reactive CSH phase develops. Samples with higher fractions of reactive regions have had less time to cure. Higher fractions of reactive regions also imply that components will diffuse through the column more quickly and smaller breakthrough volumes are observed.

If the component leached from the reactive region is not reprecipitated or captured by sample solids nearer to the column exit, then exponentially decreasing concentrations are observed in the column eluant. If the logarithm of the concentration in the column eluant is plotted against the volume of eluant issuing from the column, a straight line with a negative

Table 5-4. Correlation Matrices for Column Leaching, US1 Mix Design, 2-day Cure Time

(a) DI Leachant

	As	B	Ba	Ca	Fe	K	Mg	Na	S	Zn	pH
As	100										
B	81	100									
Ba	-48	-74	100								
Ca	87	96	-84	100							
Fe	87	94	-77	98	100						
K	89	94	-81	100	98	100					
Mg	90	94	-80	100	98	100	100				
Na	90	94	-80	100	98	100	100	100			
S	90	93	-80	100	98	100	100	100	100		
Zn	5	-13	-20	53	6	9	9	9	10	100	
pH	-54	-90	58	-74	-73	-72	-71	-71	-69	37	100

(b) pH = 3 Leachant

	As	B	Ba	Ca	Fe	K	Mg	Na	S	Zn	pH
As	100										
B	92	100									
Ba	-55	-77	100								
Ca	92	98	-73	100							
Fe	72	68	-61	81	100						
K	88	91	-83	94	88	100					
Mg	88	80	-57	89	95	92	100				
Na	89	91	-82	94	88	100	92	100			
S	86	85	-78	89	91	98	93	99	100		
Zn	63	59	-18	71	66	55	75	55	55	100	
pH	-47	-58	52	-39	11	-38	-7	-37	-28	18	100

(c) pH = 8.7 Leachant

	As	B	Ba	Ca	Fe	K	Mg	Na	S	Zn	pH
As	100										
B	96	100									
Ba	-39	-37	100								
Ca	88	91	-68	100							
Fe	85	84	-61	93	100						
K	87	90	-70	100	93	100					
Mg	87	91	-69	100	93	100	100				
Na	90	94	-56	95	90	94	95	100			
S	85	87	-65	98	96	98	98	91	100		
Zn	67	68	-57	66	58	66	66	69	56	100	
pH	-93	-98	27	-85	-77	-83	-84	-86	-80	-68	100

Table 5-5. Correlation Matrices for Column Leaching, US4 Mix Design, 2-day Cure Time

(a) DI Leachant

	As	Ni	SO4	Zn	Ca	Pb	Mg	pH
As	100							
Ni	97	100						
S	97	99	100					
Zn	91	97	98	100				
Ca	94	95	98	96	100			
Pb	-20	-16	-13	5	-2	100		
Mg	97	99	99	97	98	-12	100	
pH	62	66	70	63	68	-23	69	100

(b) pH = 3 Leachant

	As	Ba	Ni	S	Ca	Zn	Pb	Mg	Cr	pH
As	100									
Ba	69	100								
Ni	-68	-41	100							
S	-76	-43	99	100						
Ca	19	-1	24	13	100					
Zn	41	44	01	-3	-9	100				
Pb	60	36	-74	-74	-22	54	100			
Mg	-24	-08	81	77	26	32	-53	100		
Cr	18	38	-67	-58	-75	3	53	-54	100	
pH	-63	-46	83	81	81	-38	-82	54	-77	100

(c) pH = 8.7 Leachant

	As	Ni	S	Zn	Ca	Cr	Pb	Mg	pH
As	100								
Ni	-48	100							
S	16	77	100						
Zn	01	52	68	100					
Ca	09	65	85	49	100				
Cr	19	24	45	60	0	100			
Pb	-15	-20	-33	7	-47	31	100		
Mg	15	32	52	19	85	-43	-58	100	
pH	45	48	87	56	85	16	-49	73	100

slope results. The slope of the line is steeper if the reactive region makes up a larger fraction of the sample or the concentration of the waste component in the reactive region is larger.

Once the reactive CH region has been largely leached from the sample by the eluant, then the less reactive regions of the sample become the major sources of leached components. These silicate networked regions, labeled here as CSH or calcium silicate hydrate, dissolve very slowly. The leaching process from this region follows first-order kinetics so that a plot of the logarithm of the component concentration in the eluant versus the eluant volume issuing from the column is linear. A more negative slope indicates the component is more loosely bound, and a less negative slope indicates tightly bound component.

For components which are not reprecipitated in the column, a simple kinetic model may be illustrative. Extraction of components from a solid phase follows first-order kinetics with the rate law

$$-dc/dt = k\ c \qquad (1)$$

where c = concentration in the column effluent [mg/L];
k = first-order rate constant [1/sec].

Equation (1) can be integrated to yield

$$c = c_o\ e^{-kt} \qquad (2)$$

where c_o = concentration at time = 0.

Waste encapsulated in the reactive CH phase is easily extracted with rate constant k_1. The extraction of waste encapsulated in the less reactive CSH phase proceeds at a slower rate modeled with constant k_2. If both processes are assumed to be taking place simultaneously and independently, then the total rate of leaching is the sum of the two rates. The final result of the model is that the concentration in the extract is

$$[\text{extract}] = \{\text{const}\}\{CHS_o\exp(-k_1t) + CH_o\exp(-k_2t)\} \qquad (3)$$

where $k_1 > k_2$ and CHS_o and CH_o are the initial amounts of contaminants residing in the CSH and CH phases.

A prediction of this theory is that a systematic study of column leaching will reveal the relative amount of labile CH phase in samples and the behavior of individual waste components with respect to the development of the concrete lattice.

5.3.2 Column Extraction Results

Column extraction experiments were all carried out with a flow rate of 3.0 mL/min and a 50.0-gram sample. Figure 5-7 shows data for calcium extraction from US1 and US4 ferrous sulfate-stabilized waste mixes. Data for three eluants are presented: pH 3.00 acetic acid, deionized water, and pH 8.77 sodium acetate. Two S/S mix designs are shown, both with two day cure times. Calcium is not reprecipitated in the column and therefore the shape of the data is that represented by Equation (3) above. Unfortunately, the density of data was not sufficient in the beginning of the experiment to accurately define k_1 in many cases. It is important to note that the logarithmic vertical axis does not always show the same range because the concentrations being presented vary widely. The general shape of the data obtained illustrates the validity of the model developed above. Table 5-6 presents the model parameters for the latter part of the curve, CSH extraction, for the calcium data shown in Figure 5-7.

Table 5-6. Column Data Model Parameters for Calcium

Mix	Cure Time	Eluant	Intercept[a]	Slope
US1	2 days	pH 3.00	2.98	$-6x10^{-5}$
		DI H_2O	2.44	$1x10^{-5}$
		pH 8.77	2.71	$-7x10^{-5}$
US4	2 days	pH 3.00	2.84	$-9x10^{-5}$
		DI H_2O	2.30	$-2x10^{-4}$
		pH 8.50	2.42	$-3x10^{-4}$

(a) Intercept: log of the calcium concentration in mg/L

Examination of the graphs in Figure 5-7 shows that the early positive deviations from the CSH fitted line, which correspond to CH extraction, last until approximately 200 mL of eluant has passed the column for all eluants and mixes. Figure 5-8c shows the results for small volumes of DI H_2O eluant for a US1 mix cured for 390 days. Not enough data was gathered to accurately define the large volume slope but the marked difference in shape of the curve illustrates the changes apparent as S/S mixes cure.

The data for barium concentrations in column extractions of US1 S/S mix cured for two days is shown in Figure 5-9. Data is not shown for good S/S mix designs such as US4 because all barium concentrations in the eluant were at the analytical detection limit; barium is not extractable from this S/S mix. The barium data for poor S/S mixes at two day cure times have shapes expected for a system undergoing breakthrough. The large-volume exponential line meets the breakthrough rising curve at about

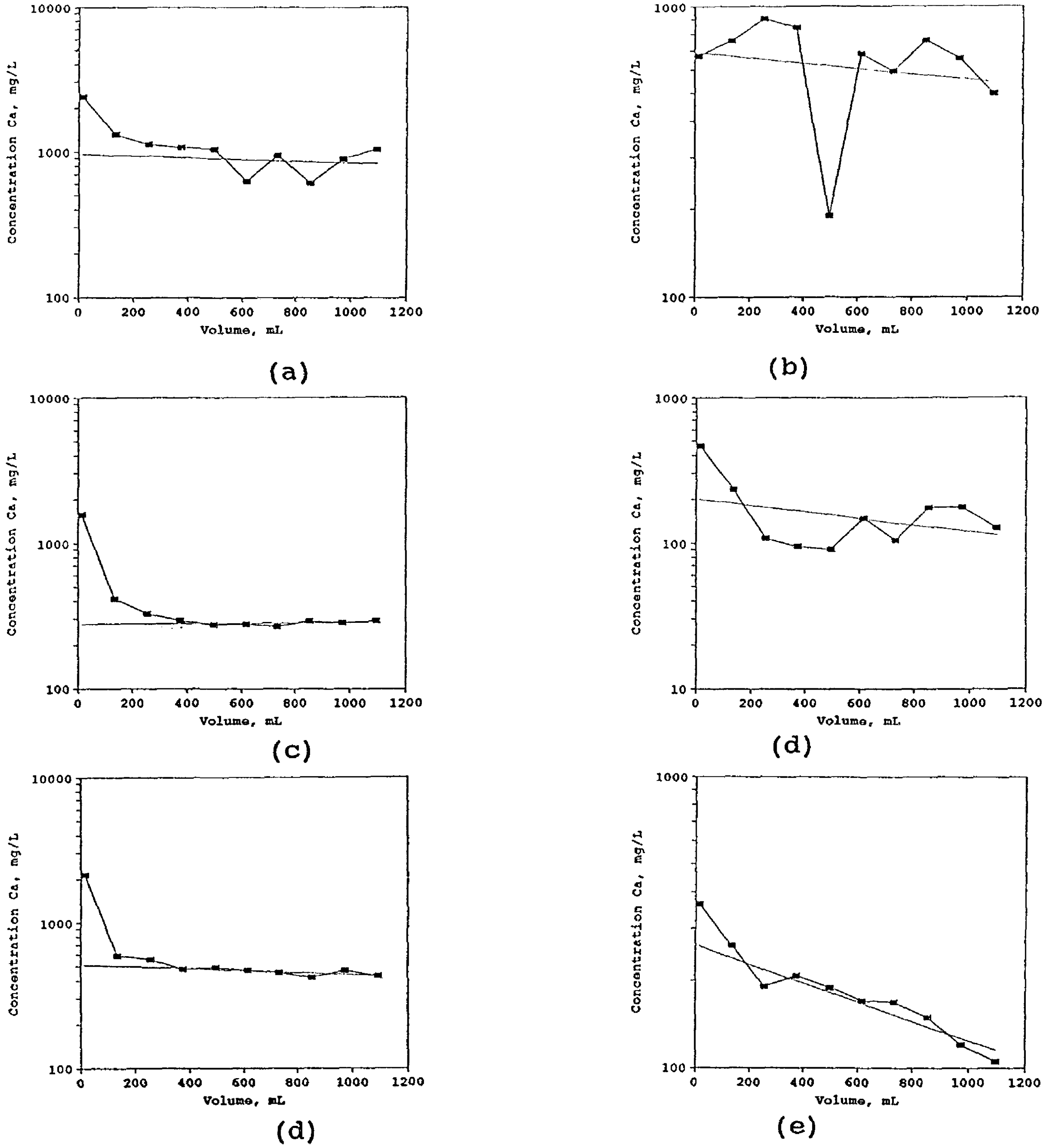

(a) (b)

(c) (d)

(d) (e)

Figure 5-7. Column Extraction Data for Calcium.
(a) Mix US1 (Table 4-2), pH 3.00 Eluant.
(b) Mix US4, pH 3.00 Eluant.
(c) Mix US1, DI H_2O Eluant.
(d) Mix US4, DI H_2O Eluant.
(e) Mix US1, pH 8.77 Eluant.
(f) Mix US4, pH 8.50 Eluant.
All samples cured for two days.

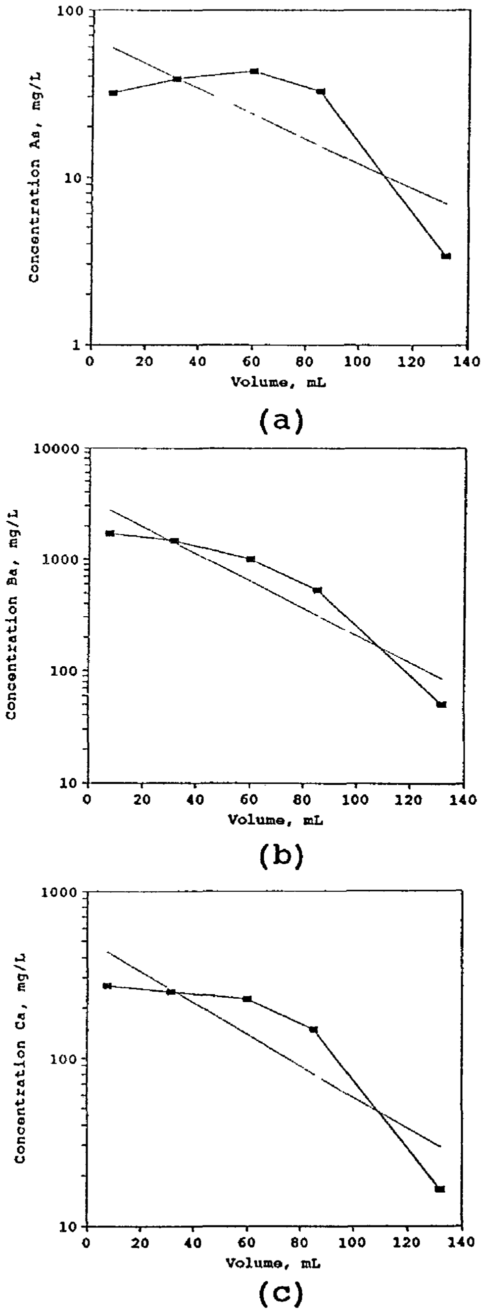

Figure 5-8. Column Extraction Data, 390-day Cure, Mix US1, DI H_2O Eluant.

(a) Arsenic (b) Barium (c) Calcium

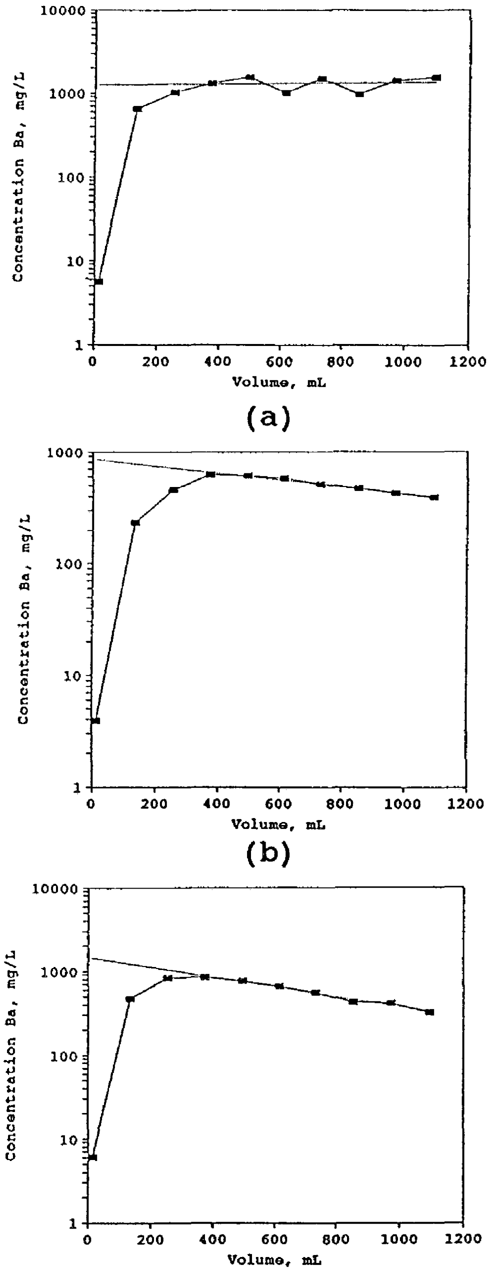

(c)

Figure 5-9. Column Extraction Data for Barium, Mix US1, 2-day Cure.

(a) pH 3.00 Eluant. (b) DI H_2O Eluant. (c) pH 8.77 Eluant

400 mL of eluant in all cases, indicating little pH dependence in the extractability of barium. However, examination of the model parameters for the CSH extraction region data shown in Table 5-7 indicates that barium extractability from a CSH matrix into a neutral solution is less than into acidic or basic solutions.

Table 5-7. Column Data Model Parameters for Barium.

Mix	Cure Time	Eluant	Intercept	Slope
US1	2-days	pH 3.00	3.10	$2x10^{-5}$
		DI H_2O	2.93	$-3x10^{-4}$
		pH 8.77	3.17	$-6x10^{-4}$

Comparison of the shapes of the barium extraction concentration curves for samples cured for two days with the shape for the same S/S mix composition cured for 390 days (Figure 5-8b) shows the drastic changes in column extraction concentrations as S/S mixes cure.

Figure 5-10 shows column extraction data for arsenic. The quality of the fit of the data to the exponential decay curve seems to be somewhat poorer than for the other elements. Reasons for this might include penetration of arsenic-containing solid particles through the eluant filtration system at the exit of the column or variability due to low concentrations. After taking this into account it is still apparent that arsenic leaching does not fit either of our simple models very well. Evidence of breakthrough-type behavior is seen in Figure 5-10, parts b, c, and f. The data points were not taken at short enough intervals to define the early behavior accurately. If the first data point is significant, then the general shape of independent first-order processes with different rate constants can be ascertained. Figure 5-8a shows the arsenic data for S/S mixes cured for 390 days. The drastic change in shape again illustrates the effects of reducing the fraction of CH phase present in the S/S mix as the sample cures.

Model parameters for the arsenic data are in Table 5-8. The relative independence from the eluant pH of the slope for poor S/S formulations indicates that the extraction of arsenic from CSH lattices fortified with ferrous sulfate additive is relatively independent of pH. The changes in slope and intercept from a poor (US1) to a good (US4) S/S formulation indicate the improvement in arsenic stabilization taking place.

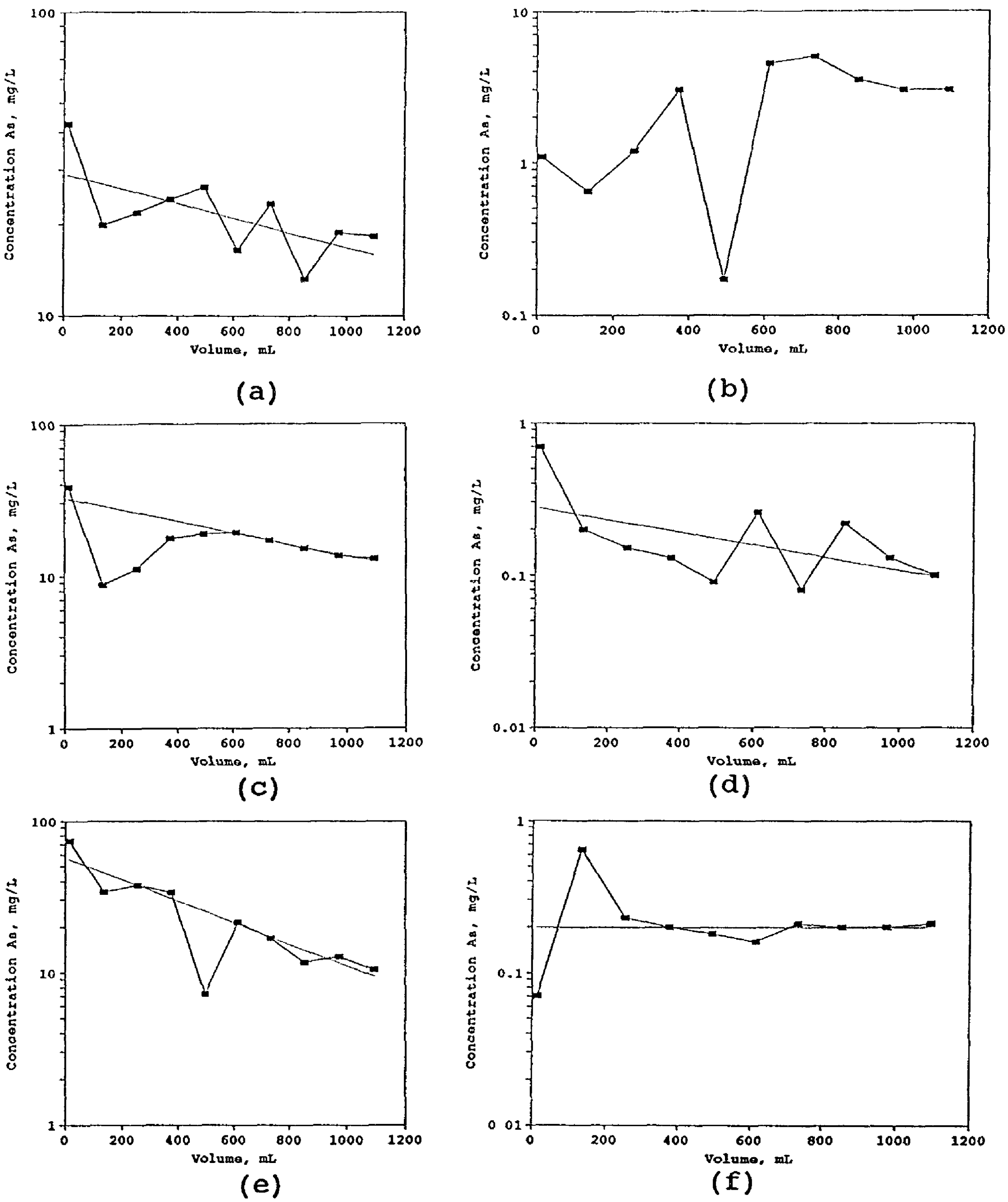

Figure 5-10. Column Extraction Data for Arsenic.

(a) Mix US1 (Table 4-2), pH 3.00 Eluant.
(b) Mix US4, pH 3.00 Eluant.
(c) Mix US1, DI H_2O Eluant.
(d) Mix US4, DI H_2O Eluant.
(e) Mix US1, pH 8.77 Eluant.
(f) Mix US4, pH 8.50 Eluant.
All samples cured for two days.

Table 5-8. Column Data Model Parameters for Arsenic

Mix	Cure Time	Eluant	Intercept	Slope
US1	2-days	pH 3.00	1.47	$-2x10^{-4}$
		DI H_2O	1.51	$-4x10^{-4}$
		pH 8.77	1.69	$-7x10^{-4}$
US4	2-days	DI H_2O	-0.55	$-4x10^{-4}$
		pH 8.50	-0.70	$-2x10^{-6}$
US1	390-days	DI H_2O	1.82	$-7x10^{-3}$

5.4 Calorimetric Analyses of Hydration Reactions

Figures 5-11 and 5-12 present data for reactions of cement with sand and cement with fly ash and sand. The ordinate is the average temperature of the tops and bottoms of two identical reaction mixtures (four points). The initial rise seen for the first three to five data points represents the time required to complete mixing of the sample, place the sample in the calorimeter, install the thermocouples and thermal isolation and achieve thermal uniformity. As can be seen in Figure 2-4, the initial hydration exotherm is complete in a cement paste sample in less than 30 minutes. The stage 3/stage 4 exotherm takes place about 500 to 700 minutes after mixing. The last exotherm experimentally observed normally takes place around 2000 minutes after mixing.

In the cement/sand mixture (Figure 5-11) the stage 3/ stage 4 is observed about 800 minutes after mixing. The first hydration isotherm was complete before data collection began. Small isotherms, about equal to the diurnal noise in the experiment, can be seen at 1700 and 2100 minutes and may be the second peak noted in Figure 2-2.

In the cement/fly ash/sand mixture (Figure 5-12) the tail of the initial hydration exotherm can be seen before 200 minutes. The stage 3/stage 4 exotherm (C_3S hydration) has been delayed to about 1000 minutes due to dilution of the matrix by the sand. The composition of the mixture was a "good mix" (mix 4, Tables 4-2 and 4-3) with fine sand substituting for the hazardous waste. The shoulder at 1700 minutes probably corresponds to C_3A hydration (Figure 2-4) although it might be due to diurnal laboratory temperature changes.

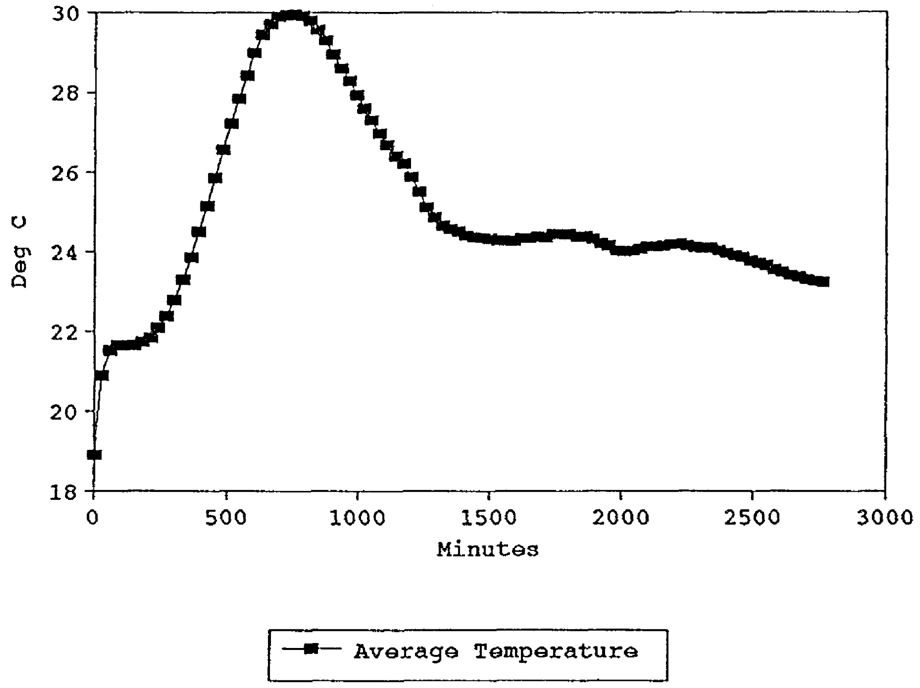

Figure 5-11. Calorimetric Curve for Cement-Sand Mix

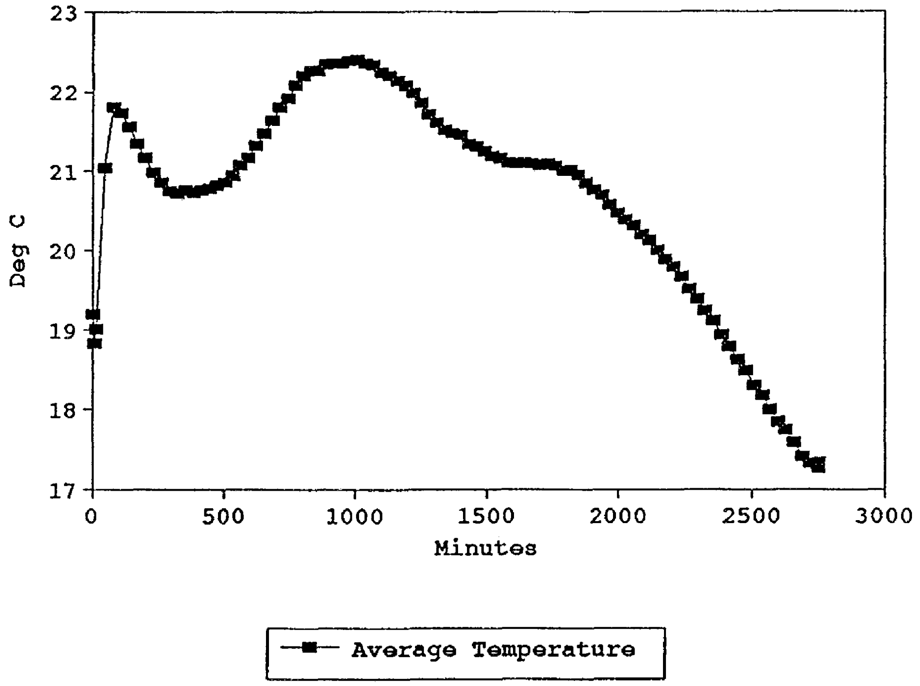

Figure 5-12. Calorimetric Curve for Cement, Fly Ash & Sand Mix

Figures 5-13 and 5-14 show the data for ferrous sulfate and ferric sulfate stabilization additives in a lean stabilized mix with a binder/waste ratio of 0.15 (mixes US1 and F1 in Table 4-2 and 4-3). Because only 10% of the total mass of the reacting system is cement/fly ash binder, the reactive ingredients are quite dilute and the rate of chemical reaction is slower. As a result, the initial hydration exotherm is observed about 80 minutes after mixing and the cement-hardening hydration reaction exotherms are much smaller and delayed more than 10%. The exotherms from the slower reactions are difficult to distinguish from experimental and ambient noise. The data show that hazardous waste stabilization mixtures will cure much slower than conventional construction concretes.

In Figures 5-15 and 5-16 are the calorimetric data using ferrous sulfate and ferric sulfate stabilization additives in richer cement/fly ash stabilizing mixes, US4 and F4. These mixes are 16% cement/fly ash binder by mass so that the chemical reactions of the binder are somewhat faster. The initial hydration isotherm has peaked by 80 minutes after mixing. The 800-minute isotherm seen in sand mixes is discernable in the ferrous sulfate experiment, although the peak is broader and less well-defined. This is probably a result of inhibition of the hydration reactions by the iron and sulfate present in excess in the mixture. The ferric sulfate experiment in Figure 5-16 was terminated early due to failure of laboratory temperature controls, leading to a widely drifting baseline.

The conclusions of the calorimetric study are that the hardening hydration reactions of stabilized waste mixtures are inhibited as a result of dilution of the reactive ingredients by the waste and through chemical interference by waste components and stabilizing additives.

5.5 Arsenite Stabilization

5.5.1 Ferrous and Ferric Sulfate Stabilization

To investigate the effect of arsenic oxidation number on stabilization, a series of experiments were carried out with a synthetically-prepared waste with a known amount of arsenic in a known oxidation state.

In Table 5-9, stabilization with ferrous sulfate and ferric sulfate is compared using a F006 waste containing sodium arsenate. The different values for the additive/waste mass ratio for ferric and ferrous sulphate were assigned so that an equal number of moles of iron were added in either case. For a binder/waste of 0.15, ferrous sulfate is significantly more effective for two reasons: the ferrous arsenate solubility product is less than the ferric arsenate solubility product; and the arsenate anions must compete with the hydroxyl ion for precipitation with the ferric ion. For a binder/waste of 0.40 with more abundance of calcium

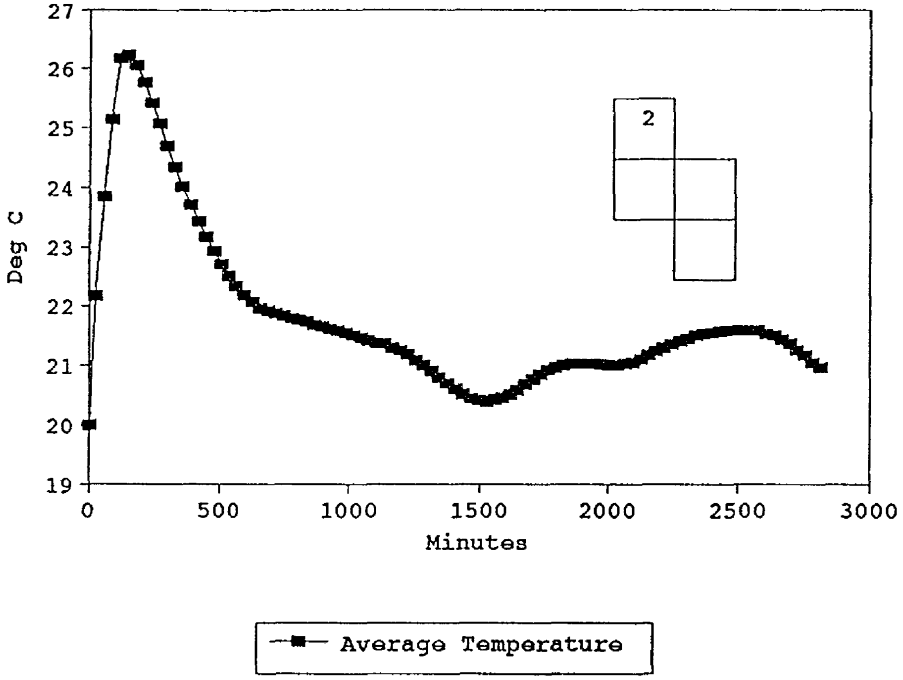

Figure 5-13. **Calorimetric Curve for Mix Design US1.** (Appendix A)

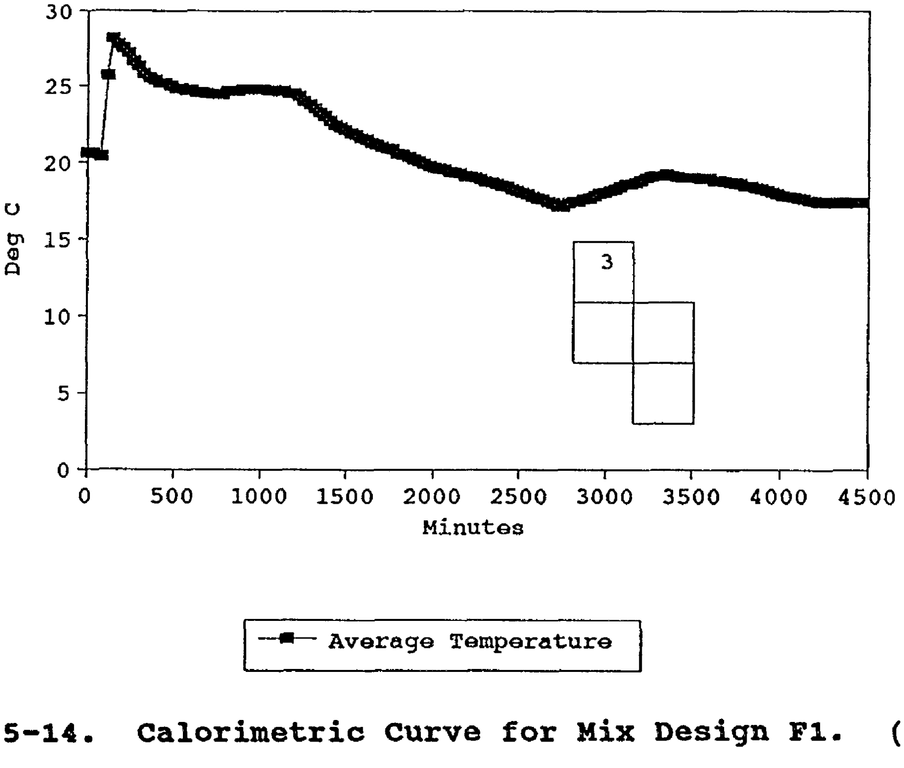

Figure 5-14. **Calorimetric Curve for Mix Design F1.** (Appendix A)

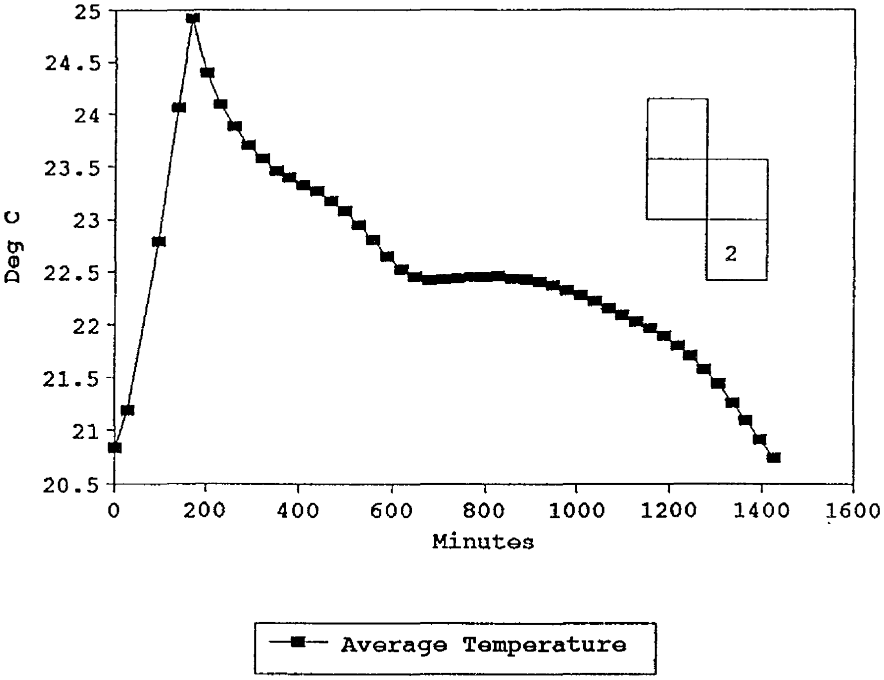

Figure 5-15. Calorimetric Curve for Mix Design US4. (Appendix A)

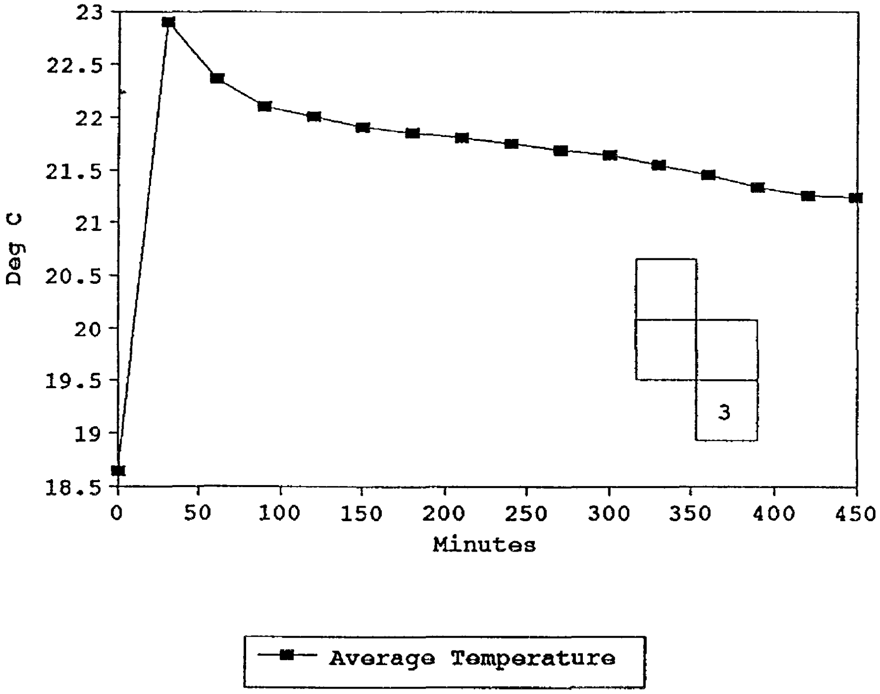

Figure 5-16. Calorimetric Curve for Mix Design F4. (Appendix A)

Table 5-9. Ferrous and Ferric Sulfate Stabilization of Arsenate Added to F006 Waste

TCLP Concentrations (mg/L)

FA1x Series

Metal	Cure Time 2-days	 60-days
As	20.9	6.05
Ca	1480	1750
Fe	0.08	0.07
S	356	16300

FA3x Series

Metal	Cure Time 2-days	 60-days
As	1.59	1.18
Ca	1490	1650
Fe	0.052	0.525
S	242	10300

	Binder F006/Arsenate Waste 0.15	 0.40
$\frac{Fe^{+3}}{As}$ mole ratio = 1.1		
$\frac{Fe^{+2}}{As}$ mole ratio = 2.0		

USA2x Series

Metal	Cure Time 2-days	 60-days
As	2.84	1.67
Ca	1500	1800
Fe	0.25	0.31
S	382	16500

USA4x Series

Metal	Cure Time 2-days	 60-days
As	2.60	0.83
Ca	2070	1820
Fe	0.208	0.77
S	684	14200

hydroxide, both ferric and ferrous sulfates yield comparable TCLP results. The large amount of sulfate in the extracts indicates the lack of barium in this modified F006 waste.

In a similar format, Table 5-10 presents results for arsenite stabilization using ferrous and ferric sulfates. Ferrous sulfate yields more effective stabilization for arsenites at either binder/waste ratio. As shown in Figures 5-17 and 5-18, the most striking result is the relative ease of stabilizing arsenate as compared to arsenite. This observation has lead to a consideration of oxidation as a pretreatment for the stabilization of arsenite wastes.

Table 5-10. Ferrous and Ferric Sulfate Stabilization of Arsenite in F006 Waste

TCLP Concentrations (mg/L)

FB1x Series

Metal	Cure Time	
	2-days	60-days
As	52.6	61.4
Ca	1580	1890
Fe	0.08	0.36
S	311	3890

FB3x Series

Metal	Cure Time	
	2-days	60-days
As	28.65	10.1
Ca	1580	1680
Fe	0.102	0.56
S	34.4	7530

$\frac{\text{Binder}}{\text{F006/Arsenate Waste}}$

	0.15	0.40
$\frac{Fe^{+3}}{As}$ mole ratio = 1.1		
$\frac{Fe^{+2}}{As}$ mole ratio = 2.0		

USB2x Series

Metal	Cure Time	
	2-days	60-days
As	23.0	24.8
Ca	1760	1780
Fe	0.49	0.57
S	34.8	68.1

USB4x Series

Metal	Cure Time	
	2-days	60-days
As	7.97	4.73
Ca	1500	1740
Fe	0.53	0.172
S	236	79.5

5.5.2 Pretreatment with Oxidation

Air oxidation and chemical oxidation with hydrogen peroxide were used to convert arsenites to arsenates for more effective stabilization. Air oxidation was accomplished by intense mixing over 45 minutes with several interruptions for redox potential measurements. Chemical oxidation of arsenite was accomplished by adding hydrogen peroxide at a mole ratio of either 1:1 or 0.5:1. Either 50 or 100 percent of the water required by the stabilization design was added to permit more effective oxidation. The experiment design is described in Table 4-6.

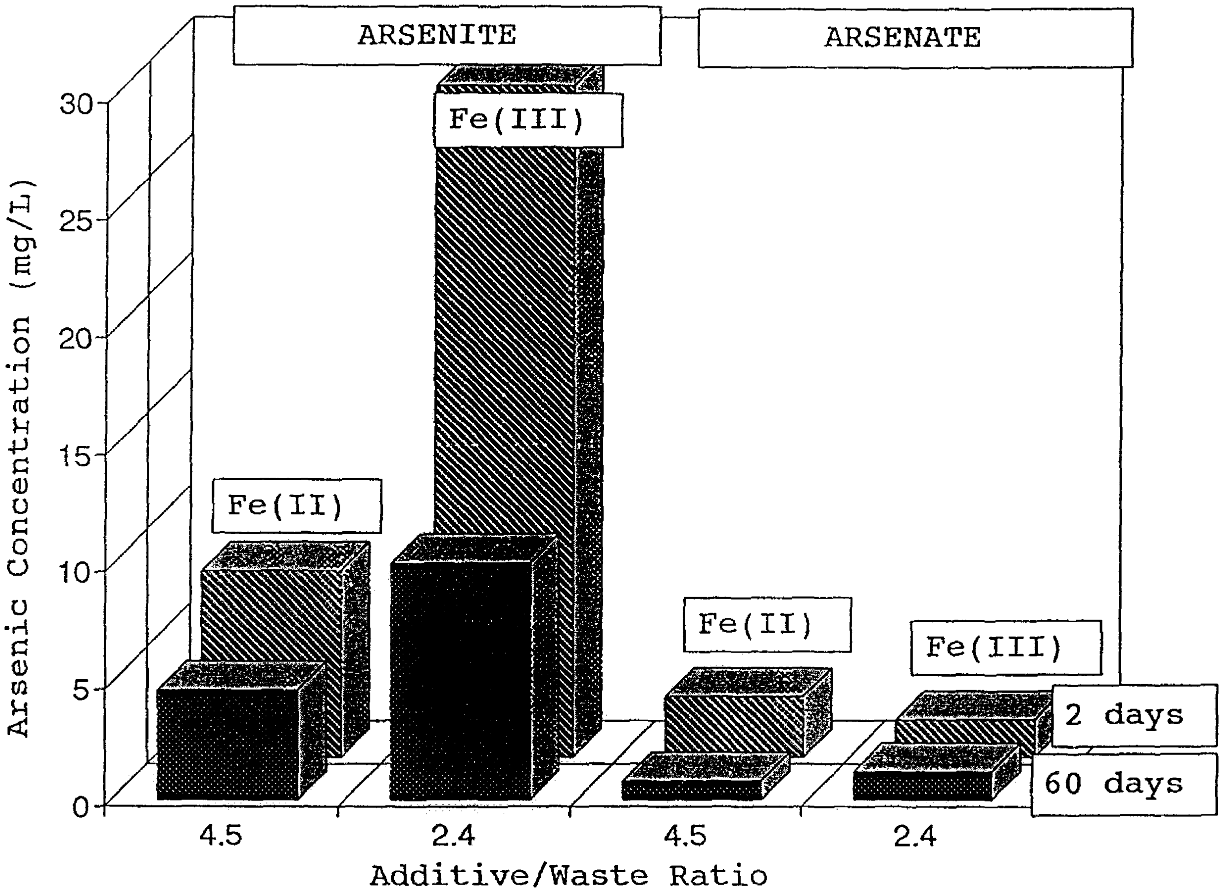

Figure 5-17. **Two-Day and Sixty-Day Stabilization of Modified Arsenate and Arsenite Waste Using Ferrous Sulfate and Ferric Sulfate Additives. Binder/Waste = 0.15**

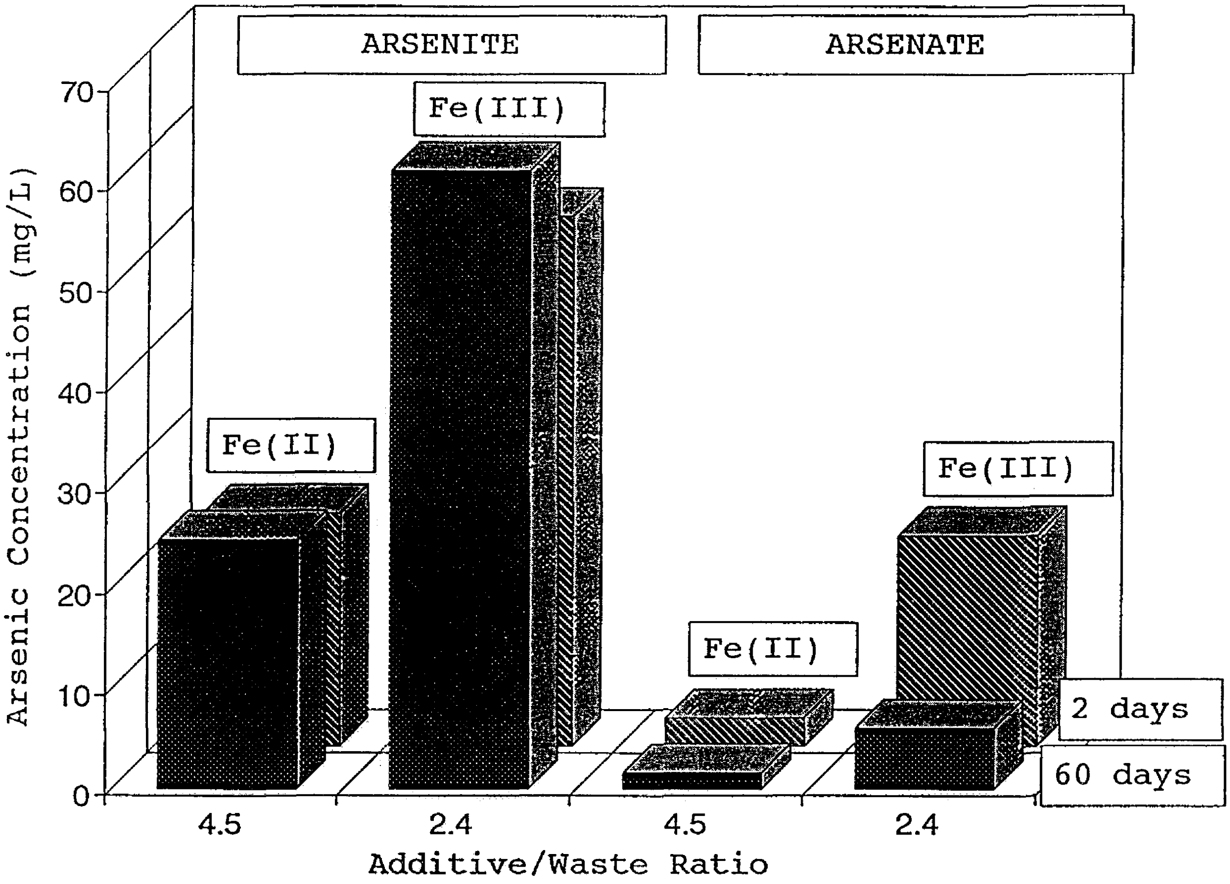

Figure 5-18. Two-Day and Sixty-Day Stabilization of Modified Arsenate and Arsenite Waste Using Ferrous Sulfate and Ferric Sulfate Additives. Binder/Waste = 0.40

After oxidative pretreatment of the waste, the cement and fly ash were added. After mixing, either ferric sulfate or ferrous sulfate was added to stabilize the arsenic. Samples were then air cured for two days before undergoing TCLP. Water is involved in the oxidation reactions as a reaction medium to allow contact between reacting species and as a reactant or product in the ideal balanced oxidation-reduction reactions. To enhance the oxidative reaction chemistry, varying fractions of the total water used in the final S/S mixture were added during the oxidative pretreatment step. The remainder of the water, if any, was added with the cement and fly ash.

Figure 5-19 presents a comparison of ferrous sulfate and ferric sulfate S/S of arsenite with air oxidation. The water to waste mass ratio indicated on the horizontal axis reflects the amount of water added during the air oxidation step. For either binder/waste ratio, lesser amounts of water will improve the performance of air oxidation, probably due to enhanced difussion through thinner aqueous films on the waste particles.

In Figure 5-20, a similar comparison is made with chemical oxidation as the pretreatment. The mole ratio of hydrogen peroxide to arsenic is indicated on the horizontal axis. Hydrogen peroxide is very effective for oxidizing arsenite to arsenate. The dramatic improvement in arsenic S/S emphasizes the relative ease of treating arsenate compared to arsenite.

Data for other elements is shown in Table 5-11. Examination of the data for calcium leads to the conclusion that oxidative pretreatment does not effect the stability of the cementitious lattice, at least in the short term. Sulfate concentrations in the TCLP extracts similarly appear to be relatively independent of the manner in which oxidative pretreatment is performed. The waste used in this set of experiments did not contain much barium, so that the extractable sulfate concentrations are quite high.

5.6 Individual Ion Effect

The TCLP results of the experimental design shown in Table 4-7 are presented in Table 5-12. A comparison of these results using a binder/waste of 0.15 with that from ferrous sulfate stabilizations is shown in Figure 5-21. This plot of arsenic versus iron/arsenic molar mix ratio also shows iron/binder ratios for each mix and the pH of the TCLP extract. The US series represents stabilization with ferrous sulfate as defined in Table 4-2. The lighter-shaded bars represent iron acetate stabilization which yields more effective stabilization of arsenic with lower iron/arsenic molar ratios.

Similar results occur for mix designs with binder/waste equal to 0.40. Iron acetate stabilizations yield arsenic concentrations of 3.84 and 0.09 mg/L for 1.5 and 3.0 iron/arsenic molar concentrations. Ferrous sulfate stabilization requires an

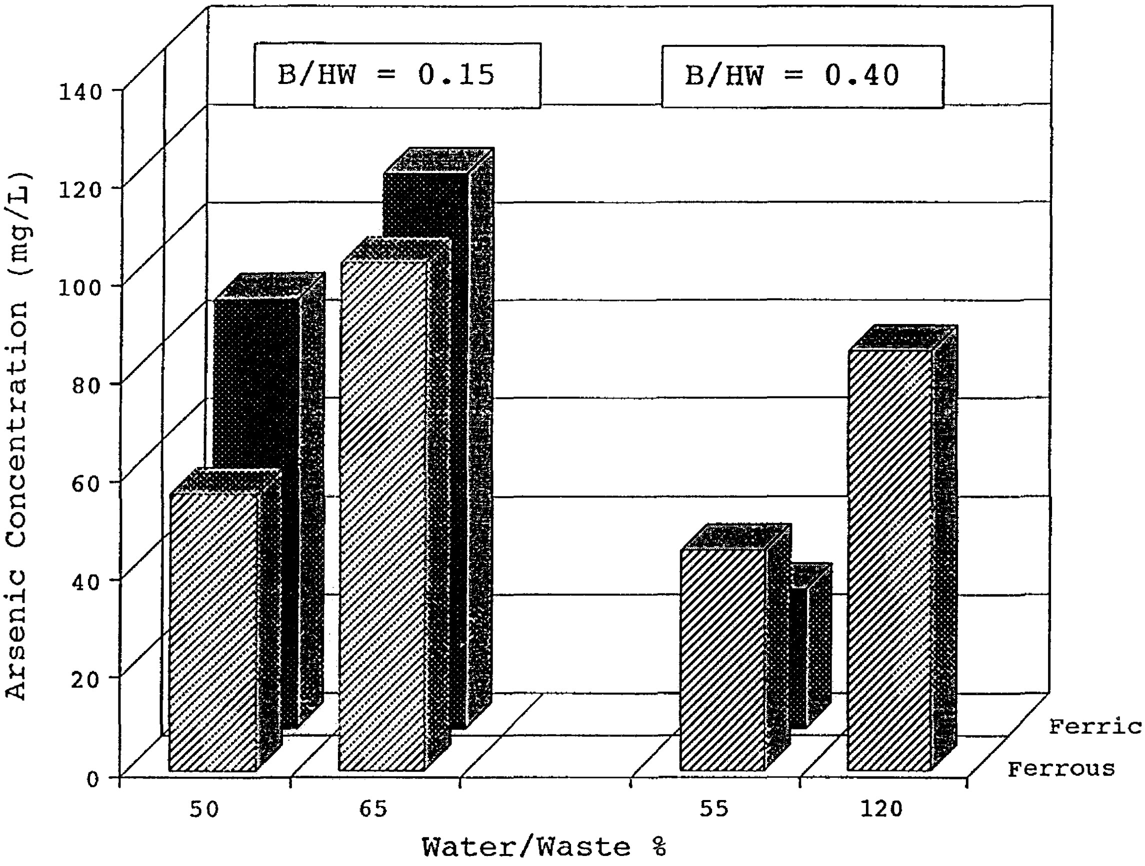

Figure 5-19. Arsenite Pretreatment by Air Oxidation, TCLP Results

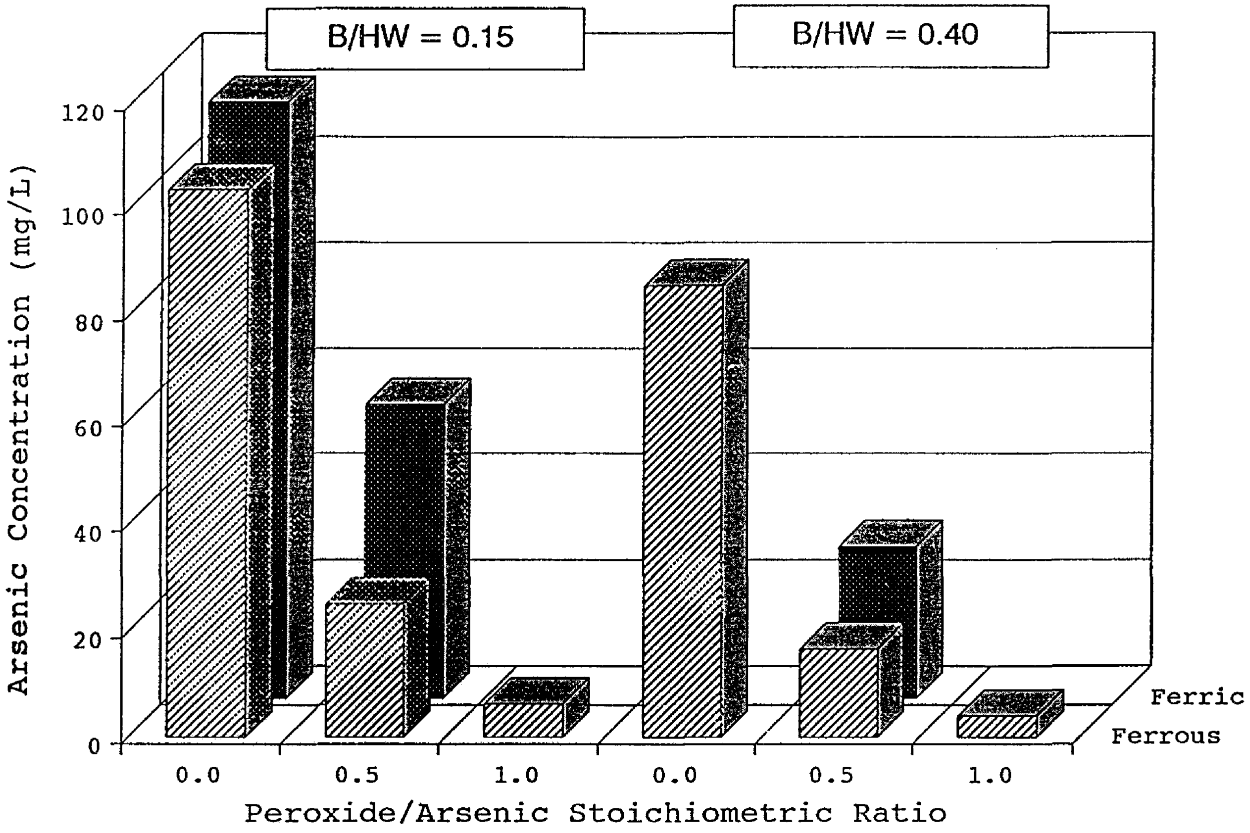

Figure 5-20. **Arsenite Pretreatment by Peroxide Oxidation, TCLP Results**

Table 5-11. Experimental Design for Arsenite Stabilization.

Binder / waste mass ratio

0.15 | 0.40

Air Oxidation

TCLP Results for USB1x (0.15)
Note. The % denotes the amount of the water added in the beginning Also if Fe(II) or Fe(III) was used is indicated.

Element	sample with 50%,Fe (II)	sample with 100%,Fe (II)	sample with 50%,Fe (III)	sample with 100%,Fe (III)
Arsenic		56 3	87 4	113
Barium		0 25	0 26	0 32
Calcium		1700	1350	1760
Iron		1 2	0 33	28 6
Sulfate		957	654	735
pH	5 8	6 6	5 9	4 7

TCLP Results for USB2x (0.40)
Note. The % denotes the amount of the water added in the beginning Also if Fe(II) or Fe(III) was used is indicated.

Element	sample with 50%,Fe (II)	sample with 100%,Fe (II)	sample with 50%,Fe (III)	sample with 100%,Fe (III)
Arsenic	44 9		28 2	
Barium	0 38		0 34	
Calcium	1070		1440	
Iron	45 8		0 18	
Sulfate	435		627	
pH	5 2	6 1	6 2	5 1

H_2O_2 Oxidation

TCLP Results for USBP1x (0.15)
Note The % denotes the amount of the water added in the beginning Also if Fe(II) or Fe(III) was used is indicated.

Element	sample with 50%,Fe (II)	sample with 100%,Fe (II)	sample with 50%,Fe (III)	sample with 100%,Fe (III)
Arsenic	33 0	17 2	57 5	53 7
Barium	1 7	1 1	1 2	1 2
Calcium	1440	1340	1300	1390
Iron	211	76 6	0 09	4 4
Sulfate	987	978	660	540
pH	5 2	5 3	6 7	4 7

TCLP Results for USBP2x (0.40)
Note The % denotes the amount of the water added in the beginning Also if Fe(II) or Fe(III) was used is indicated.

Element	sample with 50%,Fe (II)	sample with 100%,Fe (II)	sample with 50%,Fe (III)	sample with 100%,Fe (III)
Arsenic	16 2	17 1	59 6	27 9
Barium	2 7	0 35	0 55	0 33
Calcium	1280	2210	2060	1600
Iron	0 08	115	0 12	0 07
Sulfate	1280	759	660	639
pH	7 2	5 25	5 8	8 3

Table 5-12. TCLP Results Using Iron Acetate

	Binder/Waste Mass Ratio			
Mole Ratio Fe/As	0.15		0.40	
1.5	IA1x Series		IA3x Series	
	Arsenic	15.67	Arsenic	3.84
	Barium	3600.	Barium	1930.
	Iron	2.04	Iron	70.
	Sulfate	1.40	Sulfate	7.5
	Calcium	1430.	Calcium	2500.
	Extract pH	5.26	Extract pH	4.5
3.0	IA2x Series		IA4x Series	
	Arsenic	3.45	Arsenic	0.09
	Barium	3430.	Barium	1850.
	Iron	58.	Iron	21.4
	Sulfate	0.83	Sulfate	2.5
	Calcium	1650.	Calcium	2380.
	Extract pH	4.3	Extract pH	5.67

iron/arsenic ratio of 5.7 to achieve 6.2 mg/L arsenic.

The superior results of iron acetate stabilization can be explained by sulfate interference with the early cement matrix or by more favorable pH conditions. The TCLP extract pH of the iron acetate stabilizations was about 4 to 5 which is more favorable for arsenic adsorption and iron-arsenic precipitation. In contrast, the pH of extracts from ferrous sulfate stabilizations was 7 to 8.

More evidence for deleterious effects of sulfate on the early development of the cement matrix is presented in Table 5-13. Sodium sulfate is being added to precipitate barium with no iron addition for arsenic. For either binder/waste ratio, TCLP concentrations of arsenic increase significantly with increased additions of sodium sulfate.

Sulfate corrosion of stabilized forms is an explanation for the performance of certain high-sulfate mixes as discussed in Section 5.2. Moderate amounts of sulfate do not appear to be detrimental to long-term stabilizations especially those with ferrous iron.

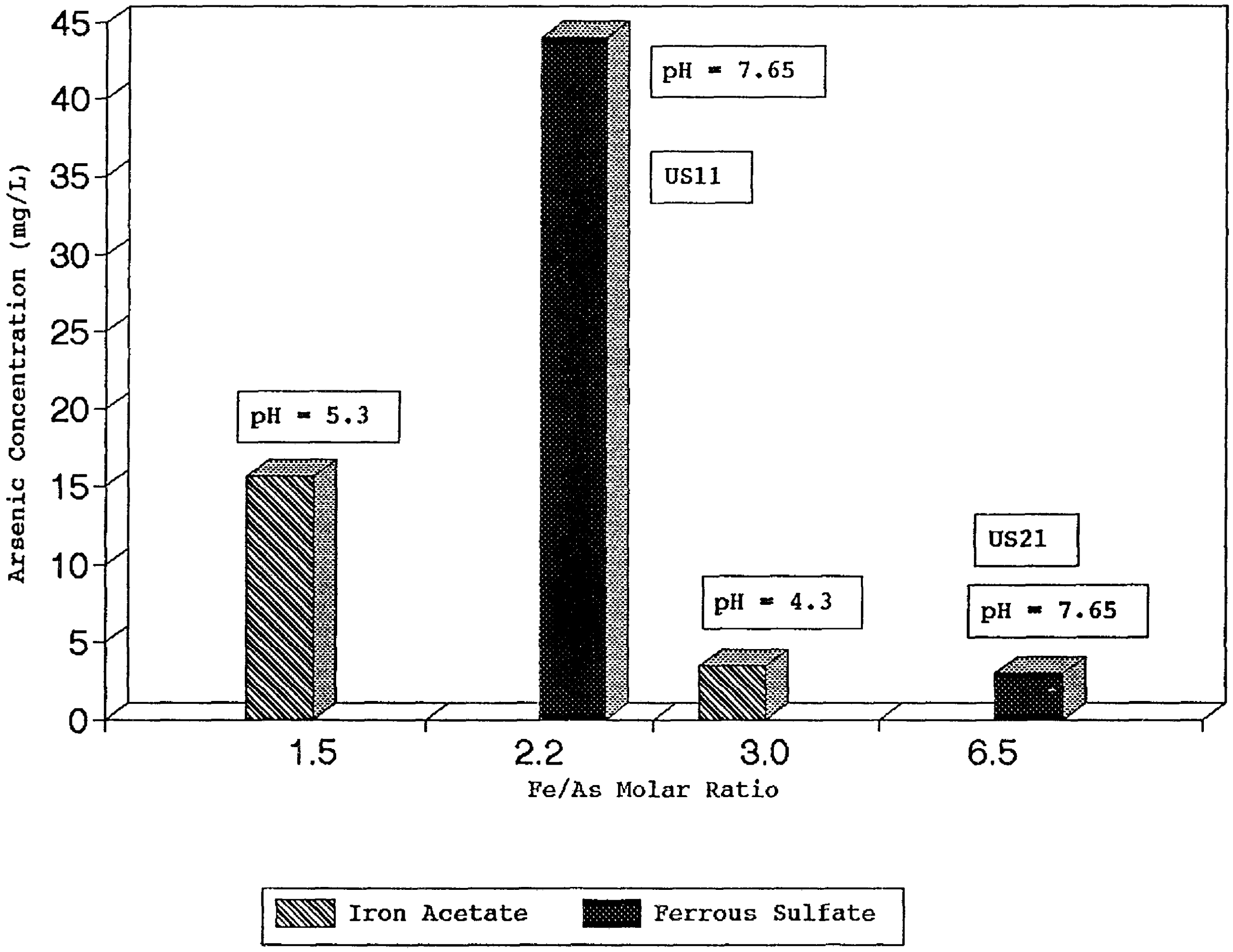

Figure 5-21. TCLP Arsenic Results for Ferrous Sulfate and Ferrous Acetate Stabilizations

Table 5-13. TCLP Results Using Sodium Sulfate

Mole Ratio SO_4^{2-}/Ba^{2+}	Binder/Waste Mass Ratio			
	0.15		0.40	
	SS1x Series		SS3x Series	
1.0	Arsenic	27.7	Arsenic	33.1
	Barium	0.582	Barium	80.6
	Iron	<0.02	Iron	0.125
	Sulfate	35.5	Sulfate	2.28
	Calcium	384.	Calcium	2370
	Extract pH	5.26	Extract pH	4.5
	SS2x Series		SS4x Series	
2.0	Arsenic	67.2	Arsenic	41.2
	Barium	0.58	Barium	0.85
	Iron	0.14	Iron	0.284
	Sulfate	715.3	Sulfate	530
	Calcium	1030	Calcium	1850
	Extract pH	4.3	Extract pH	5.67

5.7 Scanning Electron Microscope Study

Scanning electron microscope photographs and elemental dot maps are presented in Figures 5-22 to 5-26. All of these samples were cast using ferrous sulfate additive in S/S. The magnification used in these photographs is 130x so that the area of the sample shown is 0.50 mm by 0.64 mm or 0.31 mm^2.

During this discussion, a grid system modeled after commonly-used spreadsheet conventions will be used. Six cells, lettered "A" through "F", are defined across the top, each about 0.1 mm wide on the sample and 13 mm wide on the figures. Four cells, numbered "1" through "4", are defined down the left side, each about 0.1 mm on the sample and 13 mm in the figures. A feature in the lower right corner of a photo will be indicated as being located in cell "F4". The elemental dot maps are positive images, with light-colored spots representing the occurrence of an x-ray photon characteristic of the target element. The density of light spots is proportional to the surface concentration of the element at that location.

Particles of fly ash are easily recognized as spherical balls 0.05 to 0.1 mm in diameter. These particles typically have high iron concentrations and are visible as light areas on the iron elemental dot map. A fly ash particle can be seen at C4 in Figure 5-22.

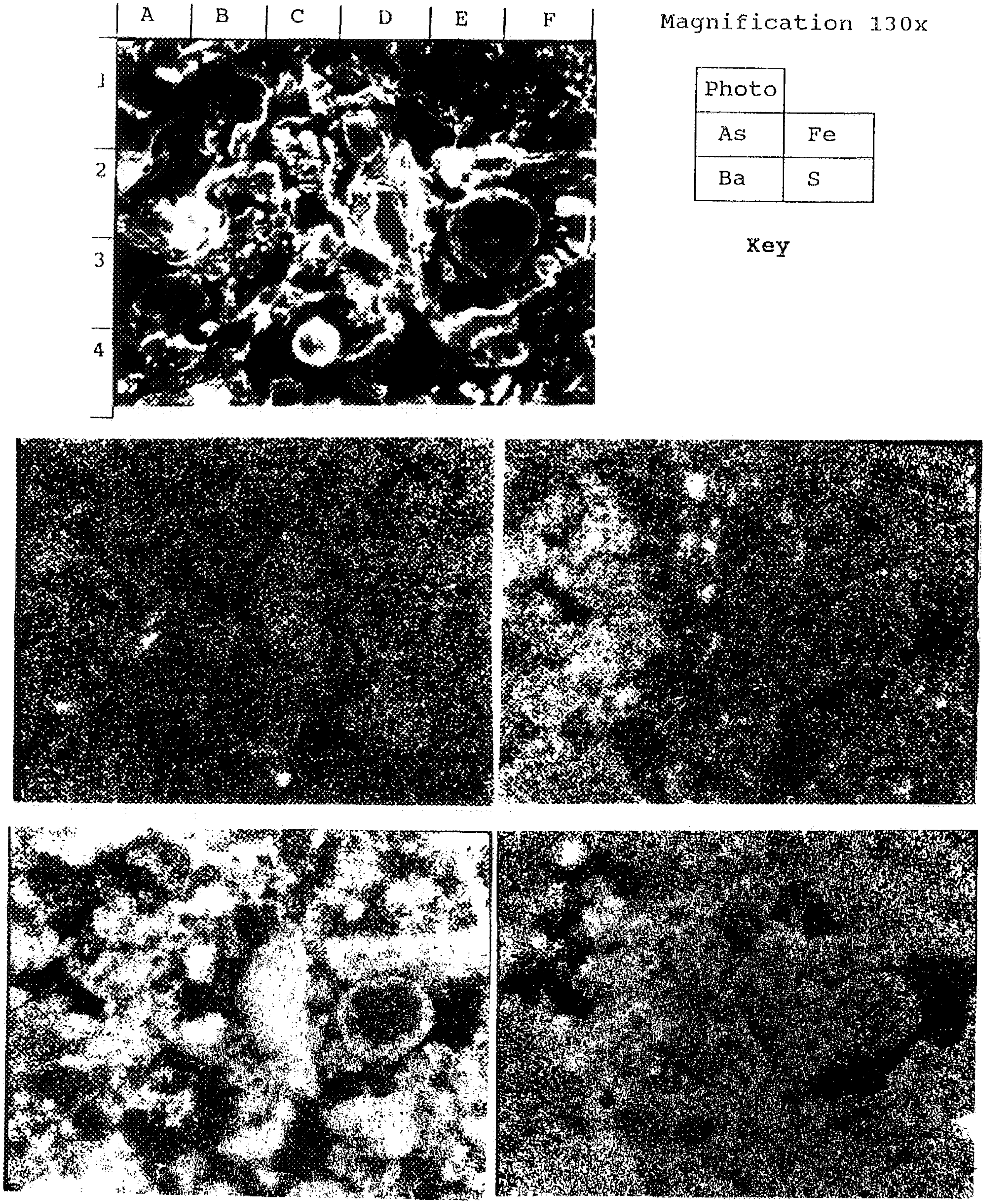

Figure 5-22. SEM Data for Sample SEM1, 2-day Cure Time

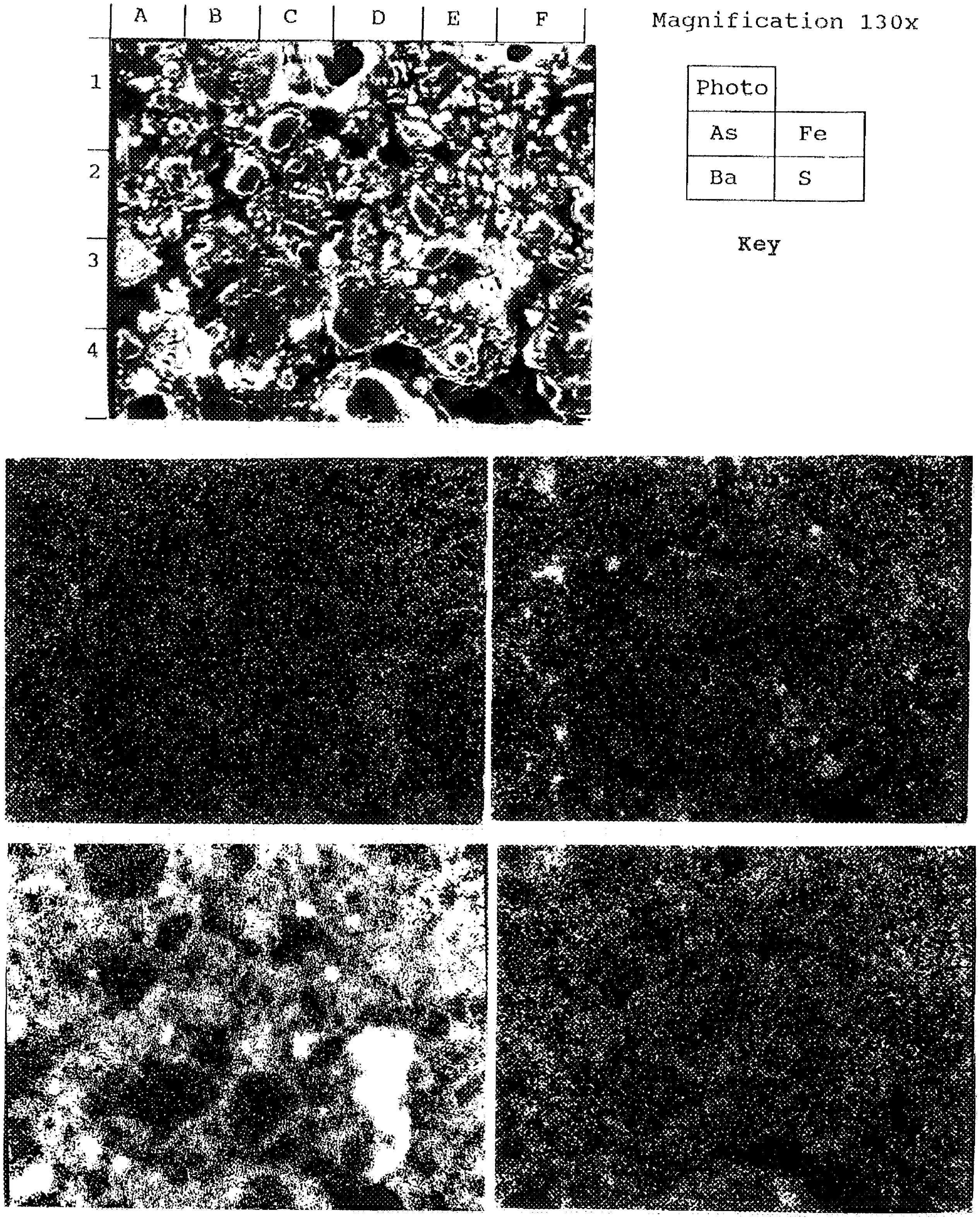

Figure 5-23. SEM Data for Sample SEM2, 60-day Cure Time

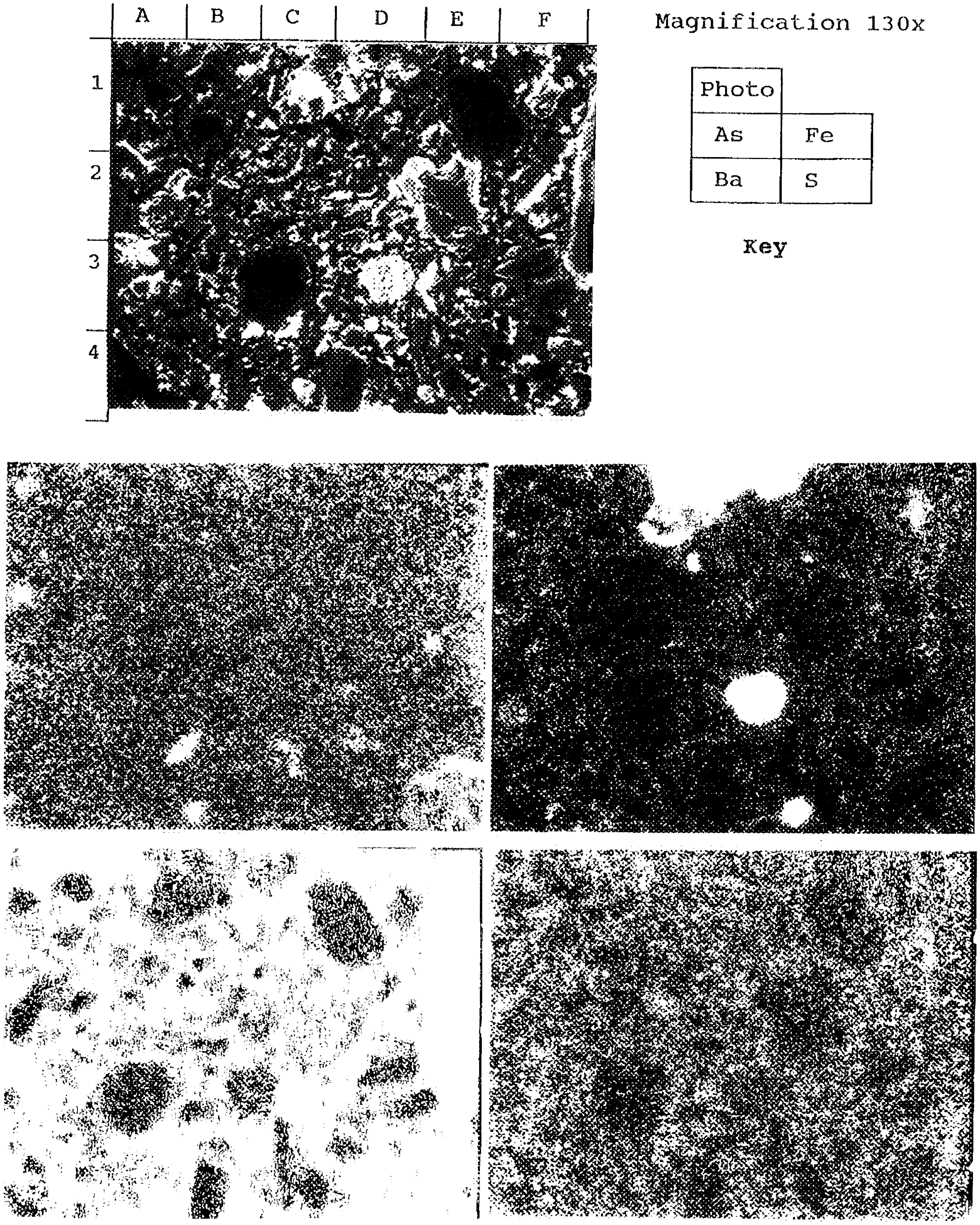

Figure 5-24. SEM Data for Sample SEM3, 365-day Cure Time

Glass particles from the industrial grinding operations which generated the D004/D005 waste are common. Glass particles can be identified by relatively straight-edged geometric-appearing shapes. Glass particles are also often characterized by voids in the iron, barium and sulfur elemental dot maps.

Calcium hydroxide (CH) gel areas, formed early in the hydration process, appear as irregularly-shaped dark areas in photographs, and as dark areas in elemental dot maps. Calcium hydroxide gel is softer than the solid components of the cement S/S mix and is often dug away in the surface preparation polishing process. The resulting hole in the surface will appear as a dark shadow in the SEM photographs.

In Figure 5-22, sample SEM1 is shown. The arsenic dot map is essentially featureless, typical of the arsenic distributions observed in this study. This sample has a cure time of two days, so that the CH gel phase is still present in significant amounts. Large zones of gel phase can be identified at locations F2, E4, C3, and A1. Integration of the areas of the recognizable gel zones and dividing by the area of the whole photograph indicates approximately 40% CH phase at two days cure time. Barium and sulfur (and to a lesser extent iron) are at reduced concentrations in the CH gel. It is difficult to recognize correlations between iron and arsenic in the dot maps. High concentrations of sulfur seem to correlate with locations of high barium, although not all high barium concentrations are correlated with sulfur concentrations. This is not surprising because about half of the barium in the waste is not extractable by TCLP. The barium concentration at E2 is perhaps an example of the inert barium component of the waste.

Figure 5-23 is for a sample of the same composition as that in Figure 5-22, but at 60 days of curing. The CH gel phase is smaller, visible only at E4 and D1. These two large areas still account for about 30% of the sample volume. The large barium hot spot at E3 has no corresponding hot spot in the sulfur dot map, so therefore it is probably part of the inert barium part of the waste. Again, very little correlation can be found between the arsenic and iron concentrations. This is not necessarily indicative of no arsenic reaction with iron because the gross amount of iron is several times the gross amount of arsenic in the S/S sample.

Figure 5-24 presents data for a sample of the same composition as shown in Figures 5-22 and 5-23. The sample in Figure 5-24 has been cured for 365 days. A fly ash particle is visible at location D3. A glass chunk is visible at location A2, and is accompanied by a high barium concentration. After 365 days of curing, very little CH gel phase is visible. Only 1.7% of the sample surface (and volume) is recognizably CH gel. The arsenic concentration at location F4 is accompanied by a visibly low concentration of iron. The number of such concentrations observed in the SEM study amount to less than 1% of the total area observed. These arsenic hot spots could account for the observation that there appears to be a minimum concentration for the TCLP concentration of arsenic, no matter what treatment is used.

Figures 5-25 and 5-26 are the data from samples using ferric sulfate additive at two different levels. Both S/S mixes had the same binder/waste ratio and were cured two days. In Figure 5-25 a prominent feature is the glass chip at location C3. This object is visible on the Ba, Fe, and S elemental dot maps as a region of low density. No apparent deviation in the arsenic dot density can be found at the location of the glass chip. The glass chip is approximately 0.12 mm long and 0.06 mm wide. In Figure 5-26 a very prominent bright feature appears at location E2. This feature appears as a region of high intensity on both the barium and arsenic dot maps, and as a region of low intensity on the iron and sulfur dot maps. This is indicative of a piece of waste material which was not broken up in the preparation of the S/S mixture. This feature is 0.2 mm long and 0.1 mm wide and is the largest single object found in the SEM observation process. A fly ash sphere is also visible at location C4 in Figure 5-26. This sphere is somewhat unique in that it is low in iron.

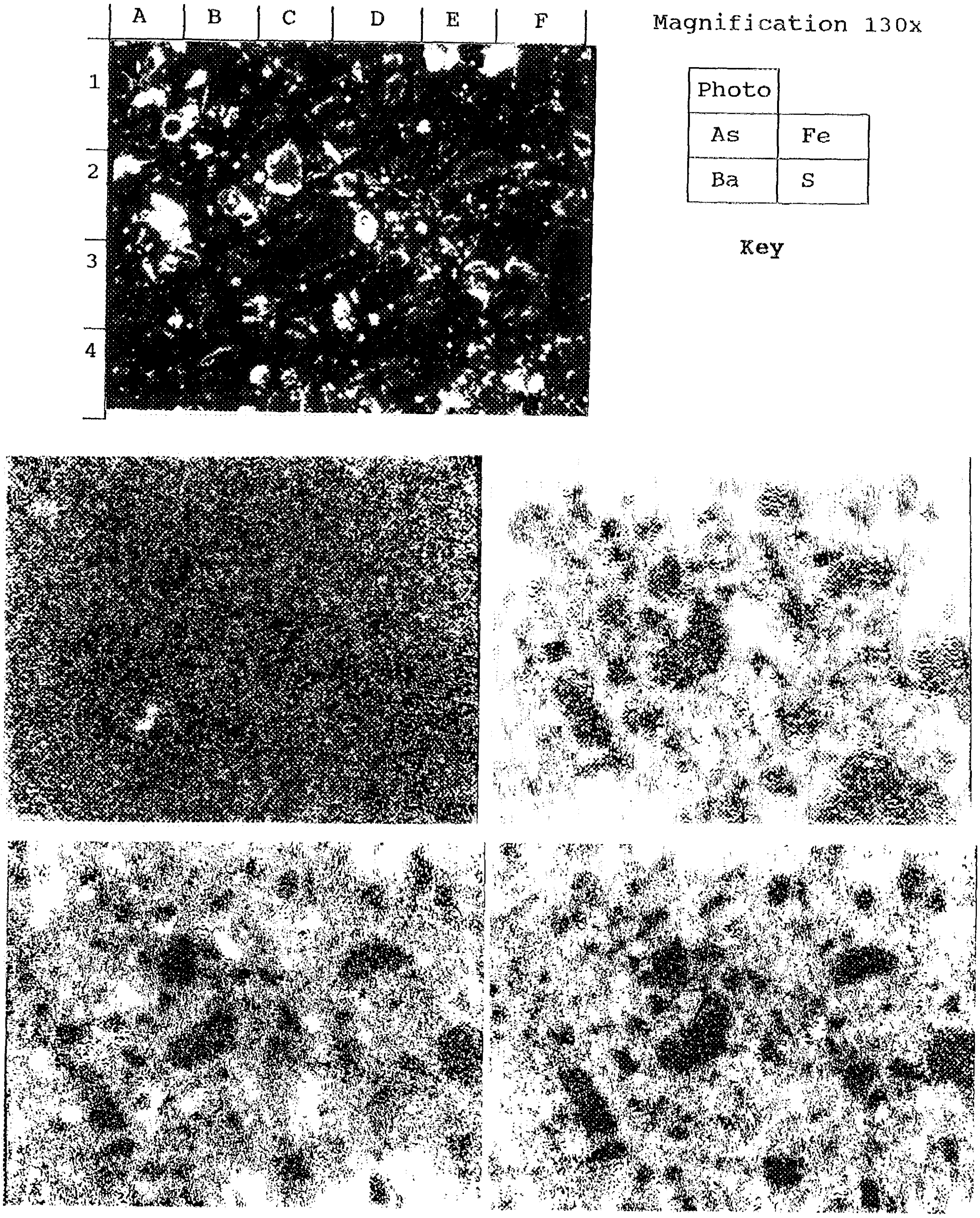

Figure 5-25. SEM Data for Sample SEM4, 2-day Cure Time

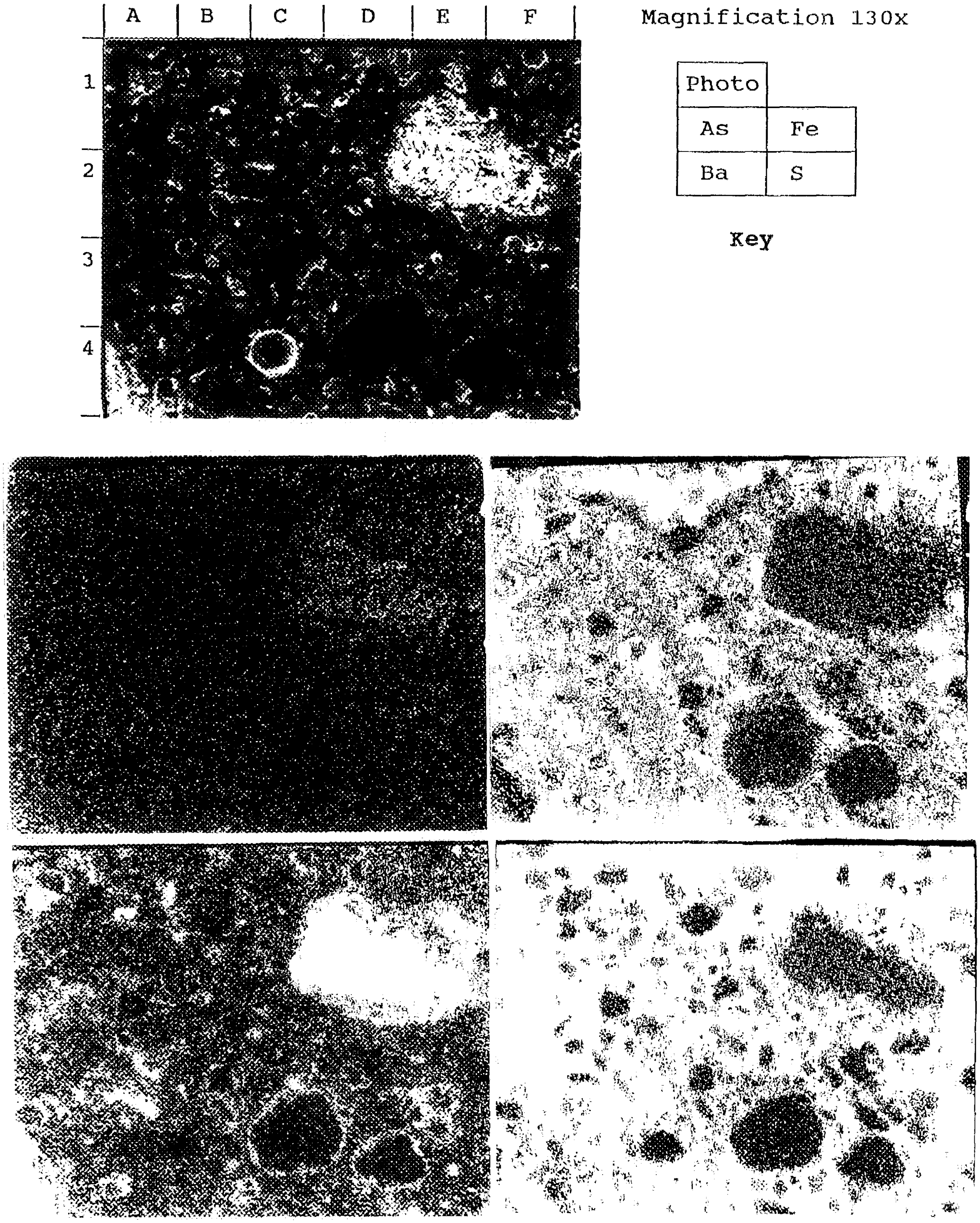

Magnification 130x

Photo	
As	Fe
Ba	S

Key

Figure 5-26. SEM Data for Sample SEM5, 2-day Cure Time

CHAPTER SIX
SUMMARY AND RECOMMENDATIONS

Table 1-1 summarizes EPA comments regarding solicited results of arsenic stabilization. These comments include no reported binder/waste ratios, no QA/QC data, and the possible interference of organics. Furthermore, the effect of cure time on treatment effectiveness had not been investigated. This summary of project findings provides recommendations and guidelines with respect to these concerns.

Inorganic arsenic was effectively stabilized for up to 540 days. There are several concerns for stabilization design: 1) the use of ferric sulfate, ferrous sulfate, or aluminum sulfate as stabilization additive; 2) arsenite versus arsenate stabilization; 3) the use of sulfate to immobilize barium; 4) binder/waste ratios and volume efficiency. Each concern is addressed and guidelines are presented below.

Precipitation of arsenic with iron in the stabilized matrix is more effective than using aluminum. Two iron salts, ferrous sulfate and ferric sulfate, were selected for experimentation because of cost and commercial availability. Ferrous sulfate is available as a K001 waste. In general, ferrous sulfate is preferred for arsenic stabilization because it is effective over a wider range of mix designs and over the long term. It is recommended that the iron(II)/ arsenic mole ratio be at least six. Slightly lower dosages of iron(II) may be effective if cure times of at least 60 days are permitted. The use of iron(III) is not recommended for arsenate stabilization since the fresh cement mix adsorbs ferric ion and does not permit adequate S/S until long cure times have elapsed. Furthermore, the ferric hydroxy-arsenic complex is a larger molecule than the ferrous arsenic compound. Ferrous stabilization is preferred to ferric stabilization because encapsulation of larger molecules in cement is more difficult.

Arsenate, As(V), is more effectively stabilized than arsenite, As(III). There are several ways to pretreat the waste so arsenite is oxidized to arsenate before stabilization. The selection of a pretreatment should be based on a knowledge of the arsenite levels in the waste. The most effective method is chemical oxidation with an appropriate reagent. Hydrogen peroxide at stoichiometric dosages and adequate mixing will provide sufficient oxidation of the arsenite. Moderate arsenite oxidation can be achieved by air oxidation using just enough water to eliminate dust escaping the mixing operation.

Barium may be encapsulated within the S/S matrix as barium sulfate. Recommended range of sulfate/barium mole ratios is 1.1 to 2.2. This ratio may be affected by the portion of barium that is extractable in the waste being stabilized. Higher dosages of sulfate are not recommended because of potential sulfate corrosion of the cement matrix over the long term. Sulfate may be introduced in any form. If additional sulfate is required beyond the amount of iron sulfate determined by the recommended mole ratio of iron/arsenic, then sodium or aluminum sulfate may also be used.

Comments in Table 1-1 also focused on the lack of information regarding binder/waste ratios and effective arsenic S/S. Mix designs in this project used a range of binder/waste ratios from 0.15 to 0.40. A binder/waste ratio of 0.15 is more volume efficient and effective mix designs were found, but there are precautions here. The mix design must be carefully controlled to the prescribed mole ratios for iron/arsenic and sulfate/barium. In practice, the heterogeneity of wastes and large scale mixing operations may preclude this close control of reagent dosages. The resulting S/S in practice may be ineffective or may pass only with extended cure times. A binder/waste ratio of 0.4 permits successful S/S over a wider range of mix designs with shorter cure times.

Project experimentation has included TCLP and dynamic column leaching. These experimental data were analyzed for 25 metals using ICP. Data analysis included mass balance and correlation studies among the metal concentrations that permit a characterization of elements: 1) those elements that are strongly bound to the matrix; 2) the fraction of metal present that is leachable; 3) a comparison of leaching rates among metals; 4) the contribution of binders and wastes to metals appearing in the extracts. Calorimetric and SEM studies conducted on selected samples also were presented to reinforce the conclusions of this project. These techniques were useful in elucidating the relative amounts and rates of leaching from different compositional areas of the curing S/S matrix.

The results of this study can be used to design S/S treatment protocols for wastes containing inorganic arsenic. However, treatment procedures for organic arsenicals have not been addressed in this study.

Industrial wastes contain a wide variety of regulated and unregulated components. The concentrations of these components vary widely in practice. Due to these wide variations, it is crucial that research developing S/S treatment procedures be carried out using representative industrial wastes.

REFERENCES

Akhter, H., L.G. Butler, S. Branz, F.K. Cartledge, and M.E. Tittlebaum. 1990. "Immobilization of As, Cd, Cr and Pb-Containing Soils by Using Cement or Pozzolanic Fixing Agents." *Journal of Hazardous Materials*, 24:145-155.

Artiola, Janick F., David Zabcik, and Sidney H. Johnson. 1990. "In Situ Treatment of Arsenic Contaminated Soil From A Hazardous Industrial Site: Laboratory Studies," *Waste Management,* 10(1):73-78.

ASTM, 1965. *Index (Inorganic) for the Powder Diffraction File and Powder Diffraction File, Sets 1-18*, American Society for Testing and Materials, Philadelphia, Pa.

Batchelor, B. 1990. "Leach Models: Theory and Application." *Journal of Hazardous Materials*, 24:255-266.

Bayasi, Z., R. Fuessle, M. Taylor. 1992. *Improvements in the Solidification of Hazardous Inorganic Wastes by Silica Fume (Microsilica) Concrete*, Final Report submitted to the State of Illinois Hazardous Waste Research and Information Center, March.

Bhattacharyya, D., A.B. Jumawan, G. Sun, C. Sund-Hagelberg, and K. Schwitzgebel. 1980. "Precipitation of heavy Metals with Sodium Sulfide: Bench-Scale and Full-Scale Experimental Results," *American Institute of Chemical Engineers,* 77(209):31-38.

Blitz, W. 1904. *Berichte* 37:1766, 3108.

Brewster, Michael D. 1992. "Removing Arsenic from Contaminated Wastewater." *Water Environment & Technology,* 4(11):54.

Cartledge, F.K, H.C. Eaton, and M. Tittlebaum, 1989. *Morphology and Microchemistry of Solidified/Stabilized Hazardous Waste Systems,* EPA Report No. EPA/600/2-89/056, November 1989.

Cartledge, Frank K. 1992. "Solidification/Stabilization of Arsenic Compounds," in U.S. EPA, *Mercury and Arsenic Wastes, Removal, Recovery, Treatment, and Disposal* Proceedings of a workshop held in Alexandria, VA, Aug. 17-20, 1992, Noyes Data Corp.

Cheng, K.Y. and P. Bishop. 1992. "Metals Distribution in Solidified/Stabilized Waste Forms after Leaching." *Hazardous Waste & Hazardous Materials,* 9(2):163-171.

Cheng, Kuang Ye and Paul L. Bishop. 1992. "Sorption, Important in Stabilized/Solidified Waste Forms." *Hazardous Waste & Hazardous Materials,* 9(3):289-296.

Chu, Peylina, Michael T. Rafferty, Thomas A. Delfino, and Richard F. Gitschlag, 1991. "Comparison of Fixation Techniques for Soil Containing Arsenic," in Tedder, D. William and Frederick G. Pohland, eds., *Emerging Technologies in Hazardous Waste Management II* Industrial and Engineering Chemistry Special Symposium sponsored by the Division of Industrial and Engineering Chemistry, Inc, American Chemical Society Atlantic City, NJ, June 4-7, 1990.
Code of Federal Regulations. 1987. "Toxicity Characteristic Leaching Procedure (TCLP)," Vol. 40, Part 268, App. I, July, pp. 692-707.

Conner, Jesse R. 1990. *Chemical Fixation and Solidification of Hazardous Wastes* Van Nostrand Reinhold NY, NY.

Cote, P.L., T.W. Constable and A. Moreira. 1987. "An Evaluation of Cement-Based Waste Forms Using the Results of Approximately Two Years of Dynamic Leaching." *Nuclear and Chemical Waste Management*, 7:129-139.
Davis, A., M.V. Ruby, and P.D. Bargstrom. 1992. "Bioavailability of Arsenic and Lead in Soils from the Butte, Montana, Mining District." *Environmental Science and Technology*, 26:461-8.

Egawa, Hiroaki, Takamasa Nonaka, and Hironori Maeda. 1985. "Studies of Selective Adsorption Resins. XXII. Removal and Recovery of Arsenic Ion in Geothermal Power Waste Solution with Chelating Resin Containing Mercapto Groups," *Separation Science and Technology,* 20(9,10):653-664.

Environmental Laboratory of the U.S. Army Engineer Waterways Experiment Station. 1980. *Guide to the Disposal of Chemically Stabilized and Solidified Waste*, Report SW-872, Interagency Agreement No. EPA-IAG-D4-0569 with Municipal Environmental Research Laboratory, Office of Research and Development, U.S. EPA, Cincinnati, OH.

Environmental Canada and Alberta Environmental Center. "Acid Neutralization Capacity Test." 1986. In *Test Methods for Solidified Waste Characterization,* Canada.

EPA. 1989. *Stabilization/Solidification of CERCLA and RCRA Wastes*, EPA/625/6-89/022. Center for Environmental Research Information and Risk Reduction Engineering Laboratory, Office of Research and Development, US EPA, Cinn. OH.

Federal Register. 1990. "Hazardous Waste Management System," Vol. 55, Part No. 61, pp. 11796ff and Part No. 126, pp. 26986ff.

Ghosh, M.M. and R.S. Teoh. 1985. "Adsorption of Arsenic on Hydrous Aluminum Oxide," *Toxic and Hazardous Wastes Proceedings of the Seventeenth Mid-Atlantic Industrial Waste Conference*, Irwin Irwin J. Kugelmann (ed.) pp. 139-155.

Gulledge, John H. and John T. O'Connor. 1973. "Removal of Arsenic (V) From Water by Adsorption on Aluminum and Ferric Hydroxides," *Journal of the American Water Works Assocation,* 65(8):548-552.

Gupta, Shailendra K. and Kenneth Y. Chen. 1978. "Arsenic Removal by Adsorption," *Journal of the Water Pollution Control Federation,* 50(3): 493-506.

Harper, Thomas R. and Neville W. Kingham. 1992. "Removal of Arsenic from Wastewater Using Chemical Precipitation Methods," *Water Environment Research,* 64(3):200-203.

Hogness, T.R. and W.C. Johnson. 1954. *Qualitative Analysis and Chemical Equilibrium,* Fourth Ed., Holt, Reinhart and Winston.

Isenburg, J. and M. Moore. 1992. "Generalized Acid Neutralizing Capacity Test." *Stabilization and Solidification of Hazardous, Radioactive, and Mixed Wastes*, 2nd Volume, ASTM STP 1123, T.M Gilliam and C.C. Wiles, Eds., American Society for Testing and Materials, Philadelphia, pp. 361-377.

Jones, Larry W. 1990. *Interferences Mechanisms in Waste Stabilization/Solidification Processes*, EPA/600/2-89/067. Risk Reduction Engineering Laboratory, Office of Research and Development, U.S. Environmental Protection Agency. Cinn. OH.

Lockemann, G. 1911. *Zeit. Koll*, 8:273.

Mindess, Sidney and J. Francis Young. 1981. *Concrete,* Prentice-Hall, Inc. Englewood Cliffs, NJ.

NAS. 1977. "Arsenic," National Academy of Sciences, Washington DC.

Neville, A.M., 1972. *Properties of Concrete*, Pitman Publishing, London.

Ortego,J.D. 1990. "Spectroscopic and Leaching Studies of Solidified Toxic Metals," *Journal of Hazardous Materials,* 24:137-44.

Ortego, J.D. 1989. *Environmental Science and Engineering,* 24:589-602.

Penrose, W.R. 1974. "Arsenic in the Marone and Aquatic Environments: Analysis, Occurence and Significance." *CRC Crit. Rev. Environ. Control,* 4:465.

"Prudent Practices for Handling Hazardous Chemicals in Laboratories", 1981. National Academy Press.

Sakata, Masahiro. 1987. "Relationship between Adsorption of Arsenic(III) and Boron by Soil and Soil Properties." *Environmental Science and Technology,* 21(11):1126-1130.

Sandesara, M. D. 1978. *Process for Disposal of Arsenic Wastes,* U.S. Patent 4,118,243.

Schlicher, R.J. and M.M. Ghosh. 1985. "Removal of Arsenic from Water by Physical-Chemical Processes." *American Institute of Chemical Engineers,* 81(243):152-164.

Sen, Asit K. and Arnab K. De. 1987. "Adsorption of Arsenic on Coal Fly Ash." *Indian Journal of Technology,* 25:259-261.

Sorum, C.H. 1960. *Introduction to Semimicro Qualitative Analysis*, Third Ed., Prentice-Hall.

Tan, L. K. and J.E. Dutrizac, 1985a. "Determination of Arsenic(III) and Arsenic(V) in Ferric Chloride-Hydrochloric Acid Leaching Media by Ion Chromatography", *Anal. Chem.,* 57, 1027-1032.

Tan, L. K. and J.E. Dutrizac, 1985b. "Determination of Arsenic(V) and Arsenic(III) in Ferric Sulfate-Sulfuric Acid Leaching Media by Ion Chromatography", *Analytical Chemistry*, 57, 2615-2620.

Urasa, I.T. and F. Ferede, 1987. "Use of Direct Current Plasma as an Element Selective Detector for Simultaneous Ion Chromatographic Determination of Arsenic(III) and Arsenic(V) in the Presence of Other Common Anions" , *Analytical Chemistry*, 59, 1563-1568.

US EPA. 1990b. *Scope of Work: Inorganics,* Document ILM01.0. CERCLA Contract Lab Program.

US EPA. 1987. *Test Methods for Evaluating Solid Waste, Physical/Chemical Methods,* _SW 846, 3 volumes, Sept. 1986 and 1 revision, Dec. 1987.

USEPA. 1990. "Land Disposal Restrictions for Thind Third Scheduled Wastes," Federal Register 55(106): 22556-22560.

Wagemann, R. 1978. "Some Theoretical Aspects of Stability and Solubility of Inorganic Arsenic in the Freshwater Environment," *Water Research*, 12:139-145.

Young, D.A. 1979. *Landfill Material,* U.S. Patent 4,142,912

MATRIX OF MIX DESIGNS FOR FERRIC SULFATE STABILIZATION OF D004/D005 WASTE (Table 4-2 repeated for ease of reference)

F1x Series

Component per 100.0 g waste	Mass g
Water	24.0
Cement	9.0
Fly Ash	6.0
$Fe_2(SO_4)_3 \cdot 9H_2O$	4.8

Important ratios:

Binder/Waste	0.15	g/g
Binder/H_2O	0.59	g/g
Fe^{3+}/binder	0.063	g/g
Fe^{3+}/As	2.1	mol/mol
SO_4^{2-}/binder	0.16	g/g
SO_4^{2-}/Ba^{2+}	0.53	mol/mol

F2x Series

Component per 100.0 g waste	Mass g
Water	24.0
Cement	9.0
Fly Ash	6.0
$Fe_2(SO_4)_3 \cdot 9H_2O$	14.4

Important ratios:

Binder/Waste	0.15	g/g
Binder/H_2O	0.53	g/g
Fe^{3+}/binder	0.19	g/g
Fe^{3+}/As	6.4	mol/mol
SO_4^{2-}/binder	0.49	g/g
SO_4^{2-}/Ba^{2+}	1.6	mol/mol

F3x Series

Component per 100.0 g waste	Mass g
Water	64.0
Cement	24.0
Fly Ash	16.0
$Fe_2(SO_4)_3 \cdot 9H_2O$	12.8

Important ratios:

Binder/Waste	0.40	g/g
Binder/H_2O	0.59	g/g
Fe^{3+}/binder	0.064	g/g
Fe^{3+}/As	5.7	mol/mol
SO_4^{2-}/binder	0.16	g/g
SO_4^{2-}/Ba^{2+}	1.4	mol/mol

F4x Series

Component per 100.0 g waste	Mass g
Water	64.0
Cement	24.0
Fly Ash	16.0
$Fe_2(SO_4)_3 \cdot 9H_2O$	38.4

Important ratios:

Binder/Waste	0.40	g/g
Binder/H_2O	0.53	g/g
Fe^{3+}/binder	0.19	g/g
Fe^{3+}/As	17.	mol/mol
SO_4^{2-}/binder	0.49	g/g
SO_4^{2-}/Ba^{2+}	4.2	mol/mol

Notes:

1. Water of hydration is taken into account in Binder/H_2O ratio.
2. 100 g waste contains 0.060 g Arsenic.
3. 100 g waste contains 13.3 g Barium of which 43% is found to be extractable in TCLP.
4. Assume 50% of Ba in waste is available for reaction in ratios calculated.

MATRIX OF MIX DESIGNS FOR FERROUS SULFATE STABILIZATION OF D004/D005 WASTE (Table 4-3 repeated for ease of reference)

US1x Series

Component per 100.0 g waste	Mass g
Water	24.0
Cement	9.0
Fly Ash	6.0
$FeSO_4 \cdot 7H_2O$	4.8

Important ratios:		
Binder/Waste	0.15	g/g
Binder/H_2O	0.57	g/g
Fe^{2+}/binder	0.064	g/g
Fe^{2+}/As	2.2	mol/mol
SO_4^{2-}/binder	0.11	g/g
SO_4^{2-}/Ba^{2+}	0.36	mol/mol

US2x Series

Component per 100.0 g waste	Mass g
Water	24.0
Cement	9.0
Fly Ash	6.0
$FeSO_4 \cdot 7H_2O$	14.4

Important ratios:		
Binder/Waste	0.15	g/g
Binder/H_2O	0.49	g/g
Fe^{2+}/binder	0.19	g/g
Fe^{2+}/As	6.5	mol/mol
SO_4^{2-}/binder	0.33	g/g
SO_4^{2-}/Ba^{2+}	1.1	mol/mol

US3x Series

Component per 100.0 g waste	Mass g
Water	64.0
Cement	24.0
Fly Ash	16.0
$FeSO_4 \cdot 7H_2O$	12.8

Important ratios:		
Binder/Waste	0.40	g/g
Binder/H_2O	0.57	g/g
Fe^{2+}/binder	0.064	g/g
Fe^{2+}/As	5.7	mol/mol
SO_4^{2-}/binder	0.11	g/g
SO_4^{2-}/Ba^{2+}	0.95	mol/mol

US4x Series

Component per 100.0 g waste	Mass g
Water	64.0
Cement	24.0
Fly Ash	16.0
$FeSO_4 \cdot 7H_2O$	38.4

Important ratios:		
Binder/Waste	0.40	g/g
Binder/H_2O	0.49	g/g
Fe^{2+}/binder	0.19	g/g
Fe^{2+}/As	17.	mol/mol
SO_4^{2-}/binder	0.33	g/g
SO_4^{2-}/Ba^{2+}	2.9	mol/mol

Notes:

1. Water of hydration is taken into account in Binder/H_2O ratio.
2. 100 g waste contains 0.060 g Arsenic.
3. 100 g waste contains 13.3 g Barium of which 43% is found to be extractable in TCLP.
4. Assume 50% of Ba in waste is available for reaction in ratios calculated.

MATRIX OF MIX DESIGNS FOR ALUMINUM SULFATE STABILIZATION OF D004/D005 WASTE (Table 4-4 repeated for ease of reference)

A1x Series

Component per 100.0 g waste	Mass g
Water	24.0
Cement	9.0
Fly Ash	6.0
$Al_2(SO_4)\cdot 18H_2O$	4.8

Important ratios:

Binder/Waste	0.15	g/g
Binder/H_2O	0.57	g/g
Al^{3+}/binder	0.026	g/g
Al^{3+}/As	1.8	mol/mol
SO_4^{2-}/binder	0.14	g/g
SO_4^{2-}/Ba^{2+}	0.45	mol/mol

A2x Series

Component per 100.0 g waste	Mass g
Water	24.0
Cement	9.0
Fly Ash	6.0
$Al_2(SO_4)\cdot 18H_2O$	14.4

Important ratios:

Binder/Waste	0.15	g/g
Binder/H_2O	0.48	g/g
Al^{3+}/binder	0.078	g/g
Al^{3+}/As	5.4	mol/mol
SO_4^{2-}/binder	0.42	g/g
SO_4^{2-}/Ba^{2+}	1.3	mol/mol

A3x Series

Component per 100.0 g waste	Mass g
Water	64.0
Cement	24.0
Fly Ash	16.0
$Al_2(SO_4)\cdot 18H_2O$	12.8

Important ratios:

Binder/Waste	0.40	g/g
Binder/H_2O	0.57	g/g
Al^{3+}/binder	0.026	g/g
Al^{3+}/As	4.8	mol/mol
SO_4^{2-}/binder	0.14	g/g
SO_4^{2-}/Ba^{2+}	1.2	mol/mol

A4x Series

Component per 100.0 g waste	Mass g
Water	64.0
Cement	24.0
Fly Ash	16.0
$Al_2(SO_4)\cdot 18H_2O$	38.4

Important ratios:

Binder/Waste	0.40	g/g
Binder/H_2O	2.1	g/g
Al^{3+}/binder	0. 79	g/g
Al^{3+}/As	14.	mol/mol
SO_4^{2-}/binder	0.42	g/g
SO_4^{2-}/Ba^{2+}	3.6	mol/mol

Notes:

1. Water of hydration is taken into account in Binder/H_2O ratio.
2. 100 g waste contains 0.060 g Arsenic.
3. 100 g waste contains 13.3 g Barium of which 43% is found to be extractable in TCLP.
4. Assume 50% of Ba in waste is available for reaction in ratios calculated.

Appendix B-1. TCLP Results for Two-Day and Sixty-Day Ferric Sulfate Stabilization of D004/D005 Waste

BINDER / D004-D005 Waste

Fe/As
(S/Ba)

0.15

0.40

2.2
(0.36)

MIX F1x

Metal (mg/L)	Cure Time(days) 2	60	365	540
As	22.1	14.4	0.59	0.57
Ba	850.	1200	2000	2320
Ca	1360	1380	1410	1480
S	10.5	6.66	<0.5	<0.5
Fe	0.62	0.90	1.6	7.2
Zn	0.10	0.12	0.84	1.1
pH	6.8	6.45		

6.0
(1.0)

MIX F2x

Metal (mg/L)	Cure Time(days) 2	60	365	540
As	0.25	0.25	15.	17.
Ba	0.55	1.36	1.9	17.3
Ca	1400	1520	1790	1540
S	230.	173.	12.7	2.67
Fe	1.01	3.24	183.	214.
Zn	0.16	1.14	1.30	1.2
pH	5.31	4.8		

MIX F3x

Metal (mg/L)	Cure Time (days) 2	60	365	540
As	20.6	15.3	0.96	0.85
Ba	0.31	0.68	88.1	125.
Ca	1840	2050	2700	2570
S	189.	152.	0.48	<0.5
Fe	0.70	0.46	27.6	18.1
Zn	0.035	0.04	1.18	1.1
pH	7.6	7.8		

17
(2.9)

MIX F4x

Metal (mg/L)	Cure Time(days) 2	60	365	540
As	0.25	0.25	3.91	13.1
Ba	0.15	0.88	0.20	6.74
Ca	1520	1670	1890	1630
S	423.	385.	454.	564.
Fe	0.61	0.50	125.	464.
Zn	0.27	0.58	1.3	1.4
pH	5.4	5.4		

Appendix B-2. TCLP Results for Two-Day and Sixty-Day Ferrous Sulfate Stabilization of D004/D005 Waste

Fe/As
(S/Ba)

BINDER / D004-D005 Waste

0.15

2.2
(0.36)

MIX US1x

Metal (mg/L)	Cure Time(days) 2	60	365	540
As	47.3	8.0	0.44	<0.25
Ba	574.	1400	2100	1660
Ca	1460	1900	2100	1470
S	9.0		3.14	<0.5
Fe	0.60		2.68	6.14
Zn	0.076	103.	0.87	1.0
pH	7.97	6.86		

6.0
(1.0)

MIX US2x

Metal (mg/L)	Cure Time(days) 2	60	365	540
As	3.16	0.11	1.48	4.64
Ba	1.11	430.	540.	520.
Ca	1650	1790	2330	2200
S	125.		0.71	1.3
Fe	0.83		20.8	61.8
Zn	0.089	222.	0.95	
pH	7.65	5.83		

0.40

MIX US3x

Metal (mg/L)	Cure Time(days) 2	60	365	540
As	4.96	0.7	0.50	0.30
Ba	0.99	2.3	0.68	188.
Ca	1490	1920	3940	3970
S	134.		115.	1.65
Fe	0.62		0.34	12.3
Zn	0.049	53.4	0.27	
pH	8.51	7.39		

17.
(2.9)

MIX US4x

Metal (mg/L)	Cure Time(days) 2	60	365	540
As	0.25	0.15	<0.25	<0.25
Ba	0.44	1.1	0.21	1.52
Ca	2240	1930	3100	3010
S	566.		395.	336.
Fe	59.5		14.4	53.1
Zn	0.67	151.	1.16	
pH	7.54	6.72		

Appendix B-3. TCLP Results for Two and Sixty-Day Aluminum Sulfate Stabilization of D004/D005 Waste

Fe/As
(S/Ba)

BINDER / D004-D005 Waste

0.15

1.8
(0.45)

MIX A1x

Metal (mg/L)	2	60	540	540
As	42.6	41.9	16.2	12.5
Ba	1110	995.	2650	2540
Ca	1270	1200	1370	1340
S	28.4	61.3	8.5	10.
Fe	0.323	0.73	1.1	1.5
Zn	<0.05	<0.05	0.94	0.81
pH	7.59	7.45		

5.1
(1.3)

MIX A2x

Metal (mg/L)	2	60	540	540
As	23.2	0.89	31.4	42.1
Ba	671.	554.	520.	584.
Ca	1350	1280	906.	1030
S	15.3	46.	16.	9.4
Fe	2.97	0.90	13.5	6.2
Zn	1.39	0.65	4.3	2.2
pH	4.62	5.22		

0.40

MIX A3x

Metal (mg/L)	2	60	540	540
As	25.9	5.32		
Ba	1.63	578.		
Ca	1740	2290		
S	139.	27.2		
Fe	0.077	2.02		
Zn	<0.05	0.81		
pH	8.02	7.75		

14.
(3.6)

MIX A4x

Metal (mg/L)	2	60	540	540
As	18.4	7.07		73.8
Ba	2.47	1.32		0.8
Ca	1760	1690		1950
S	456.	393.		351.
Fe	18.9	3.14		43.7
Zn	0.969	0.70		1.18
pH	4.89	5.19		